

# **The Impact of Myeloid Cell-restricted Insulin Receptor Deficiency on Obesity- induced Insulin Resistance**

Inaugural-Dissertation  
zur  
Erlangung des Doktorgrades  
der Mathematisch-Naturwissenschaftlichen Fakultät  
der Universität zu Köln

vorgelegt von

**Jan Mauer**

aus Köln

Köln 2008

Berichterstatter: Prof. Jens C. Brüning  
Prof. Thomas Langer

Tag der mündlichen Prüfung: 17.02.2009

<b>Figure Index</b>	<b>III</b>
<b>Table Index</b>	<b>V</b>
<b>Abbreviations</b>	<b>VI</b>
<b>1 Introduction</b>	<b>1</b>
<b>1.1 Obesity</b>	<b>1</b>
<b>1.2 Diabetes Mellitus</b>	<b>3</b>
1.2.1 Systemic and Molecular Effects of Insulin Signaling	4
<b>1.3 Obesity, Inflammation and Insulin Resistance</b>	<b>6</b>
<b>1.4 Macrophages</b>	<b>9</b>
1.4.1 The Role of Macrophages in Obesity-induced Insulin Resistance	10
1.4.2 Adipose Tissue Macrophage Heterogeneity	11
<b>1.5 Macrophages and Insulin</b>	<b>12</b>
<b>1.6 Objectives</b>	<b>13</b>
<b>2 Materials and Methods</b>	<b>14</b>
<b>2.1 Chemicals</b>	<b>14</b>
<b>2.2 Molecular Biology</b>	<b>16</b>
2.2.1 Isolation of Genomic DNA	16
2.2.2 Southern Blot Analysis	17
2.2.3 Quantification of Nucleic Acids	18
2.2.4 Polymerase Chain Reaction (PCR)	18
2.2.5 RNA Extraction, RT-PCR and Quantitative Realtime PCR	19
2.2.6 Protein Extraction	20
2.2.7 SAPK/JNK Kinase Assay	20
2.2.8 Western Blot Analysis	21
2.2.9 Gelatin Zymography	21
2.2.10 ELISA	22
<b>2.3 Cell Culture and Tissue Analysis</b>	<b>23</b>
2.3.1 Preparation of L-cell Conditioned Medium	23
2.3.2 Preparation of Palmitic Acid Media	23
2.3.3 Differentiation of Murine Bone Marrow to Macrophages	24
2.3.4 Culture of Primary Murine Macrophages	24
2.3.5 Detection of Apoptotic Cells by TUNEL Assay	24
2.3.6 Boyden Chamber Analysis	25
2.3.7 Histological Analysis and Immunohistochemistry	26
<b>2.4 Mouse Experiments</b>	<b>27</b>
2.4.1 Animals	27
2.4.2 IR <sup>Δmyel</sup> mice	27
2.4.3 Body Weight and Blood Glucose Levels	28
2.4.4 Glucose and Insulin Tolerance Test	28
2.4.5 Isolation of Adipocytes and Stromal Vascular Fraction	28
2.4.6 Isolation of Primary Peritoneal Macrophages	29
2.4.7 Isolation of Murine Bone Marrow	29
2.4.8 Glucose Transport	29
2.4.9 Hyperinsulinemic-euglycemic Clamp Studies	30
<b>2.5 Computer Analysis</b>	<b>32</b>
2.5.1 Densitometrical Analysis	32
2.5.2 Statistical Methods	32
<b>3 Results</b>	<b>33</b>
<b>3.1 Myeloid Cell-specific Disruption of the Insulin Receptor</b>	<b>33</b>

---

<b>3.2</b>	<b>The Effect of Myeloid Cell-restricted Insulin Receptor Deficiency on Diet-induced Obesity</b>	<b>35</b>
<b>3.3</b>	<b>The Effect of Myeloid Cell-restricted Insulin Receptor Deficiency on Obesity-induced Insulin Resistance</b>	<b>37</b>
<b>3.4</b>	<b>The Effect of Myeloid Cell-restricted Insulin Receptor Deficiency on Obesity-induced Inflammation</b>	<b>43</b>
<b>3.5</b>	<b>The Effect of Myeloid Cell-restricted Insulin Receptor Deficiency on Adipose Tissue Inflammation and Macrophage Accumulation</b>	<b>46</b>
<b>3.6</b>	<b>Cell-Autonomous Effects of Insulin Receptor Deficiency on Macrophages</b>	<b>51</b>
3.6.1	The Effect of Insulin on Macrophage Apoptosis	51
3.6.2	The Effect of Insulin on Pro-inflammatory Gene Expression	54
3.6.3	The Effect of Insulin on Macrophage Migration	56
<b>4</b>	<b><i>Discussion</i></b>	<b>59</b>
<b>4.1</b>	<b>Recombination Efficiency of the LysMCre Transgene</b>	<b>59</b>
<b>4.2</b>	<b>Myeloid Cell-specific Disruption of the Insulin Receptor protects against Obesity-induced Insulin Resistance</b>	<b>61</b>
<b>4.3</b>	<b>Myeloid Cell-specific Disruption of the Insulin Receptor modulates the Obesity-associated Pro-inflammatory Tone</b>	<b>62</b>
<b>4.4</b>	<b>Myeloid Cell-specific Disruption of the Insulin Receptor blunts the Inflammatory Infiltration of Adipose Tissue by Macrophages</b>	<b>63</b>
<b>4.5</b>	<b>The Effect of Metabolic Stress on Macrophages</b>	<b>65</b>
4.5.1	Insulin as a Survival Signal for Macrophages	65
4.5.2	Pro-inflammatory Effects of Insulin in Macrophages	67
4.5.3	The Effects of Insulin on Macrophage Migration	68
<b>4.6</b>	<b>Conclusions</b>	<b>70</b>
<b>5</b>	<b><i>Summary</i></b>	<b>71</b>
<b>6</b>	<b><i>Zusammenfassung</i></b>	<b>72</b>
<b>7</b>	<b><i>References</i></b>	<b>73</b>
<b>8</b>	<b><i>Acknowledgements</i></b>	<b>95</b>
<b>9</b>	<b><i>Erklärung</i></b>	<b>96</b>
<b>10</b>	<b><i>Curriculum Vitae</i></b>	<b>97</b>

## Figure Index

Fig. 1: Prevalence of overweight in the United States from 1991-2001. ....	1
Fig. 2: Prevalence of diabetes in the United States from 1991-2001. ....	3
Fig. 3: Insulin signal transduction pathway. ....	5
Fig. 4: Potential mechanisms for the inhibition of insulin signal transduction in obesity. ....	8
Fig. 5: Experimental design of the Boyden Chamber Analysis. ....	25
Fig. 6: Southern blot analysis of the insulin receptor allele in macrophages. ....	33
Fig. 7: Insulin receptor mRNA expression in macrophages. ....	34
Fig. 8: Insulin receptor protein expression in macrophages. ....	34
Fig. 9: Insulin receptor protein expression in insulin target tissues is unchanged in IR <sup>Δmyel</sup> mice. ....	35
Fig. 10: IR <sup>Δmyel</sup> mice exhibit normal weight gain upon normal chow diet and high fat feeding. ....	36
Fig. 11: IR <sup>Δmyel</sup> mice show normal high fat diet-induced increase in epididymal fat pad mass and circulating leptin concentration. ....	37
Fig. 12: Diet-induced obese IR <sup>Δmyel</sup> mice exhibit significantly reduced fasted blood glucose and insulin levels. ....	38
Fig. 13: Obese IR <sup>Δmyel</sup> mice exhibit increased glucose tolerance and insulin sensitivity. ....	39
Fig. 14: Obese IR <sup>Δmyel</sup> mice exhibit decreased hepatic glucose production. ....	40
Fig. 15: Obese IR <sup>Δmyel</sup> mice show enhanced insulin-stimulated glucose disposal in skeletal muscle. ....	41
Fig. 16: Low dose insulin-stimulated glucose uptake is enhanced in adipocytes of obese IR <sup>Δmyel</sup> mice. ....	42
Fig. 17: The obesity-associated change of serum TNF-α and adiponectin concentration is abolished in IR <sup>Δmyel</sup> mice. ....	43
Fig. 18: Obese IR <sup>Δmyel</sup> mice show reduced JNK activity in skeletal muscle. ....	44
Fig. 19: Obesity-induced change of adipokine gene expression is blunted in IR <sup>Δmyel</sup> mice. ....	45
Fig. 20: Reduced macrophage surface marker expression in adipose tissue of obese IR <sup>Δmyel</sup> mice. ....	46
Fig. 21: Adipose tissue morphology of IR <sup>Δmyel</sup> mice and control mice exposed to HFD. ....	47
Fig. 22: Quantification of adipocyte size and size distribution. ....	47
Fig. 23: Obese adipose tissue of IR <sup>Δmyel</sup> mice shows decreased formation of crown-like structures. ....	48
Fig. 24: Reduced TNF-α expression in adipose tissue-derived stromal vascular cells of IR <sup>Δmyel</sup> mice. ....	49
Fig. 25: Enhanced apoptosis in insulin receptor-deficient macrophages. ....	52
Fig. 26: Insulin enhances expression of Bcl-2 mRNA in bone marrow-derived macrophages. ....	53
Fig. 27: Insulin augments pro-inflammatory gene expression in macrophages. ....	55
Fig. 28: Insulin enhances secretion of TNF-α in macrophages. ....	56

Fig. 29: Insulin receptor deficiency impairs matrix metalloproteinase 9 expression in macrophages. .... 57

Fig. 30: Insulin receptor-deficient macrophages show impaired chemotactic abilities. .... 58

## Table Index

Table 1: Chemicals.....	16
Table 2: Oligonucleotides used to amplify the southern blot probe.....	17
Table 3: Oligonucleotides used for genotyping .....	18
Table 4: Taqman Gene Expression Assays .....	19
Table 5: Primary antibodies used for western blot analysis.....	21

## Abbreviations

A	adenosine
aa	amino acid
Akt	protein kinase B
Avertin	tribromoethyl alcohol and <i>tert</i> -amyl alcohol
β-me	β-mercaptoethanol
BMDM	bone marrow-derived macrophages
bp	base pair
c	DNA concentration
C	cytosine
°C	degrees Celsius
CAP	cbl-associated protein
cDNA	complementary DNA
cpm	counts per minute
Cre	site-specific recombinase (causes recombination)
Ctrl	Control
ddH <sub>2</sub> O	double distilled water
DEPC	diethylpyrocarbonate
dNTP	desoxynucleotide-triphosphate
DMSO	dimethylsulfoxide
DNA	desoxyribonucleic acid
DTT	1,4-Dithio-DL-threitol
ECL	enhanced chemiluminescence
EDTA	ethylene-diaminetetraacetic acid
ELISA	enzyme-linked immunosorbent assay
ERK	extracellular signal-regulated kinase
EtBr	ethidium bromide
FOXO	forkhead transcription factor
G	guanine
Glut	glucose transporter
Grb	growth factor receptor binding protein

GSK	glycogen synthase kinase
GTT	glucose tolerance test
h	hour
HEPES	N-2-hydroxyethylpiperazine-N'-2-ethansulfonic acid
i.p.	intraperitoneal
IL	interleukin
IR	insulin receptor
IRS	insulin receptor substrate
ITT	insulin tolerance test
kDa	kilodalton
loxP	locus of x (crossing) over of P1
MCP-1	macrophage chemoattractant protein 1
MIP-1 $\alpha$	macrophage inflammatory protein 1 $\alpha$
min	minute
mTOR	mammalian target of rapamycin
NaCl	sodium chloride
NaOH	sodium hydroxide
NLS	nuclear localization sequence
OD	optical density
p70S6K	p70 S6 kinase
PBS	phosphate buffered saline
PCR	polymerase chain reaction
PDK	phosphoinositide-dependent kinase
PH	pleckstrin homology
PI3K	phosphatidylinositol-3 kinase
PIP <sub>2</sub>	phosphatidylinositol-4,5-biphosphate
PIP <sub>3</sub>	phosphatidylinositol-3,4,5-triphosphate
PKA	proteinkinase A
PKC	proteinkinase C
PTB	phosphotyrosine binding
Ras	rat sarcoma
Raf	v-raf-leukemia viral oncogene
RNA	ribonucleic acid
rpm	rounds per minute

RT	room temperature
sec	second
SDS	sodium dodecyl sulfate
SH	src homology
SOS	son of sevenless
SSC	sodium chloride/ sodium citrate buffer
TAE	Tris-acetic acid-EDTA buffer
Taq Pol	polymerase from <i>Thermus aquaticus</i>
TE	Tris-EDTA buffer
TNF	tumor necrosis factor
Tris	2-amino-2-(hydroxymethyl)-1,3-propanediol
TWEEN	polyoxyethylene-sorbitan-monolaureate
U	units
v/v	volume per volume
WAT	white adipose tissue
w/v	weight per volume
wt	wildtype
5'	five prime end of DNA sequences
3'	three prime end of DNA sequences

# 1 Introduction

## 1.1 Obesity

Obesity represents a steadily increasing health threat to our society and is a major cause of morbidity and mortality. Over the last 10 years, the percentage of overweight adults in the United States has increased from 45 to 58% (Fig. 1) (1). This increment in the prevalence of overweight and obesity, a trend found not only in adults but also in children, has been observed in many other countries of the world (2-4). According to latest projections of the World Health Organisation (WHO) 1.6 billion adults are overweight and at least 400 million are obese worldwide. These numbers will presumably rise to 2.3 billion overweight and 700 million obese individuals until the year 2015 (5).

The underlying cause of excessive weight gain is a continuous imbalance between energy intake on one hand, and energy expenditure on the other (6). Enhanced susceptibility to obesity is not only attributable to genetic variation but also to a number of other factors including a global shift in diet composition towards higher amounts of fat and carbohydrates and lower amounts of vitamins, minerals and other micronutrients (7). Furthermore, decreased physical activity and a shift towards a sedentary lifestyle contribute to the obesity epidemic (8, 9).

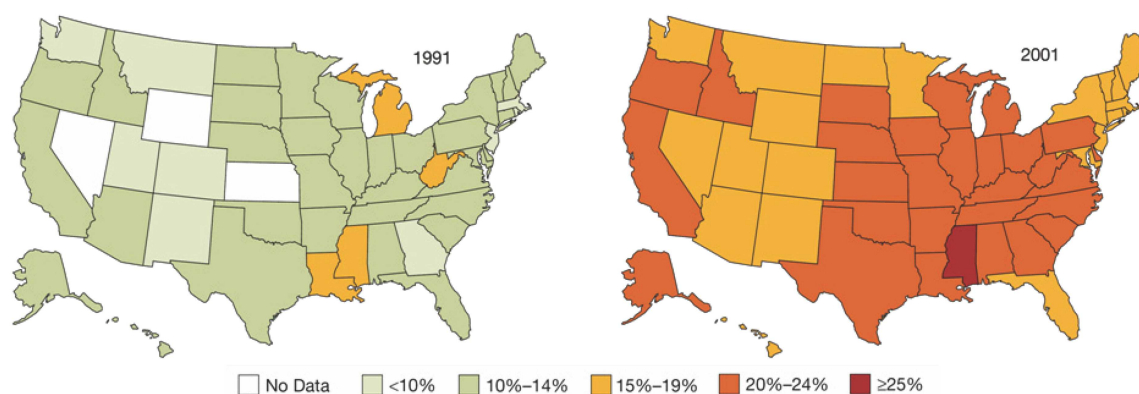


**Fig. 1: Prevalence of overweight in the United States from 1991-2001.**

Since 1991, the percentage of overweight adults has risen from 45 to 58%. Of those overweight in 2001, 56% were men and 44% were women. Mokdad et al, 2003 (1).

The most common measure for defining overweight and obesity is the body mass index (BMI) which is assessed by the ratio of body weight in kilogramm (W) and height in meters (H) multiplied by itself ( $W/H^2$ ) (10). Individuals with a BMI of 25 to 29.9  $kg/m^2$  are defined as overweight while obesity is characterized by a BMI of 30  $kg/m^2$  or higher (5). Obesity predisposes to a variety of different diseases. It represents an independent risk factor for myocardial infarction, stroke, type 2 diabetes mellitus, and certain types of cancer (11-13). Adiposity, which is the fraction of total body mass comprised of neutral lipid stored in adipose tissue, is closely correlated with important physiological parameters such as blood pressure, systemic insulin sensitivity, serum triglyceride and leptin concentrations (14-16). Several obesity-related disorders including insulin resistance, glucose intolerance, dyslipidemia, hypertension, and coronary artery disease are positively correlated with adiposity (15, 17). It has been shown that visceral fat accumulation is more closely linked to obesity-associated pathologies than overall adiposity (18). Changes in adipose tissue mass are associated with changes in the endocrine and metabolic functions of adipose tissue that connect increased adiposity to alterations in systemic physiology. For example, the concentration of circulating leptin, the most prominent adipocyte-derived hormone, positively correlates with increased adipocyte volume and number (19). Leptin functions as an important regulator of energy intake and storage, insulin sensitivity, and metabolic rate (20-22). In contrast, adiposity is negatively correlated with plasma concentrations of adiponectin, an adipocyte-derived, insulin-sensitizing hormone that decreases hepatic gluconeogenesis and increases lipid oxidation in muscle (23-25).

Visceral fat accumulation belongs to a group of risk factors including high blood pressure, high blood glucose, high levels of triglycerides and low levels of high density lipoproteins which are subsumed under the term metabolic syndrome (26). These conditions predispose for cardiovascular disease (CVD) and type 2 diabetes mellitus (T2DM) (27-29).

## 1.2 Diabetes Mellitus

Since one of the major consequences of excessive weight gain is the development of insulin resistance, it is not surprising that an increase in number of overweight and obese individuals within a population (Fig. 1) is accompanied by a rise in the occurrence of diabetes (Fig. 2). Diabetes mellitus is a chronic disease and the sixth leading cause of death in the United States. In 2007, a total of 23.6 million US citizens, representing 8% of the population, suffered from diabetes. Health care costs, whether assigned to diabetes directly or indirectly, were estimated at 174 billion USD for the year 2007 (30). According to the WHO 180 million people worldwide suffer from diabetes and these numbers are predicted to more than double by 2030. In 2005, 1.1 million people died from diabetes all over the world and an increase by more than 50% is projected for the next 10 years (31, 32).

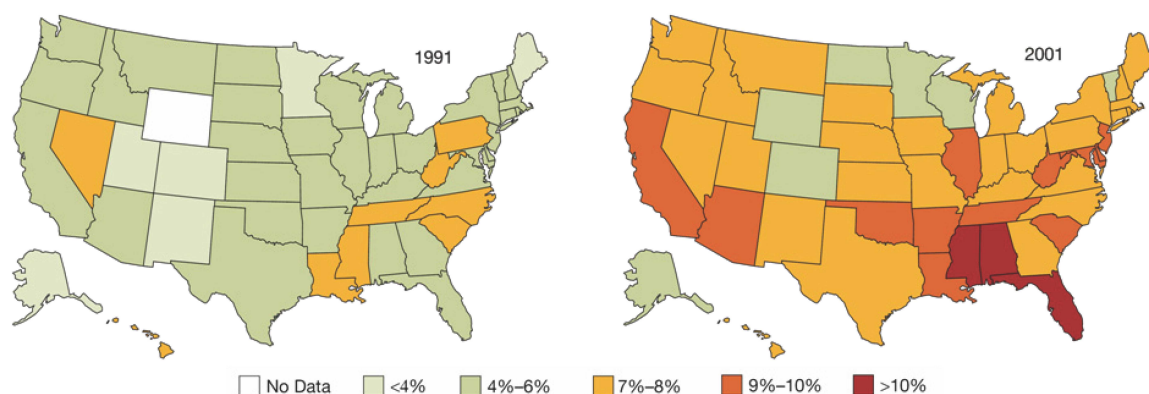


**Fig. 2: Prevalence of diabetes in the United States from 1991-2001.**

The prevalence of people diagnosed with diabetes increased to 7.9% in 2001 from 4.9% in 1990, an increase of 61%. In 2001, 3.4% of US adults (2.9% men, 3.8% women) were both obese and had diabetes, an increase of 1.4% compared to 1991. Mokdad et al, 2003 (1).

In principal, there are two idiopathic forms of diabetes known as type 1 and 2. Type 1 diabetes mellitus (T1DM), also termed juvenile diabetes or insulin-dependent diabetes (IDDM), is characterized by the loss of insulin-producing  $\beta$ -cells in the Langerhans islets of the pancreas as a result of autoimmune reactions (33). T1DM can be treated and contained by an insulin replacement therapy and dietary management (34).

Type 2 diabetes mellitus, formerly known as adult-onset diabetes, is the non-insulin-dependent (NIDDM) form of diabetes and accounts for 90-95% of all diagnosed cases of diabetes (30). This disease develops when chronic overnutrition colludes with genetic susceptibility to cause insulin resistance and a relative insulin deficiency of non-

autoimmune etiology (35, 36). When resistance to the metabolic effect of insulin occurs, the pancreas is able to compensate with expansion of  $\beta$ -cell mass and hypersecretion of the hormone (37). It is assumed that the ultimate stimulus is nutrient surplus in the blood, predominantly glucose and free fatty acids (FFA) (38-40). However, prolonged overproduction of insulin leads to progressive deterioration of  $\beta$ -cell function associated with apoptosis-driven loss of  $\beta$ -cell mass leading to subsequent progression to a type 2 diabetic state (41-43). T2DM is characterized by severe hyperglycemia and altered lipid homeostasis (44-46).

Treatment strategies for T2DM include oral agents such as sulfonylureas, biguanides and thiazolidinediones (TZD) which increase insulin secretion, insulin action and augment overall insulin sensitivity, respectively (47-50). Interestingly, anti-inflammatory drugs like salicylates can also improve insulin sensitivity (51, 52). In addition, lifestyle changes especially increased exercise and dietary adjustments including caloric restriction ameliorate T2DM morbidity (53, 54). In the long-term, diabetes is associated with complications such as atherosclerosis, retinopathy, nephropathy, neuropathy and impaired wound healing which all impose significant economical consequences (55-60).

### **1.2.1 Systemic and Molecular Effects of Insulin Signaling**

Insulin has most potent anabolic effects and promotes the synthesis and storage of carbohydrates, lipids and proteins, while inhibiting their degradation and release into the circulation (44). It controls energy homeostasis by stimulating glucose uptake in peripheral tissues and suppressing the release of stored lipids from adipose tissue (61-64). Furthermore, it increases glycolysis and inhibits gluconeogenesis in the liver (65-67).

The pleiotropic effects of insulin are mediated by binding of the hormone to its membrane-bound receptor (68). The insulin receptor (IR) belongs to the family of receptor tyrosine kinases and comprises four subunits of which two regulatory  $\alpha$ -subunits inhibit the two catalytic  $\beta$ -subunits. Upon binding of insulin, the  $\alpha$ -subunits undergo a conformational change that leads to derepression of the  $\beta$ -subunits which subsequently transphosphorylate (69). This facilitates interaction with the phosphotyrosine binding (PTB) domains of downstream signaling components (70-73) which localize to the plasma membrane by

interaction of their N-terminal Pleckstrin homology (PH) domain with lipid-bound inositol phosphates (74, 75).

There are at least nine known intracellular substrates of the insulin receptor. Four of these belong to the insulin receptor substrate (IRS) family (76-78). Others include Grb2-associated binding protein 1, p60<sup>dok</sup>, Casitas B-lineage lymphoma (Cbl), adapter protein with a pleckstrin homology and a Src homology 2 domain (APS) and isoforms of Shc (79-81). These molecules serve as docking platforms for Src-homology (SH)-2 domain-containing proteins such as the regulatory subunit of the phosphatidylinositol-3 kinase (PI3K) and the growth factor receptor binding protein (Grb)-2. Subsequent signal transduction results in the activation of the PI3K and the Ras/Raf Mitogen-activated protein (MAP)-kinase pathways (82-85).

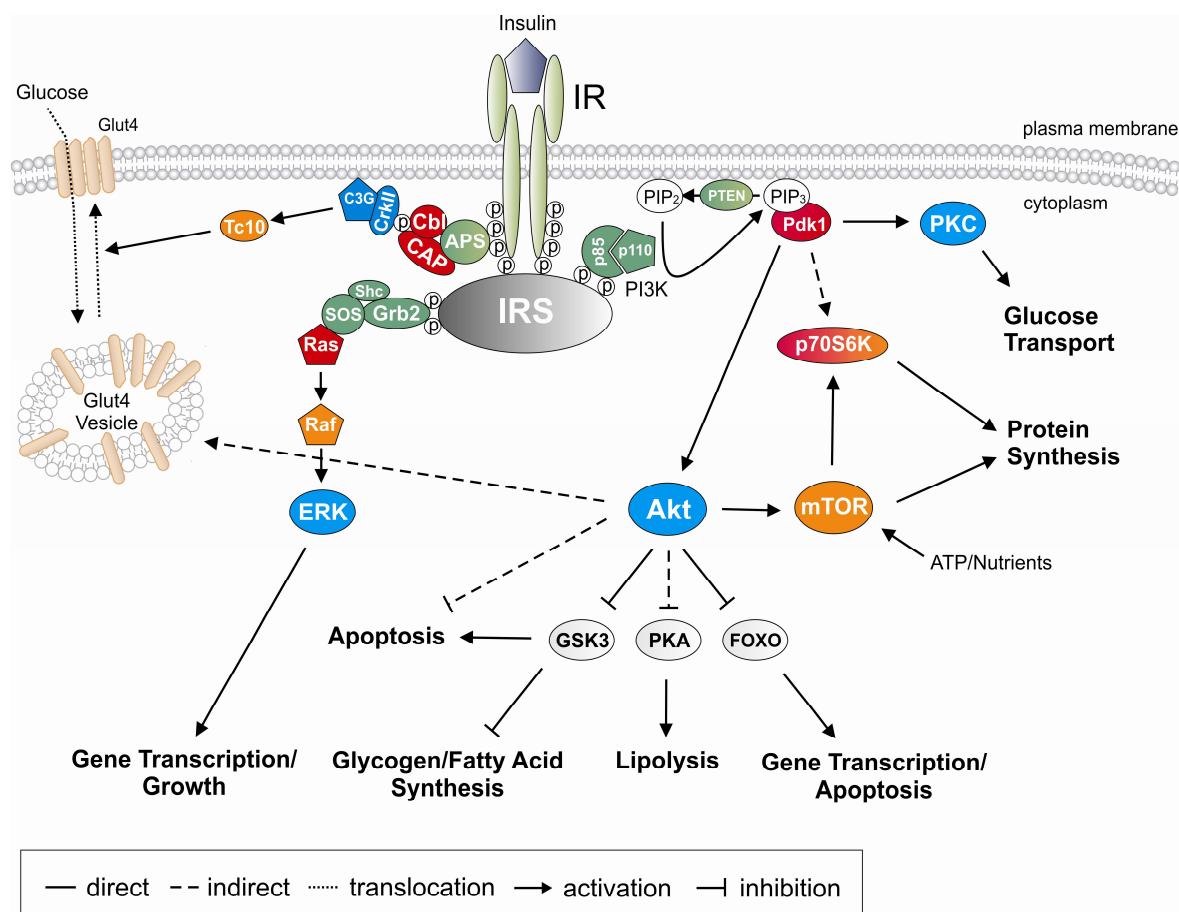


**Fig. 3: Insulin signal transduction pathway.**

Binding of insulin to the insulin receptor results in receptor trans-phosphorylation and activation leading to the recruitment and subsequent phosphorylation of insulin receptor substrates. This enables the binding of SH-2 domain containing proteins, which ultimately leads to the activation of downstream signaling pathways such as the PI3K or the Ras/Raf MAPK signaling pathway. (Abbreviations: Akt: Proteinkinase B, APS:

adaptor protein with a pleckstrin homology and an Src homology 2 domain, CAP: cbl-associated protein, ERK: extracellular signal-regulated kinase, FOXO: Forkhead transcription factor, Glut4: glucose transporter 4, Grb2: growth factor receptor binding protein 2, Gsk3: glycogen synthase kinase 3, IR: insulin receptor, IRS: insulin receptor substrate, mTOR: mammalian target of rapamycin, p70S6K: p70 S6 kinase, PI3K: phosphatidylinositol-3 kinase, PIP: phosphatidylinositol phosphate, Pdk: phosphoinositide-dependent kinase, PKA: Protein kinase A, PKC: Protein kinase C, SOS: son of sevenless, Raf: v-raf-leukemia viral oncogene, Ras: rat sarcoma)

Activation of the Ras/Raf MAP-kinase pathway leads to cellular proliferation and differentiation while no significant effect on the metabolic actions of insulin has been observed (86, 87). In contrast, insulin-induced PI3K activation mediates the vast majority of metabolic effects of the hormone including glycogen, protein and lipid synthesis, inhibition of apoptosis and stimulation of glucose transport. Most of these processes are mediated through activation of Protein kinase B/Akt (88-91). However, a PI3K-independent pathway for the regulation of glucose transport has also been identified (92). In this pathway, the insulin receptor directly recruits the adaptor protein APS and the Cbl-cbl associated protein (93) complex. Tyrosine-phosphorylated Cbl then recruits the CrkII-C3G complex to lipid rafts, leading to downstream activation of TC10 and ultimately resulting in translocation of glucose transporter (GLUT) 4 to the plasma membrane (94-98) (Fig. 3).

### **1.3 Obesity, Inflammation and Insulin Resistance**

The nutritional or metabolic state of an organism is closely linked to its immune system in a delicate balance. Malnutrition impairs immune processes thereby rendering an organism more susceptible to infectious diseases (99, 100). This arises from a reduced metabolic support under conditions of infection during which the immune system is highly dependent on the mobilization of nutrients and supply with energy to eliminate pathogens (101). In contrast, overnutrition i.e. obesity is associated with chronic, low-grade activation of the immune system and increased susceptibility to inflammatory diseases (102). This can lead to insulin resistance when inflammatory pathways interfere with insulin signaling cascades (103).

The first evidence for the importance of inflammatory signaling in obesity-induced insulin resistance was the observation that the pro-inflammatory cytokine tumor necrosis

factor (TNF)  $\alpha$  is elevated in adipose tissue of obese mice and humans and is capable of inducing insulin resistance *in vitro* (104-106). TNF- $\alpha$  acts via the TNF receptor and activates intracellular protein kinases e.g. the inhibitor of nuclear factor (NF)  $\kappa$ B kinases (IKKs) and c-jun N-terminal kinases (JNKs) (107, 108). Subsequently, these kinases mediate inhibitory phosphorylation events on serine (S307) residues of IRS molecules (109, 110). S307 phosphorylation of IRS reduces both tyrosine phosphorylation of IRS in response to insulin and its ability to associate with the insulin receptor, thus inhibiting downstream signaling and insulin action (111, 112). Inhibition or inactivation of IKK or JNK in mice has been shown to protect from obesity-induced insulin resistance (51, 52, 113-115). Aside from TNF- $\alpha$ , a variety of other inflammation-associated factors including interleukin (IL) 6, IL-1, IL-8, c-reactive protein (CRP), monocyte chemoattractant protein 1 (MCP-1, also called CCL2), vascular cell adhesion molecules (VCAMs) and matrix metalloproteinases (MMPs) are upregulated in the adipose tissue and/or circulation of obese mice and humans and have been linked to obesity and insulin resistance (93, 116-121).

In addition to these factors, the obesity-associated increase in circulating free fatty acids (FFAs) has been shown to interfere with insulin signaling in target tissues via activation of IKK, JNK and protein kinase C (PKC) (122-127). This interference is mediated via at least two mechanisms. On one hand, FFAs induce inflammatory signaling cascades by activation of toll-like receptors (TLRs). TLRs belong to a family of pattern-recognition receptors that play a crucial role in activating the pro-inflammatory response after contact with microbial pathogens (128). The best characterized member of this receptor family is TLR4 which recognizes lipopolysaccharides (LPS), components of the bacterial cell wall. Signal transduction after contact with LPS is mediated through intracellular binding of myeloid differentiation factor 88 (MyD88) to the Toll/IL-1 receptor (TIR) domain of the receptor and subsequent activation of the NF $\kappa$ B pathway. This leads to expression of pro-inflammatory cytokines and chemokines and other effectors of the innate immune response (129).

Besides LPS, whose lipid component is sufficient to mediate TLR signaling, saturated fatty acids have the full potential to promote TLR4 activation *in vitro* (130, 131). Disruption of TLR4 in mice has been demonstrated to partially protect these animals from obesity-induced insulin resistance and substantially reduce the negative effect of systemic lipid infusion on glucose metabolism and muscle insulin action (132). In addition to TLR signaling, FFA activate inflammatory serine kinases by intermediates of their intracellular

processing pathways such as  $\beta$ -oxidation in the mitochondria, storage to triglyceride depots and conversion into ceramides (133-136).

Another important aspect of obesity-induced insulin resistance is the development of endoplasmic reticulum (ER) stress. Under normal conditions, the ER is the site of protein folding and assembly by chaperones (137). However, obesity generates conditions of glucose or nutrient deprivation, inundation with fatty acids or increased expression of secretory proteins that elevate the demand on the ER leading to accumulation of unfolded or misfolded proteins.

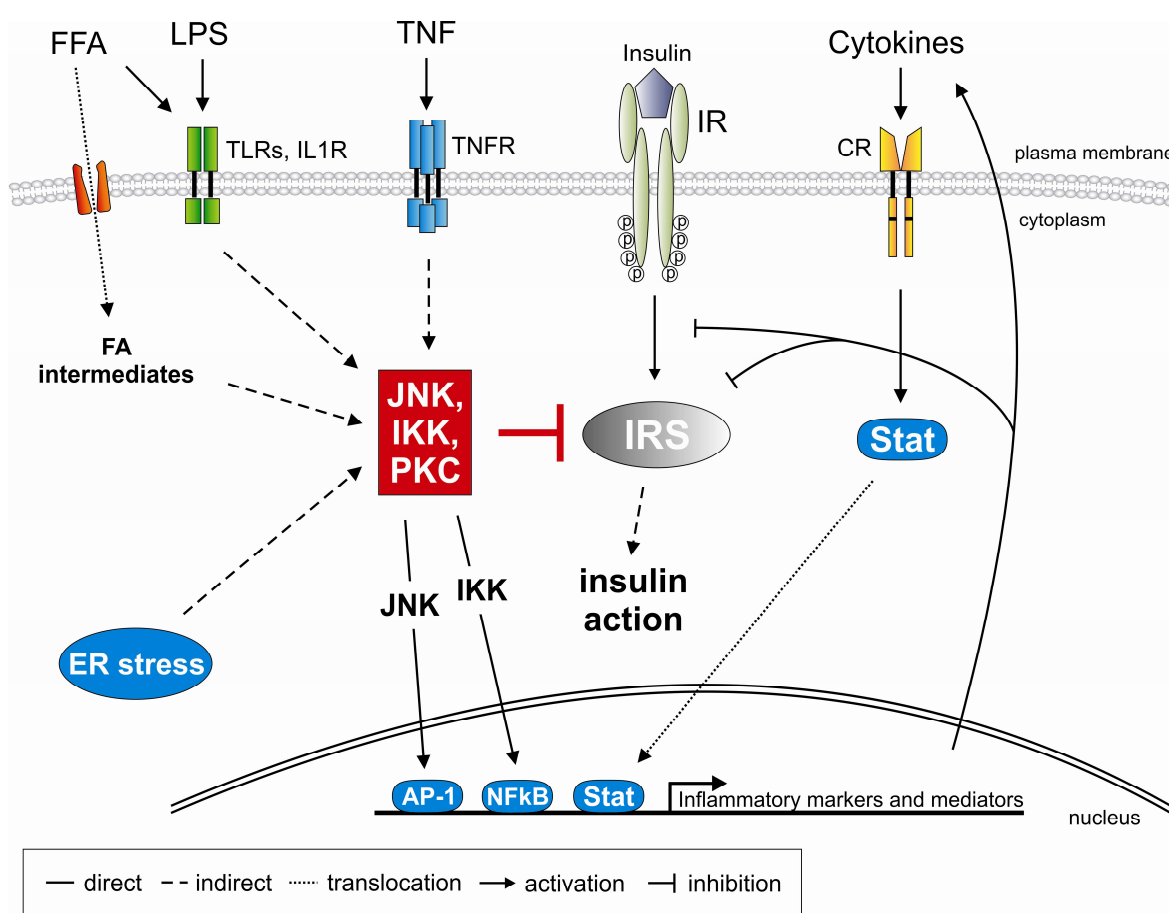


**Fig. 4: Potential mechanisms for the inhibition of insulin signal transduction in obesity.**

Obesity increases circulating inflammatory cytokine and free fatty acid concentration. This leads to activation of cell surface receptors which then induce serine kinases like c-jun N-terminal kinase (JNK), inhibitor of NF $\kappa$ B kinase (IKK) complex and protein kinase c (PKC) isoforms. These kinases then mediate inhibitory serine (S307) phosphorylation events on insulin receptor substrates (IRS) thereby blocking insulin action. Additionally, transcription factors nuclear factor  $\kappa$ B (NF $\kappa$ B), activator protein (AP) 1 and signal transducer and activator of transcription (Stat) activate inflammatory gene expression thereby enhancing production and secretion of inflammatory markers and mediators. Furthermore, endoplasmic reticulum (ER) stress and intermediates of fatty acid metabolism may activate stress kinases. (Abbreviations: CR:

cytokine receptor, FFA: free fatty acid, FA: fatty acid, IL1R: interleukin-1 receptor, IR: insulin receptor, IRS: insulin receptor substrate, LPS: lipopolysaccharide, TLR: toll-like receptor, TNF: tumor necrosis factor, TNFR: TNF receptor)

This in turn triggers the unfolded protein response (UPR) which enhances the transcription of genes involved in assembly, folding, modification and degradation of proteins to normalize ER function (138). It has been suggested that failure of this adaptive response leads to activation of various cell death effectors such as Bax, Bak and caspases (139-141). Nevertheless, the UPR not only affects gene transcription and pro-apoptotic factors but also activates stress kinases like JNK and expression of pro-inflammatory cytokines via the IKK/NF $\kappa$ B axis which ultimately induces insulin resistance (142-144). A recent study demonstrated that the genetic disruption of x-box protein (XBP) 1, a transcription factor that mediates expression of ER chaperones, leads to increased ER stress, activation of JNK and induction of insulin resistance via serine-phosphorylation of IRS in diet-induced obese mice (138). Furthermore, treatment of diet-induced obese mice with orally active chemical chaperones reverses these effects on ER stress and JNK and improves tissue insulin sensitivity (145). These findings underline the importance of ER stress and inflammatory signals in the development of obesity-induced insulin resistance.

## **1.4 Macrophages**

In general, macrophages belong to the mononuclear phagocyte system which also includes monocytes and their lineage-committed precursors (146). The first step of macrophage development takes place in the bone marrow where myeloid progenitors differentiate into monocytes. Monocytes in turn enter the circulation and give rise to tissue-resident macrophage populations throughout the body (147). Recruitment of monocytes to peripheral tissues and differentiation into macrophages is enhanced by pro-inflammatory, metabolic and immune stimuli (148). Macrophages are classically defined to belong to the innate immune system and, due to their ubiquitous distribution, represent a first line of defense against invading pathogens (149). Their main functions are the maintenance of tissue homeostasis and initiation of the inflammatory response. Furthermore, macrophages harbor pronounced chemotactic and phagocytotic abilities and contribute to tissue remodeling and repair (150). Macrophage dysfunction is associated

with a variety of diabetes-associated diseases such as atherosclerosis, retinopathy, nephropathy, neuropathy and impaired wound healing (151, 152).

#### **1.4.1 The Role of Macrophages in Obesity-induced Insulin Resistance**

In obesity, the adipose tissue is an important initiator of the inflammatory response since it not only serves as a storage depot for excess calories, but is also capable of secreting fatty acids, hormones, cytokines and chemokines which then act in both endocrine and paracrine fashion (153). Although it mainly consists of adipocytes, the adipose tissue also contains preadipocytes, endothelial cells and immune cells which all reside in the stromal vascular fraction. During expansion of the adipose tissue in obesity, local hypoxia occurs due to hypoperfusion with blood vessels. This microhypoxia induces activation of JNK and NF $\kappa$ B signaling cascades and increases inflammatory gene expression, leading to secretion of chemokines and, ultimately, adipocyte death (154). Chemokines that are released into the circulation during these events attract macrophages which then surround dead adipocytes for removal of cell debris and tissue remodeling (155). In addition, these macrophages secrete pro-inflammatory cytokines and chemokines thereby inducing insulin resistance in adjacent adipocytes and recruiting more macrophages from the vascularity to the fat tissue (156).

Accumulation of macrophages in adipose tissue is an important hallmark of adiposity, a condition in which these cells represent 40% of the total adipose cell content in contrast to only 10% in lean counterparts (157). Conditional disruption of pro-inflammatory kinases JNK1 and IKK $\beta$  specifically in myeloid cells protected mice from diet-induced insulin resistance, decreased the inflammatory tone and blocked accumulation of macrophages in adipose tissue in different models of obesity (114, 158). Interestingly, although JNK1 and IKK $\beta$  remained intact in all organs despite immune cells, no effect on adiposity was observed in these studies. Furthermore, conventional disruption of MCP-1, which is an important chemoattractant for immune cells, or its receptor CCR2, prevented the accumulation of macrophages in adipose tissue of obese mice and improved overall insulin sensitivity (159, 160). These studies clearly indicate that systemic inflammation alone can affect insulin sensitivity and that the obesity-associated inflammatory state is mainly mediated through the myeloid compartment of the immune system and infiltration of immune cells into adipose tissue.

### 1.4.2 Adipose Tissue Macrophage Heterogeneity

Macrophages can be divided into at least two subgroups, M1 and M2 (161). M1-cells are defined as "classically activated" macrophages, which are induced by interferon (IFN)  $\gamma$  and LPS. These macrophages secrete pro-inflammatory cytokines (e.g. TNF- $\alpha$ , IL-6, IL-12) and produce high levels of nitric oxide (NO) via inducible nitric oxide synthase (iNOS) expression (162). In addition, they show increased reactivity to fatty acids and LPS. M2-cells or "alternatively activated" macrophages are induced by IL-4 or IL-13 and display a more anti-inflammatory phenotype since they produce high levels of IL-10 and IL-1 decoy receptor and only secrete low levels of pro-inflammatory cytokines. M2 macrophages are generally involved in tissue repair and remodeling (163).

Recently, it has been demonstrated that macrophages invading the adipose tissue of obese animals exhibit a different polarization compared to the cells identified in the adipose tissue of lean animals. Freshly recruited macrophages are positive for surface markers F4/80, CD11b and CD11c and have a pronounced pro-inflammatory profile showing high reactivity to LPS and FFA allocating them to the M1 subgroup (164). In contrast, resident adipose tissue macrophages in lean animals also express F4/80 and CD11b surface markers, but lack CD11c expression almost completely. These cells exhibit an M2/anti-inflammatory profile showing reduced expression of IL-6, iNOS and CCR2 (165). Notably, the obesity-induced switch in the adipose tissue macrophage activation state is not dependent on the conversion of resident M2 macrophages to an M1 phenotype but arises from a localized recruitment of inflammatory macrophage subtypes out of the circulation (166). An important mediator of M1 to M2 polarization of macrophages is the nuclear receptor peroxisome proliferator-activated receptor (PPAR)  $\gamma$  which acts as a lipid sensor (167) and whose conditional disruption in myeloid cells has been shown to impair alternative activation of macrophages and predisposes for obesity-induced insulin resistance and glucose intolerance (168). Activation of PPAR $\gamma$  in macrophages e.g. by treatment with TZDs polarizes towards an M2 phenotype, thus also providing an explanation for the beneficial effect of these compounds on insulin sensitivity in humans (169). Recently, the importance of M1 vs. M2 macrophages in obesity-induced insulin resistance has been demonstrated by Patsouris and colleagues. In this study, ablation of CD11c-positive cells in obese, insulin resistant mice lead to a drastic decrease in inflammatory marker expression and normalized insulin sensitivity to that of lean controls (170).

According to these findings, it is clear that activated macrophages infiltrate the adipose tissue in obesity. However, another important question asks which signals lead to activation of macrophages in this context. Obesity provides an extracellular environment that is enriched with lipids, pro-inflammatory cytokines, chemokines and even gut-derived bacterial compounds which can activate macrophages (171). Among the receptors activated by these signals, TLRs are the most intensively investigated family. Disruption of TLR2 or TLR4 or both prevent the activation of inflammation in macrophages by FFA (172, 173). In addition to FFA, cytokines derived from expanding adipose tissue, ER stress and also microhypoxia, whose central mediator hypoxia inducible factor (HIF) was shown to be crucial for the regulation of macrophage function (174), can activate inflammatory pathways in these cell types.

## 1.5 Macrophages and Insulin

Until now, only few studies have been performed to investigate the effect of insulin itself on macrophage activation and function. Primary monocytes and macrophages express insulin receptors as they were used to study insulin binding affinities and receptor turnover in the 1970s (175-177). The functionality of the insulin receptor on monocytes was demonstrated first when insulin was shown to modulate Fc receptor expression on these cells (178). Furthermore, insulin augments the bacteriocidal properties of macrophages against *Salmonella typhimurium* and enhances their chemotactic activity towards pancreatic  $\beta$ -cell islets *in vitro* (179, 180). Approximately 10 years later, Costa-Rosa and colleagues further investigated insulin's effect on macrophage key functions. They demonstrated that insulin does not affect cell migration, at least in response to thioglycolate and Bacille Calmette-Guérin (BCG), but significantly enhances phagocytosis,  $H_2O_2$  production and glucose metabolism in macrophages (181).

More recent studies demonstrated that insulin induces TNF- $\alpha$  mRNA and protein expression in an ERK-dependent manner and promotes survival in a human monocytic cell-line (182, 183). Moreover, the same cell-line, when exposed to LPS followed by insulin treatment, shows enhanced secretion of TNF- $\alpha$  and IL-1 $\beta$  compared to LPS alone (184). The role of insulin in cell survival was also demonstrated in primary murine macrophages. Treatment with insulin increased protein levels of anti-apoptotic B-cell

lymphoma (Bcl) 2 and induced XBP-1 and 78 kDa glucose response protein (GRP78), which are both involved in the UPR (185).

The concept of insulin's role in macrophage survival was further supported when Han et al. demonstrated that in a mouse model of atherosclerosis, transplantation of bone marrow from insulin receptor-deficient animals into a low density lipoprotein (LDL) receptor-deficient background, leads to advanced lesion formation (186). This was ascribed to increased ER stress and apoptosis in IR-deficient macrophages due to elevated scavenger receptor A (SRA) expression and enhanced uptake of oxidized LDL. Interestingly, our lab demonstrated in a similar study that myeloid cell-autonomous IR-deficiency decreases formation of atherosclerotic plaques in mice (187). Here, IR-deficient primary macrophages displayed unaltered uptake and efflux of cholesterol. Furthermore, IR-deficient macrophages exhibited decreased expression and secretion of IL-6 after stimulation with LPS indicating a reduced inflammatory response in these cells.

Taken together, insulin exerts a variety of effects on macrophage function including survival, phagocytosis, migration and inflammatory gene expression. However, until today, the role of macrophage insulin receptor signaling in obesity-induced insulin resistance remains elusive.

## **1.6 Objectives**

To study the role of insulin signal transduction in macrophages in obesity-induced insulin resistance, mice with a conditional disruption of the insulin receptor specifically in myeloid cells were generated. The aim of this study was to physiologically characterize these animals under normal chow and high fat diet. In addition, we sought to study glucose metabolism in insulin target tissues by euglycemic-hyperinsulinemic clamp analysis. Also, the impact of myeloid cell insulin receptor deficiency on obesity-associated inflammation, both locally and systemically, was to be investigated. Furthermore, we wanted to analyze the action of insulin in primary macrophages in a cell-autonomous fashion in relation to migration/chemotaxis, apoptosis and inflammation.

## 2 Materials and Methods

### 2.1 Chemicals

Size markers for agarose gel electrophoresis (Gene Ruler DNA Ladder Mix) and for SDS-PAGE (Prestained Protein Ladder Mix) were obtained from MBI Fermentas, St. Leon-Rot, Germany. RedTaq DNA Polymerase and 10 x RedTaq buffer were purchased from Sigma-Aldrich, Seelze, Germany.

<b>Chemical</b>	<b>Supplier</b>
$\epsilon$ -aminocaproic acid	Sigma-Aldrich, Seelze, Germany
2-Deoxy-D-[1- <sup>14</sup> C]-Glucose	Amersham, Freiburg, Germany
Acetone	KMF Laborchemie, Lohmar, Germany
Acrylamide	Roth, Karlsruhe, Germany
Agarose (Ultra Pure)	Invitrogen, Karlsruhe, Germany
Amyloglucosidase	Roche, Mannheim, Germany
Aprotinin	Sigma-Aldrich, Seelze, Germany
Benzamidine	Sigma-Aldrich, Seelze, Germany
$\beta$ -Mercaptoethanol ( $\beta$ -ME)	AppliChem, Darmstadt, Germany
Bovine serum albumin (BSA)	Sigma-Aldrich, Seelze, Germany
BSA essentially fatty acid free	Sigma-Aldrich, Seelze, Germany
Bradford reagent	Bio-Rad, München, Germany
Bromphenol blue	Merck, Darmstadt, Germany
Calcein	Invitrogen, Karlsruhe, Germany
Chloroform	Merck, Darmstadt, Germany
D-[3- <sup>3</sup> H]-Glucose	Amersham, Freiburg, Germany
Desoxy-Ribonucleotid-Triphosphates (dNTPs)	Amersham, Freiburg, Germany
Dextran sulfate	AppliChem, Darmstadt, Germany
Dimethylsulfoxide (DMSO)	Merck, Darmstadt, Germany
Dithiothreitol (DTT)	Boehringer, Mannheim, Germany
Enhanced Chemiluminescence (ECL) Kit	Perbio Science, Bonn, Germany
Ethanol, absolute	AppliChem, Darmstadt, Germany
Ethidium bromide	Sigma-Aldrich, Seelze, Germany
Ethylendiamine tetraacetate (EDTA)	AppliChem, Darmstadt, Germany

---

Fetal Calf Serum (FCS)	Gibco BRL, Eggenstein, Germany
Gelatine	Sigma-Aldrich, Seelze, Germany
Glacial acetic acid	Roth, Karlsruhe, Germany
Glucose	DeltaSelect, Pfullingen, Germany
Glycerol	Serva, Heidelberg, Germany
Hydrochloric acid (37 %)	KMF Laborchemie, Lohmar, Germany
Insulin	Novo Nordisk, Bagsværd, Denmark
Isopropanol	Roth, Karlsruhe, Germany
Ladderman™ DNA Labeling Kit	Cambrex Bio Science, Verviers, Belgium
Leptin	Sigma-Aldrich, Seelze, Germany
Lipopolysaccharide (LPS)	Sigma-Aldrich, Seelze, Germany
MCP-1	Sigma-Aldrich, Seelze, Germany
Methanol	Roth, Karlsruhe, Germany
Non-essential amino acids	Gibco BRL, Eggenstein, Germany
Palmitate	Sigma-Aldrich, Seelze, Germany
Penicillin/Streptomycin Solution	Gibco BRL, Eggenstein, Germany
Phenol-Chloroform-Isoamyl alcohol	AppliChem, Darmstadt, Germany
Phenylmethylsulfonylfluoride (PMSF)	Sigma-Aldrich, Seelze, Germany
Phosphate buffered saline (PBS)	Gibco BRL, Eggenstein, Germany
Potassium hydroxide	Merck, Darmstadt, Germany
Proteinase K	Roche, Mannheim, Germany
RPMI 1640	Gibco BRL, Eggenstein, Germany
Salmon sperm DNA	Sigma-Aldrich, Seelze, Germany
Sodium acetate	AppliChem, Darmstadt, Germany
Sodium chloride	AppliChem, Darmstadt, Germany
Sodium dodecyl sulfate	AppliChem, Darmstadt, Germany
Sodium hydroxide	AppliChem, Darmstadt, Germany
Sodium fluoride	Merck, Darmstadt, Germany
Sodium orthovanadate	Sigma-Aldrich, Seelze, Germany
Sodium pyruvate	Gibco BRL, Eggenstein, Germany
Sucrose	AppliChem, Darmstadt, Germany
Tetramethylethylenediamine	Sigma-Aldrich, Seelze, Germany
Thioglycollate	Sigma-Aldrich, Seelze, Germany
Tramadolehydrochloride	Grünenthal GmbH, Stolberg, Germany
Avertin	Sigma-Aldrich, Seelze, Germany

---

Trishydroxymethylaminomethane	AppliChem, Darmstadt, Germany
Triton X-100	Appllichem, Darmstadt, Germany
Tween 20	Appllichem, Darmstadt, Germany
Western Blocking Reagent	Roche, Mannheim, Germany

---

**Table 1: Chemicals**

## 2.2 Molecular Biology

Standard methods of molecular biology were performed according to Sambrook and Russell (1989), unless stated otherwise.

### 2.2.1 Isolation of Genomic DNA

Mouse tail biopsies were incubated 2-3 hours (h) in lysis buffer (100 mM Tris-HCl (pH 8.5), 5 mM EDTA, 0.2% (w/v) SDS, 0.2 M NaCl, 500 µg/ml proteinase K) in a thermomixer (Eppendorf, Hamburg, Germany) at 56°C. Peritoneal macrophages were incubated in lysis buffer at 56°C overnight. Precipitation was performed by addition of one equivalent of isopropanol. After centrifugation and a single washing step with 70% (v/v) ethanol, the DNA pellet was dried at room temperature (RT) for 30 minutes and resuspended in double distilled water (ddH<sub>2</sub>O).

For Southern blot analysis, 100 mg of murine tissue were digested in lysis buffer containing 1 g/ml of proteinase K overnight in a thermomixer at 56°C. Samples were centrifuged to discard debris and an equal volume of phenol-chloroform-isoamyl alcohol mixture ((v/v/v) 25:24:1, saturated with 100 mM Tris (pH 8.0)) was added to the supernatant. Following centrifugation, the aqueous phase was transferred to a fresh vial and mixed with an equivalent of chloroform. After centrifugation, DNA was precipitated from the supernatant as described above and resuspended in TE buffer (10 mM Tris-HCl (pH 8), 1 mM EDTA) containing 50 µg/ml RNaseI.

### 2.2.2 Southern Blot Analysis

10 µg of phenol-chloroform-extracted DNA were digested overnight at 37°C, with 50 U of NcoI restriction enzyme (MBI Fermentas GmbH, St. Leon-Rot, Germany), and separated electrophoretically on a 0.8% (w/v) agarose gel at 60 V. The DNA was subsequently transferred to a Hybond<sup>TM</sup>-N+ nylon membrane (Amersham, Braunschweig, Germany) by an alkaline capillary transfer (189) and crosslinked to the membrane by baking at 80°C for 20 min. A probe was PCR-amplified using customized primers (Table 2) and labelled with [<sup>32</sup>P]-dCTP using the Ladderman<sup>TM</sup> DNA Labeling Kit (TaKaRa; Cambrex Bio Science, Verviers, Belgium). Membranes were equilibrated in 2 x SSC and then prehybridized at 65°C for 4 h in hybridization solution (1 M NaCl, 1% (w/v) SDS, 10% (w/v) dextran sulfate, 50 mM Tris-HCl (pH 7.5), 250 µg/ml sonicated salmon sperm DNA). The radioactively labelled probe was then added to the prehybridization solution. Hybridization of the probe to its corresponding sequence on the nylon membrane was performed overnight at 68°C in a rotating cylinder. Unspecifically bound probe was removed by washing the membrane initially with 2 x SSC / 0.1 % (w/v) SDS, followed by 1 x SSC / 0.1% (w/v) SDS, if necessary. All washes were performed at 68°C under gentle shaking for 10-20 min. After each wash, the membrane was monitored with a Geiger counter and the washes were stopped when radioactivity reached 50 to 200 cps. The membrane was then sealed in a plastic bag and exposed to X-ray film (Kodak XAR-5 or BioMAX MS; Eastman Kodak) at -80°C. Films were developed in an automatic developer (Agfa, Köln, Germany).

Probe	Primer	Sequence (5'-3')	Orientation
IR	<i>NcoI5'</i>	CCATGGGTCCATAACCTATC	sense
IR	<i>NcoI3'</i>	AGTGATGAGATGGCTCATTAG	antisense

**Table 2: Oligonucleotides used to amplify the southern blot probe**

All primer sequences are displayed in 5'-3' order. Primer orientation is designated "sense" when coinciding with transcriptional direction. All primers were purchased from Eurogentec, Cologne, Germany.

### 2.2.3 Quantification of Nucleic Acids

Nucleic acid concentration was assessed by measuring the sample absorption at 260 nm with a NanoDrop® ND-1000 UV-Vis Spectrophotometer (Peqlab, Erlangen, Germany). An optical density of 1 corresponds to approximately 50 µg/ml of double-stranded DNA, 40 µg/ml of RNA and 33 µg/ml of ssDNA. The 260/280 nm absorbance ratio was used as a measure of purity for nucleic acid samples. A ratio of ~1,8 was accepted as pure DNA and a ratio of ~2,0 as pure RNA.

### 2.2.4 Polymerase Chain Reaction (PCR)

The PCR method (190, 191) was used to genotype mice for the presence of floxed alleles or transgenes with customized primers listed in Table 2. Reactions were performed in a Thermocycler iCycler PCR machine (Bio-Rad, München, Germany) or in a Peltier Thermal Cycler PTC-200 (MJ Research, Waltham, USA). All amplifications were performed in a total reaction volume of 25 µl, containing a minimum of 50 ng template DNA, 25 pmol of each primer, 25 µM dNTP Mix, 10 x RedTaq reaction buffer and 1 unit of RedTaq DNA Polymerase. Standard PCR programs started with 4 minutes (192) denaturation at 95°C, followed by 30 cycles consisting of denaturation at 95°C for 45 seconds (sec), annealing at oligonucleotide-specific temperatures for 30 sec and elongation at 72°C for 30 sec and a final elongation step at 72°C for 7 min. PCR-amplified DNA fragments were applied to 1% - 2% (w/v) agarose gels (1 x TAE, 0.5 mg/ml ethidium bromide) and electrophoresed at 120 V.

Primer	Sequence (5'-3')	T <sub>Annealing</sub> [°C]	Orientation
<i>LysMCre5'</i>	CTC TAG TCA GCC AGC AGC TG	59	sense
<i>LysMCre3'</i>	ATG TTT AGC TGG CCC AAA TGT	59	antisense
<i>IR5'</i>	GAT GTG CAC CCC ATG TCT G	58	sense
<i>IR3'</i>	CTG AAT AGC TGA GAC CAC AG	58	antisense
<i>IRA</i>	GGG TAG GAA ACA GGA TGG	58	sense

**Table 3: Oligonucleotides used for genotyping**

All primer sequences are displayed in 5'-3' order. Primer orientation is designated "sense" when coinciding with transcriptional direction. All primers were purchased from Eurogentec, Cologne, Germany.

### 2.2.5 RNA Extraction, RT-PCR and Quantitative Realtime PCR

Total RNA from murine cells and tissues was extracted using the Qiagen RNeasy Kit (Qiagen, Hilden, Germany). 1 µg of each RNA sample was reversely transcribed using the Eurogentec RT Kit (Eurogentec, Cologne, Germany) according to manufacturer's instructions. The cDNA was subsequently amplified using an ABI Prism 7900HT Fast Real-time PCR System (Applied Biosystems, Foster City, USA).

Probe	Catalogue N°
Adiponectin	Mm00456425_m1
Bax	Mm00432050_m1
Bcl-2	Mm00477631_m1
CCl2	Mm00441242_m1
CCl3	Mm00441258_m1
F4/80	Mm00802530_m1
Gusb	Mm00446953_m1
Hprt1	Mm00446968_m1
IL-6	Mm00446190_m1
Insr	Mm00439693_m1
Leptin	Mm00434759_m1
Mac-2	Mm00802901_m1
TNF-α	Mm00443258_m1

**Table 4: Taqman Gene Expression Assays**

All assays were purchased from Applied Biosystems, Foster City, USA.

Relative expression of Adiponectin, CCl-2, CCl-3, F4/80, Leptin, Mac-1, Mac-2 and TNF-α mRNA was determined using standard curves based on white adipose tissue cDNA. Samples were adjusted for total cDNA content by Glucuronidase beta (Gusb) and hypoxanthine guanine phosphoribosyl transferase (Hprt-) 1 mRNA quantitative Realtime PCR. Calculations were performed by a comparative method ( $2^{-\Delta\Delta CT}$ ). In brief, the amplification plot is the plot of fluorescence versus PCR number. The threshold cycle value (Ct) is the fractional PCR cycle number at which the fluorescent signal reached the

detection threshold. Therefore, the input cDNA copy number and Ct are inversely related. Data were analyzed with the Sequence Detector System (SDS) software version 2.1 (ABI) and Ct value was automatically converted to fold change RQ value ( $(RQ) = 2^{-\Delta\Delta CT}$ ). The RQ values from each gene were then used to compare the gene expression across all groups.

### 2.2.6 Protein Extraction

Cell pellets or snap-frozen tissues were disrupted in lysis buffer (50 mM HEPES (pH 7.4), 1% (v/v) Triton X-100, 0.1 M sodium fluoride, 10 mM EDTA, 50 mM sodium chloride, 10 mM sodium orthovanadate, 0.1% (w/v) SDS, 10 µg/ml aprotinin, 2 mM benzamide, 2 mM phenylmethylsulfonyl fluoride (PMSF)) by resuspension and gentle vortexing or by usage of a polytron homogenizer (IKA Werke, Staufen, Germany), respectively. Particulate matter was removed by centrifugation for 1 h at 4°C. The supernatant was transferred to a fresh vial and protein concentration was determined using a Bradford assay. Protein extracts were diluted to 5 mg/ml with lysis buffer and 4 x SDS sample buffer (125 mM Tris-HCl (pH 6.8), 5% (w/v) SDS, 43.5% (w/v) glycerol, 100 mM DTT, and 0.02% (v/v) bromophenol blue), incubated at 95°C over 5 min and stored at -80°C.

### 2.2.7 SAPK/JNK Kinase Assay

A c-Jun fusion protein linked to agarose beads (SAPK/JNK Kinase assay #9810; Cell Signaling, Danvers, MA, USA) was used to pull down SAPK/JNK enzyme from liver and skeletal muscle protein extracts. Immunoprecipitation was performed by overnight incubation at 4°C. After two washes with lysis buffer and kinase buffer, 200 µM ATP was supplemented to the precipitate. The phosphorylation reaction was carried out at 30°C and stopped after 30 min by addition of 4 x SDS sample buffer. Detection of phospho-c-Jun by western blot analysis was used to measure SAPK activity.

## 2.2.8 Western Blot Analysis

Frozen protein extracts were thawed at 95°C for 5 min, then separated on 10-15% (v/v) SDS polyacrylamide gels (193) and blotted onto PVDF membranes (Bio-Rad, München, Germany). Membranes were then incubated with 1% (v/v) blocking reagent (Roche, Mannheim, Germany) for 1 h at RT. Subsequently, primary antibodies (Table 5) diluted in 0.5% (v/v) blocking solution were applied overnight at 4°C. PVDF membranes were then washed four times for 5 min with 1 x TBS/0.01 (v/v) Tween. After 1 h incubation at RT with the respective secondary antibodies, membranes were washed 4 times for 10 min with 1 x TBS/0.01 (v/v) Tween, rinsed in 1 x TBS, incubated for 1 min in Pierce ECL Western Blotting Substrate (Perbio Science, Bonn, Germany), sealed in a plastic bag and exposed to chemiluminescence film (Amersham, Braunschweig, Germany). Films were developed in an automatic developer.

Antibody	Catalogue N°	Distributor	Dilution
Actin	A5441	Sigma Aldrich, Seelze, Germany	1:10000
Akt	9272	Cell Signaling, Danvers, MA, USA	1:1000
p-Akt (Ser473)	9271	Cell Signaling, Danvers, MA, USA	1:1000
p-c-jun (Ser63)	9810 (101)	Cell Signaling, Danvers, MA, USA	1:1000
IRβ (C-19)	sc-711	Santa Cruz, Heidelberg, Germany	1:200
SAPK/JNK	9252	Cell Signaling, Danvers, MA, USA	1:1000

**Table 5: Primary antibodies used for western blot analysis**

All respective secondary antibodies were purchased from Sigma Aldrich, Seelze, Germany, and used in a 1:1000 dilution.

## 2.2.9 Gelatin Zymography

Cell culture supernatants were purified from lower molecular weight proteins (<50 kDa) by centrifugation through Microcon<sup>®</sup> YM-50 Centrifugal Filter Units (# 42415, Millipore, Billerica, MA, USA) for 10 minutes at RT. After determination of the protein concentration by a Bradford assay, 10 µg total protein were diluted with 4xSDS sample buffer (100 mM Tris, 10% (v/v) glycerol, 0.5% (w/v) SDS, 0.05% (w/v) bromophenol

blue) and separated on a 10% (v/v) SDS polyacrylamide gel (containing 0.1 mg/ml (w/v) gelatine) at 20 mA with 1xSDS running buffer (3 g/l (w/v) Tris base, 14.4 g/l (w/v) glycine, 1 g/l (w/v) SDS, pH 8.3). Subsequently, the gel was soaked in 2.5% (v/v) Triton X-100 for 1h at RT. After three fast washing steps with ddH<sub>2</sub>O, the gel was transferred to MMP activation buffer (50 mM Tris-HCl, 5 mM CaCl<sub>2</sub>, pH 8) and incubated at 37°C overnight in a humidified chamber to carry out the digestion reaction. Following three 5 min washes with ddH<sub>2</sub>O, the gel was stained with 2.5 g/l (w/v) Coomassie brilliant-blue R-250 for 1 h at RT. Levels of gelatinolytic activity were revealed by destaining with 40% (v/v) methanol until the bands appeared clearly, then the gel was wrapped in plastic foil and scanned on a Canon Canoscan 8800F.

### **2.2.10 ELISA**

Mouse insulin (Mouse/Rat Insulin ELISA; Crystal Chem, Downers Grove, IL, USA), leptin (ACTIVE<sup>®</sup> Murine Leptin ELISA; Diagnostics Systems Laboratories, Webster, TX, USA), TNF- $\alpha$  (Quantikine Mouse TNF-alpha/TNFSF1A ELISA; R&D Systems, Wiesbaden, Germany), IL-6 (Quantikine Mouse IL-6 ELISA; R&D Systems, Wiesbaden, Germany), adiponectin (Quantikine Mouse Adiponectin/Acrp30 ELISA; R&D Systems, Wiesbaden, Germany) and MMP-9 (Quantikine Mouse MMP-9 (total) ELISA; R&D Systems, Wiesbaden, Germany) concentration in serum or cell culture supernatant was determined using mouse standards according to manufacturer's guidelines and measured on a Precision Microplate Reader (Emax; Molecular Devices GmbH, München, Germany).

## 2.3 Cell Culture and Tissue Analysis

### 2.3.1 Preparation of L-cell Conditioned Medium

L929 fibroblasts were seeded on 175 cm<sup>2</sup> tissue culture flasks in 50 ml DMEM (supplemented with 10% (v/v) heat inactivated FCS, 1% (v/v) glutamine, 1% (v/v) penicillin-streptomycin). After confluency was reached, 50 ml fresh medium was added to the flasks and cells were incubated without further medium exchange for 14 days at 37°C and 5% CO<sub>2</sub>. At the end of the incubation period, medium from different flask was pooled, sterile-filtered through a 0.22 µm membrane and aliquoted to 50 ml Falcon tubes. L-cell conditioned medium (LCM) was stored at -80°C until use.

### 2.3.2 Preparation of Palmitic Acid Media

Preparation of 20% BSA: Essentially fatty acid free bovine serum albumin (20% (w/v) BSA, # A6003, Sigma-Aldrich, Seelze, Germany) was layered on top of PBS and allowed to percolate overnight at 4°C without stirring. After sterile filtering into aliquots, fatty acid free BSA was stored at 4°C until the experiment.

Preparation of 20 mM palmitic acid: Palmitic acid solution was prepared freshly before each experiment. 15 ml NaOH (0,01 N) were warmed to 70°C. Subsequently, 84 mg palmitic acid (# P5585, Sigma-Aldrich, Seelze, Germany) were added and incubated for 20-30 min at 70°C. During the incubation period, 50-100 µl aliquots of 1 N NaOH were added and the mixture was vortexed several times until the solution cleared.

Preparation of palmitic acid medium: Complexing was performed immediately after palmitic acid was dissolved completely. 0.5 ml of 20 mM palmitic acid solution were added to 1.65 ml prewarmed (37°) 20% fatty acid free BSA by vortexing at lowest speed without introducing any bubbles. Complexes were added immediately to 17.85 ml of prewarmed (37°C) RPMI 1640 (supplemented 1% (v/v) glutamine and 1% (v/v) penicillin-streptomycin). Palmitic acid medium (500 µM palmitic acid, 250 µM BSA) was then filter sterilized through a 0.22 µm membrane and stored at 4°C for up to one week.

### 2.3.3 Differentiation of Murine Bone Marrow to Macrophages

Bone marrow cells were plated at a concentration of  $1-2 \times 10^6$  cells/ml in RPMI 1640 (Invitrogen GmbH, Karlsruhe, Germany; supplemented with 10% (v/v) heat inactivated FCS, 1% (v/v) glutamine, 1% (v/v) penicillin-streptomycin and 10% (v/v) LCM) on 15 cm bacterial petridishes. After 6-8 days, medium was renewed followed by further incubation until day 10. Adherent cells were removed from the plates with TrypLE™ Express (Gibco BRL, Eggenstein, Germany), counted and seeded for further experiments in RPMI 1640 with LCM. Preceding all the experiments, cells were washed two times with sterile PBS and, if stimulated with insulin, serum-starved for 16-20 h.

### 2.3.4 Culture of Primary Murine Macrophages

Cells were plated at a density of  $1 \times 10^6$ /ml on tissue culture dishes (Greiner Bio-One GmbH, Frickenhausen, Germany) in RPMI 1640 (supplemented with 10% (v/v) heat inactivated FCS, 1% (v/v) glutamine, 1% (v/v) penicillin-streptomycin) and were allowed to adhere overnight at 37°C, 5% CO<sub>2</sub> and 95% humidity. On the next day, adherent cells were washed once with PBS followed by further incubation in RPMI 1640. Preceding all the experiments, cells were washed two times with sterile PBS and, if stimulated with insulin, serum-starved for 16-20 h.

### 2.3.5 Detection of Apoptotic Cells by TUNEL Assay

For assessment of apoptosis in primary macrophages, the DeadEnd™ Fluorometric TUNEL system (# G3250, Promega Corporation, Madison, WI, USA) was used. The protocol for adherent cells was carried out according to the manufacturer's instructions. Initially, cells were grown directly on glass cover slips in 6-well tissue culture dishes. After a 24 h stimulation period, cells were fixed by incubation in 4% (w/v) paraformaldehyde (PFA) for 20 min at 4°C. After two washing steps with PBS, cells were permeabilized with 0.2% (v/v) Triton X-100 in PBS for 5 min at RT. Following two additional washing steps with PBS, equilibration buffer was added to the slides and incubated for 10 min at RT. After removal of equilibration buffer, incorporation of fluorescein-12-dUTP by rTdT enzyme was carried out at 37°C in the dark for 60 min. The

reaction was stopped by addition of 2x SSC and after three washing steps with PBS, slides were mounted with Vectashield DAPI medium (# H-1200, Vector Laboratories Inc, Burlingame, CA, USA) and analyzed under a fluorescence microscope. Quantification of DAPI- and FITC-positive cells was performed using AxioVision 4.2 (Carl Zeiss MicroImaging GmbH, Oberkochen, Germany).

### 2.3.6 Boyden Chamber Analysis

General design: In a Boyden Chamber, two compartments are separated by a porous membrane through which cells can migrate (Fig. 5). Chemotactic gradients can be set up by placing different concentrations of the putative chemoattractant in the upper and lower chambers. The use of this chamber requires that the cells under test have to move in three dimensions and are able to squeeze through the pores (5-10  $\mu\text{m}$  diameters) of the particular filter. The Boyden chamber is reproducible and the chemokinetic, chemotactic response easy to quantify.

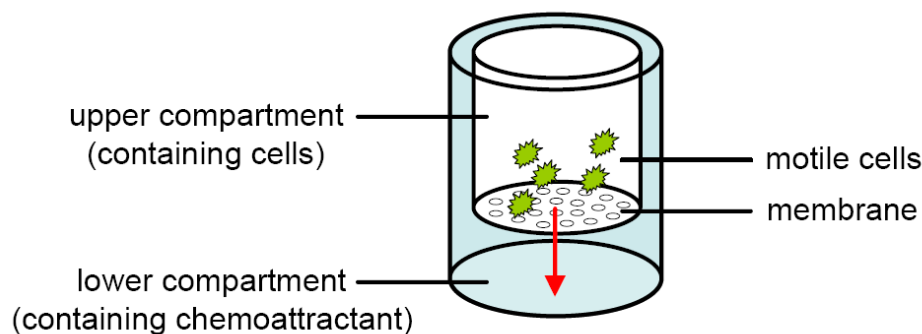


**Fig. 5: Experimental design of the Boyden Chamber Analysis.**

Two isolated compartments are separated by a porous membrane (pore size dependent on cell type). The lower compartment contains medium substituted with a chemoattractant (e.g. MCP-1). The medium in the upper compartment is the same as in the lower compartment but lacks the chemoattractant. Motile cells are placed into the upper compartment and migrate against (arrow) the concentration gradient into the lower compartment.

Experimental setup: A ChemoTx<sup>®</sup> Chemotaxis System ( Neuro Probe Inc., Gaithersburg, MD, USA) comprised of a 96-well inner plate coated with a partially hydrophobic polycarbon filter (pore size 5  $\mu\text{m}$ ; upper compartment) and a base plate (lower compartment). The cell suspension can be loaded directly onto the membrane.

Preparation of cells: The chemotaxis assay was carried out with bone marrow-derived macrophages of control and IR<sup>Δmyel</sup> mice. Macrophages were lifted from the culture dish by gentle scraping. After two washing steps with PBS, cells were incubated in 2 ml of PBS (supplemented with 3μM Calcein, Molecular Probes/Invitrogen Corp., Karlsruhe, Germany) for 20 min at 37°C. Following two additional washing steps with PBS, cells were resuspended in incubation buffer (RPMI 1640 supplemented with 10% (v/v) heat inactivated FCS, 1% (v/v) glutamine) and cell number was adjusted to 5x10<sup>6</sup> cells/ml.

Assay procedure and analysis: The chemoattractant was dissolved in incubation buffer and added to the lower compartments in the desired concentration. Incubation buffer without chemoattractant was used as a negative control (random migration). 29 μl of the cell suspension were loaded onto the membrane and chemotaxis was carried out at 37°C in a humidified chamber. After a migration period of 120 min, the inner plate was removed and cells on the upper surface of the filter were detached with a rubber scraper. Green fluorescence of adherent cells on the lower surface was detected with a Cytofluor analyser (Filter: excitation 485 nm, emission 530 nm; Global Medical Instrumentation Inc., Ramsey, MN, USA). Data was collected in triplicates for three independent experiments.

### **2.3.7 Histological Analysis and Immunohistochemistry**

White adipose tissue of diet-induced obese Control and IR<sup>Δmyel</sup> mice was dissected, fixed overnight in 4% (w/v) PFA and then embedded for paraffin sections. Subsequently, 7 μm thin sections were deparaffinized and stained with hematoxylin and eosin (H&E) for general histology or with Mac-2/Galectin-3 antibody (#CL8942AP; Cedarlane Laboratories Ltd, Burlington, ON, Canada) for detection of adipose tissue macrophages. Immunohistochemistry was performed as previously described (155). Quantification of adipocyte size and Mac-2-positive area was performed using AxioVision 4.2 (Carl Zeiss MicroImaging GmbH, Oberkochen, Germany).

## 2.4 Mouse Experiments

General animal handling was performed as described by Hogan (194) and Silver (195).

### 2.4.1 Animals

Mice were housed in a virus-free facility at 22-24°C on a 12 h light/ 12 h dark cycle with the light on at 6 a.m. and were either fed a normal chow diet (NCD; Teklad Global Rodent 2018; Harlan Winkelmann GmbH, Borchon, Germany) containing 53.5% (w/v) carbohydrates, 18.5% (w/v) protein and 5.5% (w/v) fat or a high fat diet (HFD; C1057; Altromin GmbH, Lage, Germany) containing 32.7% (w/v) carbohydrates, 20% (w/v) protein, and 35.5% (w/v) fat (55.2% of calories from fat). All animals had access to water *ad libitum*. Food was only withdrawn if required for an experiment. At the end of the study period, animals were sacrificed by CO<sub>2</sub> anesthesia or cervical dislocation. All animal procedures and euthanasia were reviewed by the animal care committee of the University of Cologne, approved by local government authorities (Bezirksregierung Köln) and were in accordance with National Institutes of Health guidelines.

### 2.4.2 IR<sup>Δmyel</sup> mice

To disrupt the insulin receptor allele specifically in myeloid cells, mice homozygous for the loxP-flanked insulin receptor allele (IR<sup>flox/flox</sup>) (196) were bred with mice homozygous for the LysMCre transgene (197). LysMCre<sup>+/-</sup>IR<sup>flox/wt</sup> mice were further crossed with IR<sup>flox/flox</sup> mice to achieve homozygosity for the loxP-flanked allele. Breeding colonies were maintained by mating IR<sup>flox/flox</sup> (30) mice and LysMCre <sup>+/-</sup>IR<sup>flox/flox</sup> mice (IR<sup>Δmyel</sup>). All metabolic experiments were carried out with male mice backcrossed for at least 10 generations onto a C57BL/6 background.

### **2.4.3 Body Weight and Blood Glucose Levels**

Body weight and blood glucose levels were monitored weekly and at 20 weeks of age, respectively. Blood glucose values were determined from whole venous blood using an automatic glucose monitor (GlucoMen<sup>®</sup> GlycÓ; A. Menarini Diagnostics, Neuss, Germany).

### **2.4.4 Glucose and Insulin Tolerance Test**

Glucose tolerance tests (GTT) were performed on animals that had been fasted overnight for 16 hours. Insulin tolerance tests (ITT) were performed on random fed mice. Animals were injected with either 2 g/kg body weight of glucose or 0.75 U/kg body weight of human regular insulin into the peritoneal cavity. Glucose levels were determined in blood collected from the tail tip immediately before and 15, 30 and 60 minutes after the injection, with an additional value determined after 120 minutes for the GTT.

### **2.4.5 Isolation of Adipocytes and Stromal Vascular Fraction**

Animals were sacrificed and subcutaneous and epididymal fat pads were removed under sterile conditions. Adipocytes were isolated by collagenase (1 mg/ml) digestion for 45 min at 37°C in DMEM/Ham's F-12 1:1 (DMEM/F12) containing 0.1% (w/v) BSA. Digested tissues were filtered through sterile 150 µm nylon mesh and centrifuged at 250 x g for 5 min. The floating fraction consisting of pure isolated adipocytes was then removed and washed three more times before proceeding to experiments. The pellet, representing the stromal vascular fraction containing preadipocytes, macrophages and other cell types, was resuspended in erythrocyte lysis buffer consisting of 154 mM NH<sub>4</sub>Cl, 10 mM KHCO<sub>3</sub>, and 0.1 mM EDTA for 10 min.

### 2.4.6 Isolation of Primary Peritoneal Macrophages

8-20 week old IR<sup>Δmyel</sup> mice or control mice were injected intraperitoneally with 2 ml thioglycollate medium (4% in PBS (w/v)) to induce a sterile peritonitis. On day 4 *post* injection, the animals were sacrificed by CO<sub>2</sub> anesthesia and cells were collected by peritoneal lavage with sterile PBS. Following centrifugation, cells were resuspended in erythrocyte lysis buffer for 3 min at RT. After one additional wash with PBS, cells were resuspended in RPMI 1640 (supplemented with 10% (v/v) heat inactivated FCS, 1% (v/v) glutamine, 1% (v/v) penicillin-streptomycin) and live cells were counted in 4% (w/v) trypan blue. Cell numbers were adjusted to 1\*10<sup>6</sup>/ml and stored on ice for further experiments.

### 2.4.7 Isolation of Murine Bone Marrow

8-20 week old mice were sacrificed by CO<sub>2</sub> anesthesia, rinsed in 70% (v/v) ethanol and femurs and tibias were dissected. After removal of all muscle tissue, bones were cut at the ends and bone marrow was flushed with a 26 G needle in sterile, ice-cold PBS. After dispersion and resuspension with the same needle, cells were spun down at 1.200 rpm for 5 min at 4°C. Cells were resuspended in erythrocyte lysis buffer and incubated for 3 min at RT. After one additional wash with PBS, cells were resuspended in RPMI 1640 (supplemented with 10% (v/v) heat inactivated FCS, 1% (v/v) glutamine, 1% (v/v) penicillin-streptomycin and 10% (v/v) LCM) and live cells were counted in 4% (w/v) trypan blue. Cell numbers were adjusted to 1\*10<sup>6</sup>/ml and stored on ice for further experiments.

### 2.4.8 Glucose Transport

For the determination of glucose transport, isolated adipocytes from the fat depots were stimulated with 0.1, 1, 10 and 100 nM insulin for 30 min then incubated for 30 min with 3 μM U-<sup>14</sup>C-glucose. Immediately after incubation, adipocytes were fixed with osmic acid, incubated for 48 hours at 37°C and radioactivity was quantified after the cells had been decolorized (198).

### 2.4.9 Hyperinsulinemic-euglycemic Clamp Studies

**Catheter Implantation:** At the age of 16-20 weeks, male mice were anesthetized by intraperitoneal injection of avertin and adequacy of the anesthesia was ensured by the loss of pedal reflexes. A Micro-Renathane catheter (MRE 025; Braintree Scientific Inc., MA, USA) was inserted into the right internal jugular vein, advanced to the level of the superior vena cava, and secured in its position in the proximal part of the vein with 4-0 silk; the distal part of the vein was occluded with 4-0 silk. After irrigation with physiological saline solution, the catheter was filled with heparin solution and sealed at its distal end. The catheter was subcutaneously tunneled, thereby forming a subcutaneous loop, and exteriorized at the back of the neck. Cutaneous incisions were closed with a 3-0 silk suture and the free end of the catheter was attached to the suture in the neck as to permit the retrieval of the catheter on the day of the experiment. Mice were intraperitoneally injected with 1 ml of saline containing 15 $\mu$ g/g body weight of tramadolhydrochloride and placed on a heating pad in order to facilitate recovery.

**Clamp Experiment:** Only mice that had regained at least 90% of their preoperative body weight after 6 days of recovery were included in the experimental groups. After starvation for 15 hours, awake animals were placed in restrainers for the duration of the clamp experiment. After a D-[3-<sup>3</sup>H]Glucose (Amersham Biosciences, UK) tracer solution bolus infusion (5  $\mu$ Ci), the tracer was infused continuously (0.05  $\mu$ Ci/min) for the duration of the experiment. At the end of the 40-minute basal period, a blood sample (50  $\mu$ l) was collected for determination of the basal parameters. To minimize blood loss, red blood cells were collected by centrifugation and reinfused after being resuspended in saline. Insulin (human regular insulin; NovoNordisc Pharmaceuticals, Inc., NJ, USA) solution containing 0.1% (w/v) BSA (Sigma-Aldrich, Germany) was infused at a fixed rate (4  $\mu$ U/g/min) following a bolus infusion (40  $\mu$ U/g). Blood glucose levels were determined every 10 minutes (B-Glucose Analyzer; Hemocue AB, Sweden) and physiological blood glucose levels (between 120 and 150 mg/dl) were maintained by adjusting a 20% glucose infusion (DeltaSelect, Germany). Approximately 60 minutes before steady state was achieved, a bolus of 2-Deoxy-D-[1-<sup>14</sup>C]Glucose (10  $\mu$ Ci, Amersham) was infused. Steady state was ascertained when glucose measurements were constant for at least 30 min at a fixed glucose infusion rate and was achieved within 100 to 130 min. During the clamp experiment, blood samples (5  $\mu$ l) were collected after the infusion of the 2-Deoxy-D-[1-<sup>14</sup>C]Glucose at the time points 0, 5, 15, 25, 35 min etc. until reaching the steady state. During the steady state, blood samples (50  $\mu$ l) for the measurement of steady state

parameters were collected. At the end of the experiment, mice were killed by cervical dislocation, and brain, liver, WAT and skeletal muscle tissue were dissected and stored at -20°C.

Assays: Plasma [3-<sup>3</sup>H]Glucose radioactivity of basal and steady state samples was determined directly after deproteinization with 0.3 M Ba(OH)<sub>2</sub> and 0.3 M ZnSO<sub>4</sub> and also after removal of <sup>3</sup>H<sub>2</sub>O by evaporation, using a liquid scintillation counter (Beckmann, Germany). Plasma Deoxy-[1-<sup>14</sup>C] Glucose radioactivity was directly measured in the liquid scintillation counter. Tissue lysates were processed through Ion exchange chromatography columns (Poly-Prep<sup>R</sup> Prefilled Chromatography Columns, AG<sup>R</sup>1-X8 formate resin, 200-400 mesh dry; Bio Rad Laboratories, CA, USA) to separate 2-Deoxy-D-[1-<sup>14</sup>C]Glucose (2DG) from 2-Deoxy-D-[1-<sup>14</sup>C]Glucose-6-Phosphate (2DG6P).

Calculations: Glucose turnover rate ( $\text{mg} \times \text{kg}^{-1} \times \text{min}^{-1}$ ) was calculated as the rate of tracer infusion (dpm/min) divided by the plasma glucose-specific activity (dpm/mg) corrected for body weight. HGP ( $\text{mg} \times \text{kg}^{-1} \times \text{min}^{-1}$ ) was calculated as the difference between the rate of glucose appearance and glucose infusion rate. In vivo glucose uptake for each tissue ( $\text{nmol} \times \text{g}^{-1} \times \text{min}^{-1}$ ) was calculated based on the accumulation of 2DG6P in the respective tissue and the disappearance rate of 2DG from plasma as described previously (199).

## **2.5 Computer Analysis**

### **2.5.1 Densitometrical Analysis**

Protein expression was assessed by western blot analysis and bands were measured in intensity per mm<sup>2</sup> using the Quantity One Software (Bio-Rad, München, Germany). After background subtraction, each sample was normalized to an internal loading control. Average protein expression of control mice was set to 100% and compared to protein expression of knockout animals unless stated otherwise.

### **2.5.2 Statistical Methods**

Data sets were analyzed for statistical significance using a two-tailed unpaired student's t test. All *p* values below 0.05 were considered significant.

### 3 Results

#### 3.1 Myeloid Cell-specific Disruption of the Insulin Receptor

The lysozyme M gene is expressed specifically in cells of the myeloid lineage (200). Crossing mice carrying a loxP-flanked allele with mice containing a targeted insertion of the *cre* cDNA into the endogenous lysozyme M locus has been shown to promote efficient disruption of loxP-flanked alleles in these cell types (201). Clausen et al. reported a deletion-efficiency of 83-98% in mature macrophages and of 100% in granulocytes.

To disrupt the insulin receptor allele specifically in myeloid cells ( $IR^{\Delta myel}$ ), mice homozygous for the loxP-flanked insulin receptor allele ( $IR^{lox/lox}$ ) and heterozygous for a Cre recombinase under the control of the lysozyme M promoter (LysMCre) were generated.

To analyze recombination of the loxP-flanked fourth exon of the insulin receptor allele, bone marrow of control mice and  $IR^{\Delta myel}$  mice was first isolated and differentiated *in vitro* into macrophages. Southern blot analysis was performed with genomic DNA from the resulting cell population. As shown in Fig. 6, transgenic expression of the Cre cDNA under the control of the lysozyme M promoter lead to a recombination efficiency of ~90% in these cells.

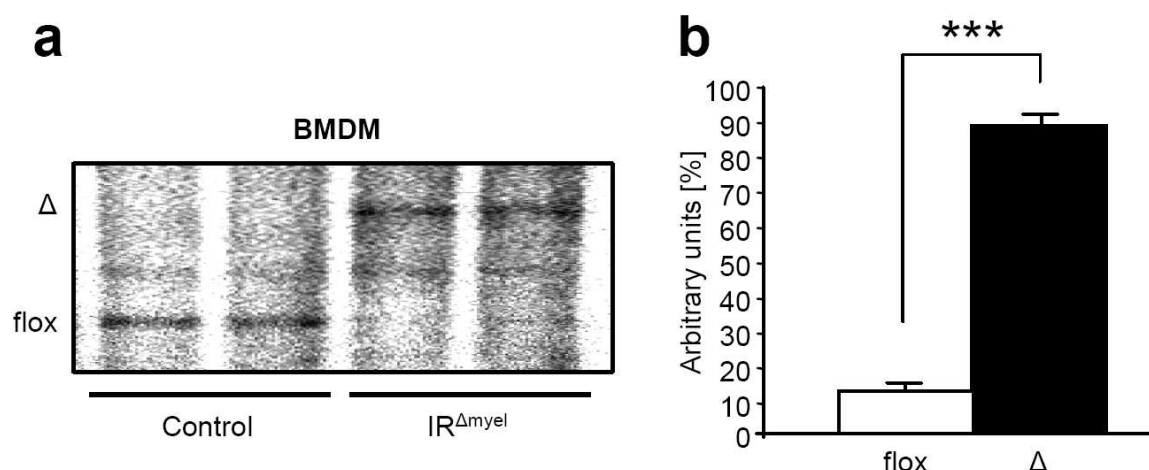


**Fig. 6: Southern blot analysis of the insulin receptor allele in macrophages.**

(a) Southern blot analysis of genomic DNA isolated from bone marrow-derived macrophages (BMDM) from control mice and  $IR^{\Delta myel}$  mice (b) Densitometrical quantification of the deleted versus the floxed allele band in macrophages of  $IR^{\Delta myel}$  mice. (flox = loxP-flanked allele band (2.5 kb),  $\Delta$  = deleted allele band (5 kb); All data are presented as mean  $\pm$  SEM; \*\*\*  $p \leq 0,001$ ; n = 3 vs. 3)

Furthermore, bone marrow-derived macrophages were analyzed for expression of insulin receptor mRNA by realtime PCR. As depicted in Fig. 7, expression of the insulin receptor mRNA was reduced by ~80% in cells from IR<sup>Δmyel</sup> mice compared to control mice.

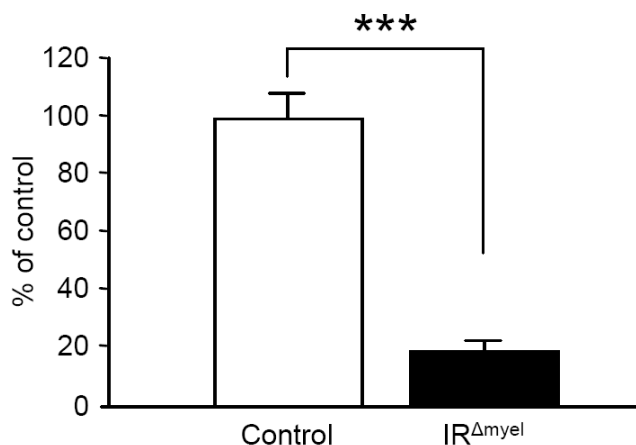


**Fig. 7: Insulin receptor mRNA expression in macrophages.**

Insulin receptor mRNA expression was assessed by quantitative realtime PCR in bone marrow-derived macrophages from control and IR<sup>Δmyel</sup> mice; Hprt1 was used as endogenous control; (All data are presented as mean  $\pm$  SEM; \*\*\*  $p \leq 0,001$ ; n = 4 vs 4)

To exclude the possibility that the residual mRNA expression detected by realtime PCR analysis might lead to significant amounts of insulin receptor protein expression, western blot analysis was performed. Analysis of peritoneally-elicited macrophages demonstrated the complete absence of the insulin receptor protein on these cells (Fig. 8). However, as depicted in Fig. 9, protein expression of the insulin receptor was robust and unchanged in insulin target tissues of IR<sup>Δmyel</sup> mice compared to control mice.

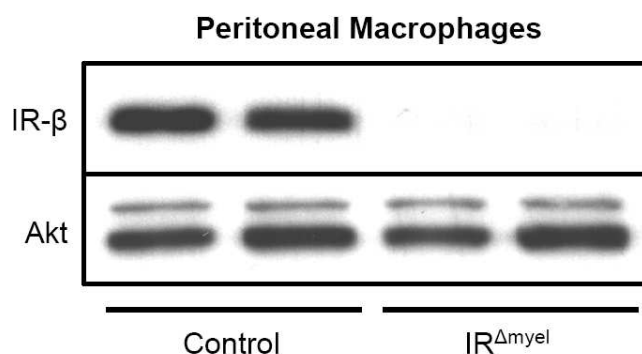


**Fig. 8: Insulin receptor protein expression in macrophages.**

Western blot analysis of insulin receptor  $\beta$  subunit (IR- $\beta$ ) and protein kinase B/Akt (loading control) expression in peritoneal macrophages of control mice and IR<sup>Δmyel</sup> mice.

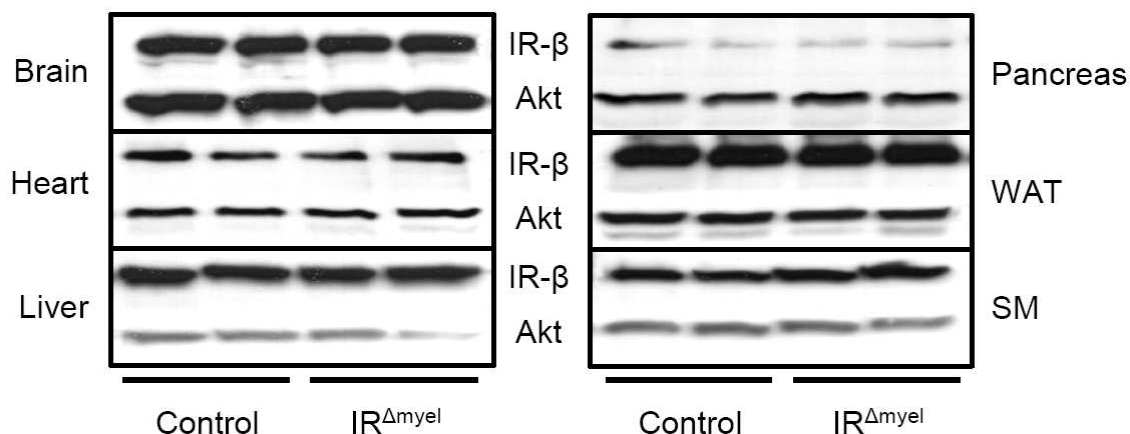


**Fig. 9: Insulin receptor protein expression in insulin target tissues is unchanged in  $IR^{\Delta myel}$  mice.**

Western blot analysis of insulin receptor  $\beta$  subunit (IR- $\beta$ ) and protein kinase B/Akt (loading control) expression. Proteins were extracted from brain, heart, liver, pancreas, white adipose tissue (WAT) and skeletal muscle (SM) of control mice and  $IR^{\Delta myel}$  mice.

In summary, conditional gene targeting using the lysozyme M promoter to drive Cre expression leads to efficient and specific depletion of the insulin receptor in peritoneal and bone marrow-derived macrophages without affecting metabolically relevant tissues, such as brain, liver and skeletal muscle.

### 3.2 The Effect of Myeloid Cell-restricted Insulin Receptor Deficiency on Diet-induced Obesity

To investigate the impact of myeloid cell-restricted insulin receptor deficiency on diet-induced obesity, control mice and  $IR^{\Delta myel}$  mice were fed either a normal chow (NCD) or were exposed to a high fat diet (HFD) for 12 weeks. Under NCD both groups exhibited indistinguishable growth curves reaching approximately 30 g body weight after 16 weeks (Fig. 10a). When exposed to a HFD control mice and  $IR^{\Delta myel}$  mice significantly gained weight over animals exposed to NCD. However, both animal groups gained weight to a similar extent with an average maximum of 45 g after 16 weeks of age (Fig. 10b).

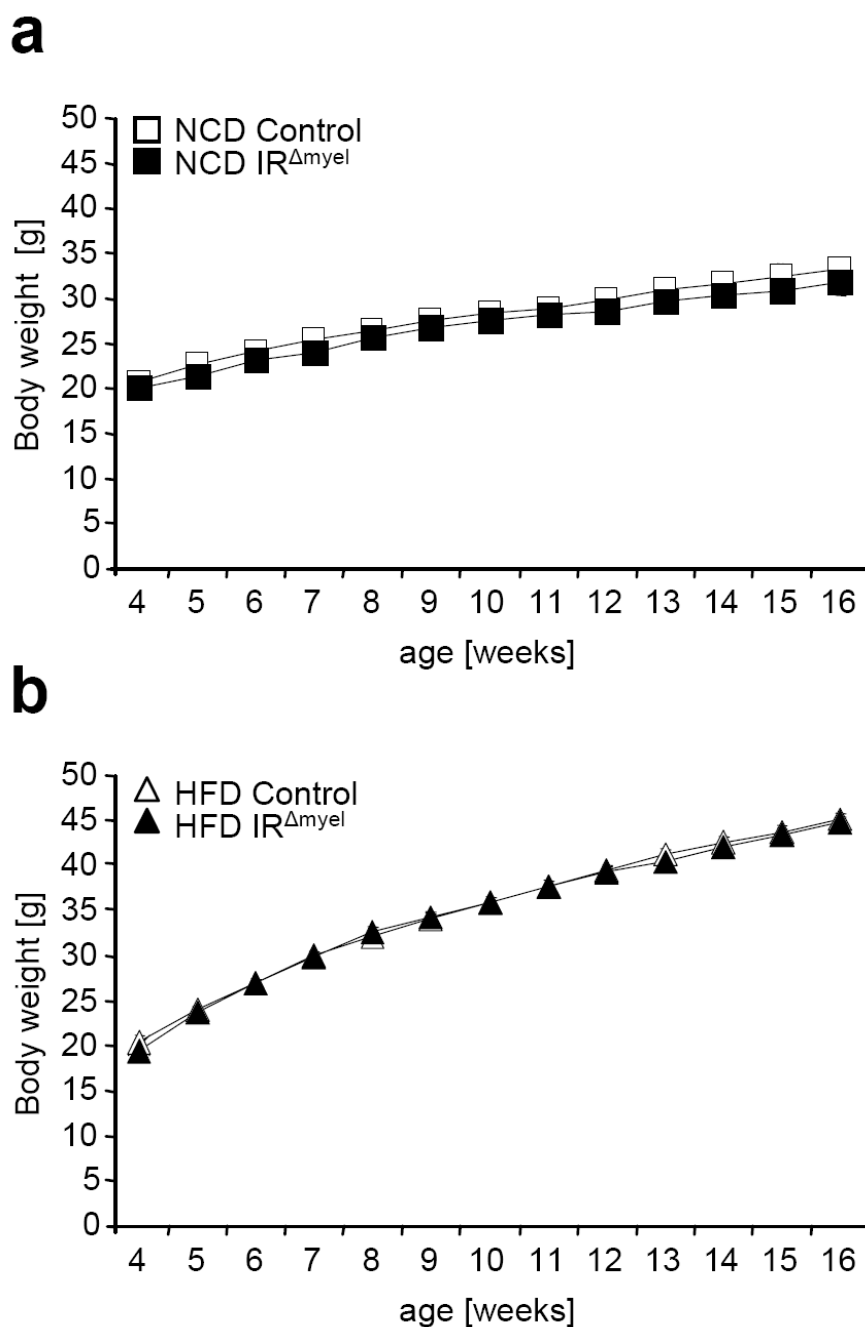


**Fig. 10: IR<sup>Δmyel</sup> mice exhibit normal weight gain upon normal chow diet and high fat feeding.**

(a) Body weight curves of control mice and IR<sup>Δmyel</sup> mice exposed to normal chow diet (NCD). Weight gain was monitored from the age of 4 to 16 weeks. (b) Body weight curves of control mice and IR<sup>Δmyel</sup> mice exposed to HFD. Weight gain was monitored from the age of 4 to 16 weeks. From week 6 onwards, exposure to HFD led to a significantly higher average weight compared to NCD. (All data are presented as mean  $\pm$  SEM; NCD n = 15 vs 14; HFD n = 30 vs 30)

In accordance, epididymal fat pad mass was drastically increased upon high fat feeding, but unchanged between groups (Fig. 11a). An increase of circulating leptin is positively correlated with obesity thereby representing an important indicator for the degree of adiposity. Accordingly, serum leptin concentrations were significantly increased

after 12 weeks of HFD in control mice and IR<sup>Δmyel</sup> mice compared to lean animals (Fig. 11b) while no difference was observed between both genotypes.

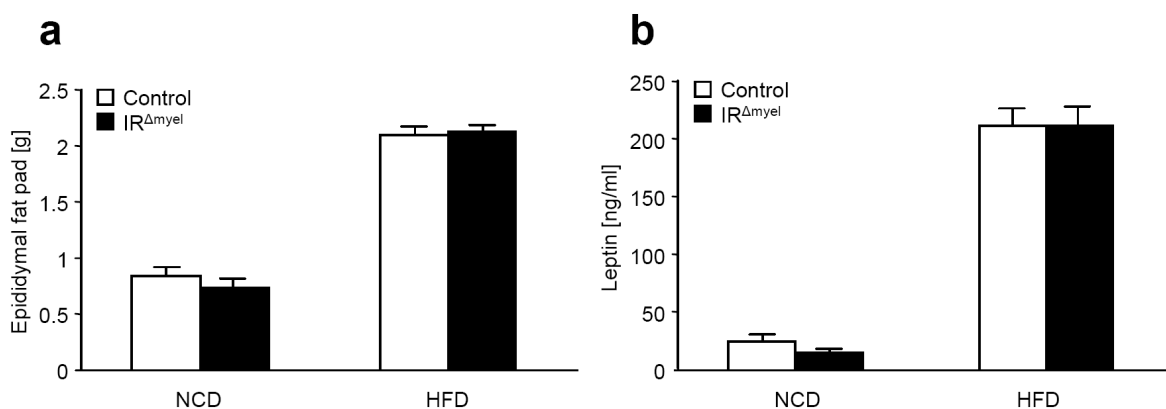


**Fig. 11: IR<sup>Δmyel</sup> mice show normal high fat diet-induced increase in epididymal fat pad mass and circulating leptin concentration.**

(a) Epididymal fat pad mass in control mice and IR<sup>Δmyel</sup> mice. Animals were dissected after 16 weeks on either NCD or HFD and adipose tissue weight was measured. (b) Serum leptin concentrations in control mice and IR<sup>Δmyel</sup> mice were determined by ELISA. Serum was isolated after 16 weeks of age on either NCD or HFD. (NCD n = 11 vs 10; HFD n = 10 vs 10; All data are presented as mean ± SEM)

Taken together, these results indicate that myeloid cell-restricted insulin resistance does not affect the development of obesity upon high fat feeding.

### 3.3 The Effect of Myeloid Cell-restricted Insulin Receptor Deficiency on Obesity-induced Insulin Resistance

Severe obesity is strongly associated with hyperglycemia and hyperinsulinemia. These two parameters represent important indicators for reduced insulin sensitivity or even insulin resistance. To investigate the effect of myeloid cell-autonomous insulin signaling on obesity-induced insulin resistance, glucose metabolism of IR<sup>Δmyel</sup> mice was analyzed. Fasted blood glucose levels and insulin levels were determined as a first measure of glucose homeostasis in these animals (Fig. 12a, b). On NCD, both genotypes displayed average fasted blood glucose concentration of ~60 mg/dl and average fasted serum insulin concentration of ~2 pg/ml after 16 weeks of age. Surprisingly, IR<sup>Δmyel</sup> mice on HFD had significantly reduced fasted blood glucose compared to control mice although both groups clearly developed hyperglycemia. Consistently, fasted serum insulin levels were

significantly reduced in obese  $IR^{\Delta myel}$  mice compared to control mice while no difference was observed under NCD.

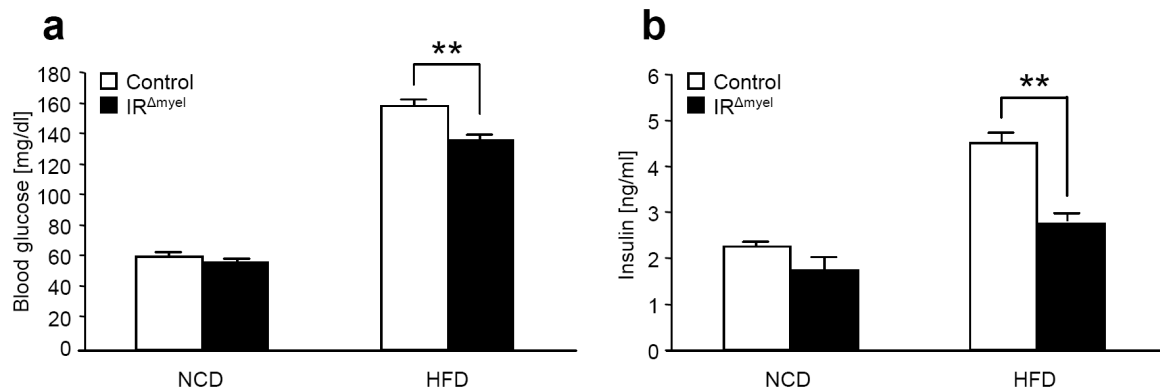


**Fig. 12: Diet-induced obese  $IR^{\Delta myel}$  mice exhibit significantly reduced fasted blood glucose and insulin levels.**

Fasted blood glucose concentration (a) and fasted insulin concentration (b) of 16 week old control mice and  $IR^{\Delta myel}$  mice fed either NCD or HFD. (All data are presented as mean  $\pm$  SEM; NCD n = 11 vs 10; HFD n = 10 vs 10; \*\* $p \leq 0.01$ )

After 16 weeks on either NCD or HFD, control mice and  $IR^{\Delta myel}$  mice were challenged in a glucose tolerance test (GTT, Fig. 13a). While lean mice (NCD) of both groups responded identically to an exogenous glucose challenge,  $IR^{\Delta myel}$  mice fed a high fat diet performed significantly better than control mice. Also, during insulin tolerance testing (ITT, Fig. 13b), diet-induced obese  $IR^{\Delta myel}$  mice displayed significantly higher insulin sensitivity than their littermate controls.

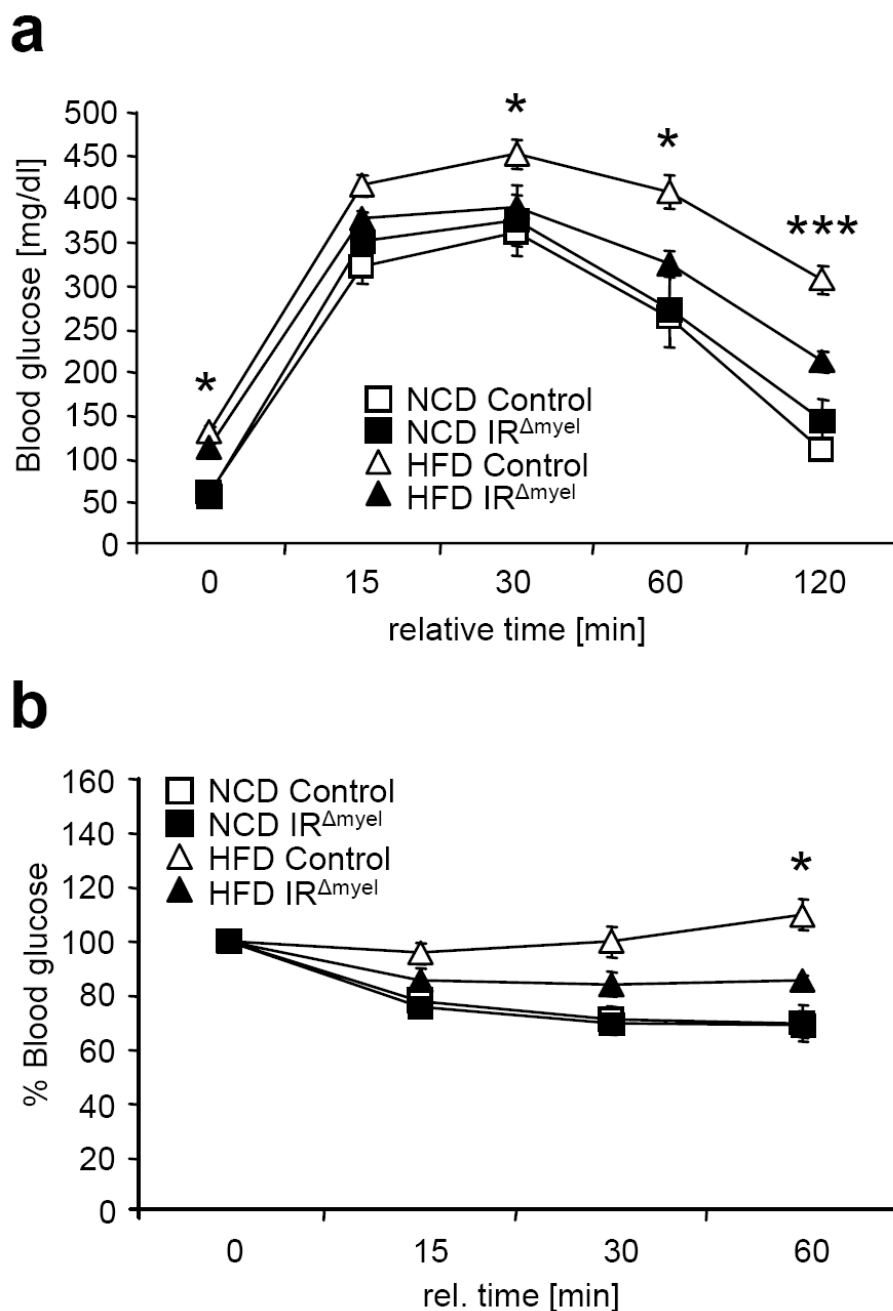


**Fig. 13: Obese IR<sup>Δmyel</sup> mice exhibit increased glucose tolerance and insulin sensitivity.**

(a) GTT analysis was performed with 16 week old control mice and IR<sup>Δmyel</sup> mice fed either NCD or HFD for 16 weeks. (NCD n = 6 vs 7; HFD n = 20 vs 20). (b) ITT analysis was performed with 16 week old control mice and IR<sup>Δmyel</sup> mice fed either NCD or HFD. (All data are presented as mean ± SEM; NCD n = 6 vs 5; HFD n = 14 vs 13; \*p ≤ 0.05; \*\*\*p ≤ 0.001 HFD control versus HFD IR<sup>Δmyel</sup>)

To further elucidate which insulin target tissues are responsible for the enhanced glucose metabolism in diet-induced obese IR<sup>Δmyel</sup> mice, euglycemic-hyperinsulinemic clamp analyses were performed. Hepatic glucose production (HGP) was assessed in control mice and IR<sup>Δmyel</sup> mice after 12 weeks on HFD. Although no difference was

observed in insulin's ability to suppress HGP, the basal i.e. non-suppressed glucose production was significantly reduced in livers of obese IR<sup>Δmyel</sup> mice (Fig. 14).

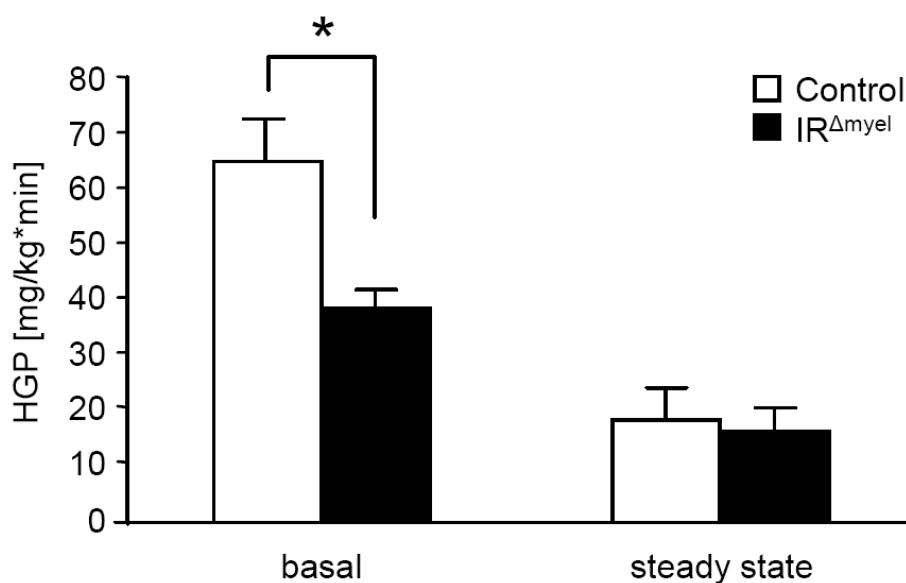


**Fig. 14: Obese IR<sup>Δmyel</sup> mice exhibit decreased hepatic glucose production.**

Hepatic glucose production (HGP) in 16 week old HFD-fed control mice and IR<sup>Δmyel</sup> mice was determined before (basal) and during (steady-state) euglycemic-hyperinsulinemic clamp analysis. (All data are presented as mean ± SEM; n = 10 vs 13; \*p ≤ 0.05)

Since WAT, skeletal muscle and brain represent major target tissues for insulin-stimulated carbohydrate uptake, glucose disposal rate was determined in these organs. As depicted in Fig. 15, glucose uptake during the clamp was drastically enhanced in skeletal muscle of obese IR<sup>Δmyel</sup> mice compared to obese control mice. In contrast, uptake into the WAT and brain was, at least under clamp conditions, unaltered between the two genotypes.

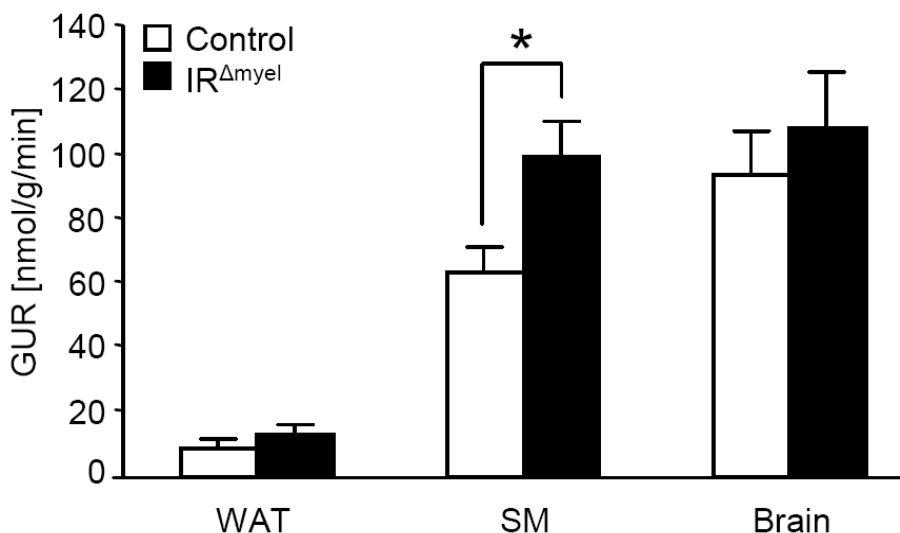


**Fig. 15: Obese IR<sup>Δmyel</sup> mice show enhanced insulin-stimulated glucose disposal in skeletal muscle.**

Steady-state insulin-stimulated glucose uptake rate (202) was determined in euglycemic-hyperinsulinemic clamp analysis. GUR was measured in WAT, skeletal muscle (SM) and brain of obese control mice and IR<sup>Δmyel</sup> mice after 16 weeks of HFD. (All data are presented as mean  $\pm$  SEM; n = 10 vs 13; \*p  $\leq$  0.05)

Responsiveness of the adipose tissue to the metabolic effects of insulin is crucial for maintenance of energy homeostasis. Its role in the development of T2DM, especially in the context of immune cell/adipocyte crosstalk, is of central importance to the concept of obesity-induced insulin resistance. Therefore, it was mandatory to further investigate adipocyte-autonomous insulin signaling in IR<sup>Δmyel</sup> mice. To this end, adipocytes of control mice and IR<sup>Δmyel</sup> mice were isolated and stimulated with different doses of insulin *in vitro*. Although no difference in glucose uptake could be observed after stimulation with 1, 10 and 100 nm insulin adipocytes of IR<sup>Δmyel</sup> mice took up significantly more glucose compared to control mice when stimulated with a concentration of 0,1 nm insulin (Fig. 16).

These data indicate that myeloid cell-restricted insulin receptor deficiency, despite enhancing glucose uptake in skeletal muscle, also improves insulin action in adipocytes by shifting the dose response curve without altering the maximal response.

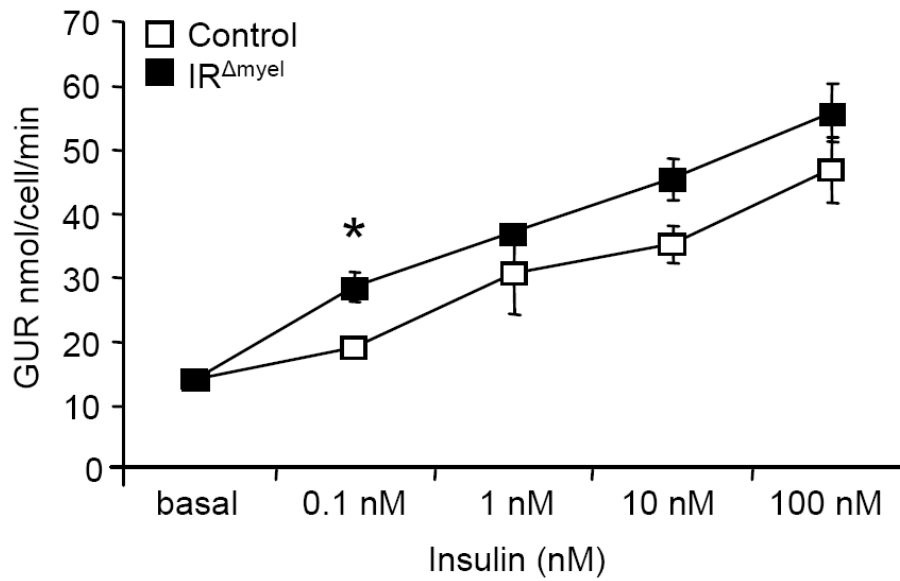


**Fig. 16: Low dose insulin-stimulated glucose uptake is enhanced in adipocytes of obese IR<sup>Δmyel</sup> mice.**

Freshly isolated adipocytes of control mice and IR<sup>Δmyel</sup> mice were stimulated with 0, 0.1, 1, 10 and 100 nM insulin *in vitro* and glucose uptake rate (202) was determined. (All data are presented as mean  $\pm$  SEM; n = 5 vs 5; \*p  $\leq$  0.05)

In conclusion, myeloid cell-specific disruption of the insulin receptor protects against obesity-induced insulin resistance by reducing basal hepatic glucose production and facilitating insulin-stimulated glucose disposal in skeletal muscle and adipose tissue.

### 3.4 The Effect of Myeloid Cell-restricted Insulin Receptor Deficiency on Obesity-induced Inflammation

Obesity is associated with a local and systemic rise in inflammatory markers originating from activated immune cells infiltrating the white adipose tissue. This increase of cytokines activates pro-inflammatory pathways in insulin target tissues leading to the induction of JNK and NF $\kappa$ B signaling which can either directly or indirectly block insulin signaling components. To analyze the pro-inflammatory effect of high fat feeding in IR $^{\Delta myel}$  mice, serum cytokine concentrations were determined. As shown in Fig. 17, HFD induced an increase in the concentration of circulating TNF- $\alpha$  and reduced that of adiponectin in control mice. This response to high fat feeding could not be observed in IR $^{\Delta myel}$  mice. TNF- $\alpha$  concentration in blood serum of obese IR $^{\Delta myel}$  mice remained unchanged compared to lean animals. Similarly, adiponectin concentration was unaltered between IR $^{\Delta myel}$  mice on NCD compared to HFD.

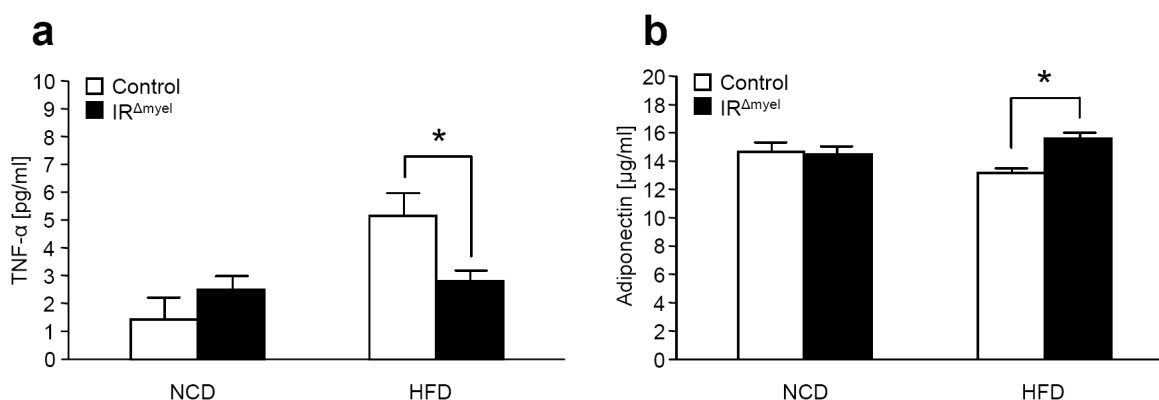


**Fig. 17: The obesity-associated change of serum TNF- $\alpha$  and adiponectin concentration is abolished in IR $^{\Delta myel}$  mice.**

Serum concentration of TNF- $\alpha$  (a) and adiponectin (b) was measured by ELISA in control mice and IR $^{\Delta myel}$  mice fed either NCD or HFD for 16 weeks. (All data are presented as mean  $\pm$  SEM; NCD n = 12 vs 13; HFD n = 20 vs 20; \* $p \leq 0.05$ )

As previously described, the chronic low-grade inflammatory state encountered in obese subjects leads to insulin resistance in insulin target tissues at least partially due to increased JNK activity. To directly measure the activation state of this signaling pathway, an *in vitro* assay for the determination of JNK activity was performed. Liver and skeletal muscle protein extracts from obese control mice and IR $^{\Delta myel}$  mice were analyzed and significantly lower JNK activity was detected in skeletal muscle of the latter (Fig. 18). This

indicates that despite unaltered obesity in IR<sup>Δmyel</sup> mice, the systemic, obesity-associated proinflammatory tone is reduced.

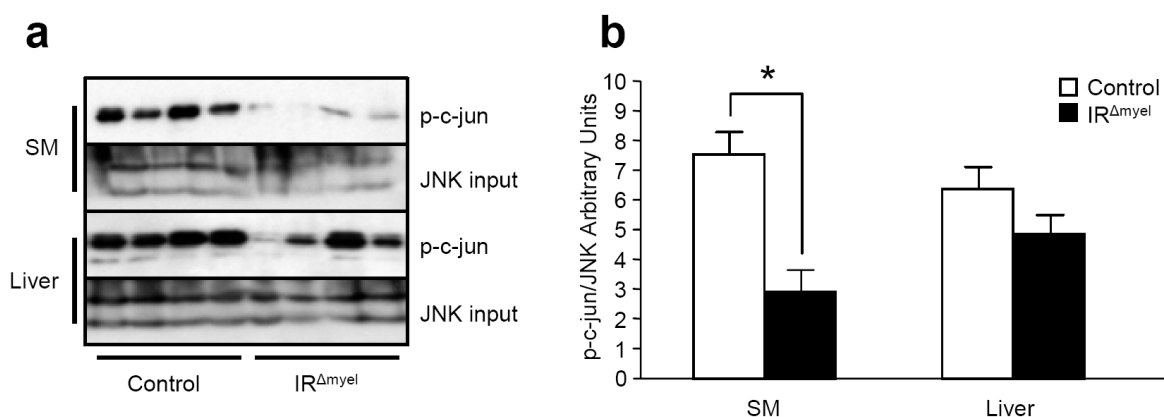


**Fig. 18: Obese IR<sup>Δmyel</sup> mice show reduced JNK activity in skeletal muscle.**

Protein extracts from skeletal muscle (SM) and liver of HFD-fed control mice and IR<sup>Δmyel</sup> mice were analyzed for JNK activity. Western blots showing the *in vitro* phosphorylation of c-jun (a) were densitometrically quantified (b). Total JNK levels from the initial lysate (JNK input) were used as a loading control. (All data are presented as mean  $\pm$  SEM; n = 6 vs 6; \*p  $\leq$  0.05)

Local increase of inflammatory cytokine and chemokine expression in adipose tissue is a hallmark of obesity. Therefore, mRNA levels of the pro-inflammatory cytokine TNF- $\alpha$ , the chemokines CCL2 and CCL3 and adiponectin were determined in WAT samples of control mice and IR<sup>Δmyel</sup> mice (Fig. 19). As expected, high fat feeding significantly increased inflammatory gene expression in WAT of control mice. In contrast, exposure to HFD failed to induce TNF- $\alpha$  and CCL3 gene expression in IR<sup>Δmyel</sup> mice to the extent observed in the controls. Also, adiponectin mRNA expression was significantly elevated in obese IR<sup>Δmyel</sup> mice compared to control mice. CCL2 mRNA levels were slightly decreased but the difference did not reach significance.

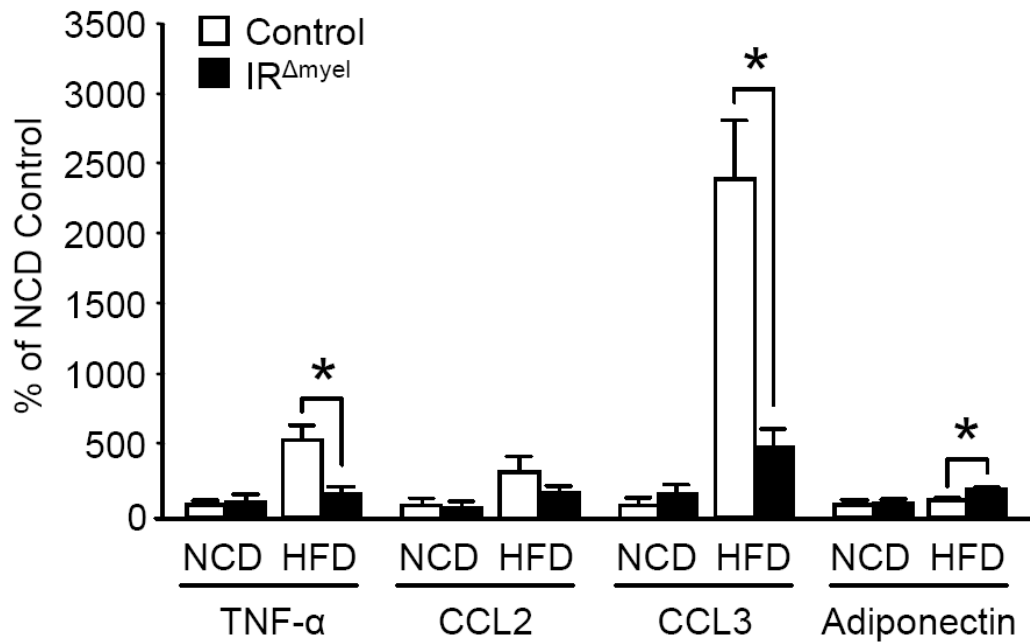


**Fig. 19: Obesity-induced change of adipokine gene expression is blunted in IR<sup>Δmyel</sup> mice.**

WAT samples of control mice and IR<sup>Δmyel</sup> mice fed either NCD or HFD were analyzed by quantitative realtime PCR. Relative mRNA levels of TNF- $\alpha$ , CCL2, CCL3 and adiponectin were measured in 16 week old mice. Hprt1 mRNA was used as endogenous control. (All data are presented as mean  $\pm$  SEM; n = 8 vs 8; \*p  $\leq$  0.05)

In conclusion, myeloid cell-autonomous insulin resistance diminishes the typical, obesity-associated rise in circulating inflammatory markers and activation of inflammatory protein kinase JNK in peripheral organs. Furthermore, a local and systemic increase in adiponectin mRNA and protein levels, respectively, was observed.

### 3.5 The Effect of Myeloid Cell-restricted Insulin Receptor Deficiency on Adipose Tissue Inflammation and Macrophage Accumulation

Since macrophages have been shown to contribute significantly to the enhanced inflammatory profile of the expanding adipose tissue under obesity, gene expression of a macrophage-specific marker (F4/80) was determined in this tissue. As expected, obesity led to a substantial increase in F4/80 mRNA expression (Fig. 20a) in white adipose tissue of diet-induced obese control mice compared to lean animals. However, while lean mice from both genotypes showed the same expression level of F4/80 mRNA, the obesity-induced increase of this marker was significantly blunted in HFD-fed  $IR^{\Delta myel}$  mice. Nevertheless, the cell-autonomous expression of F4/80 was unchanged between bone marrow-derived macrophages of both genotypes, neither at the basal level nor after stimulation with palmitic acid (Fig. 20b).

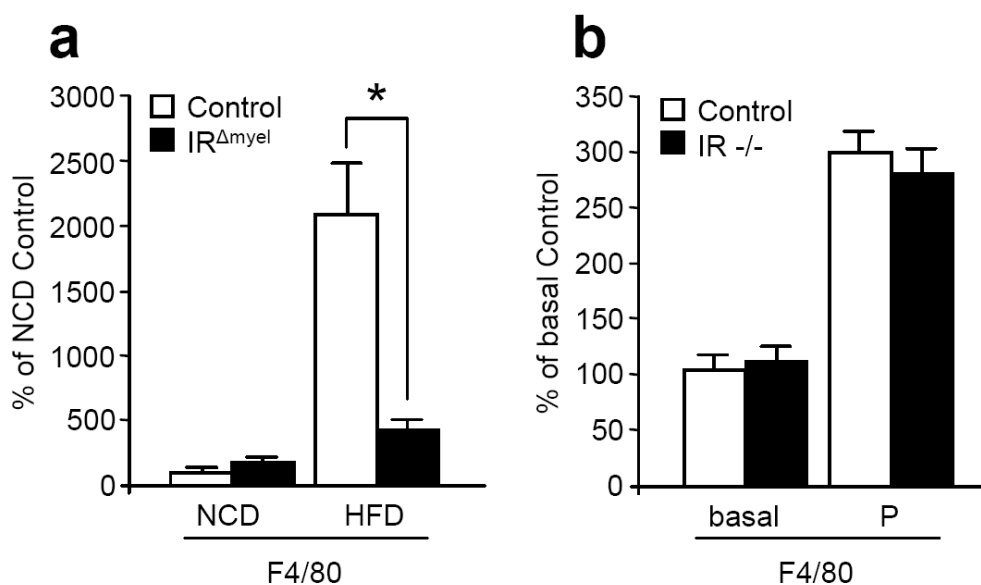


**Fig. 20: Reduced macrophage surface marker expression in adipose tissue of obese  $IR^{\Delta myel}$  mice.**

F4/80 mRNA expression was assessed by quantitative realtime PCR analysis in (a) WAT of NCD and HFD fed control mice and  $IR^{\Delta myel}$  mice and (b) untreated (basal) or palmitic acid (P, 500  $\mu$ M) stimulated bone marrow-derived macrophages from control mice and  $IR^{\Delta myel}$  mice. Hprt1 mRNA was used as endogenous control (All data are presented as mean  $\pm$  SEM; WAT n = 5 vs 5; BMDM n = 4 vs 4; \*p  $\leq$  0.05)

Moreover, white adipose tissue was analyzed microscopically for changes in morphology. As depicted in Fig. 21, when stained with hematoxylin and eosin (H&E)

adipose tissue morphology was indistinguishable between obese control mice and IR<sup>Δmyel</sup> mice.

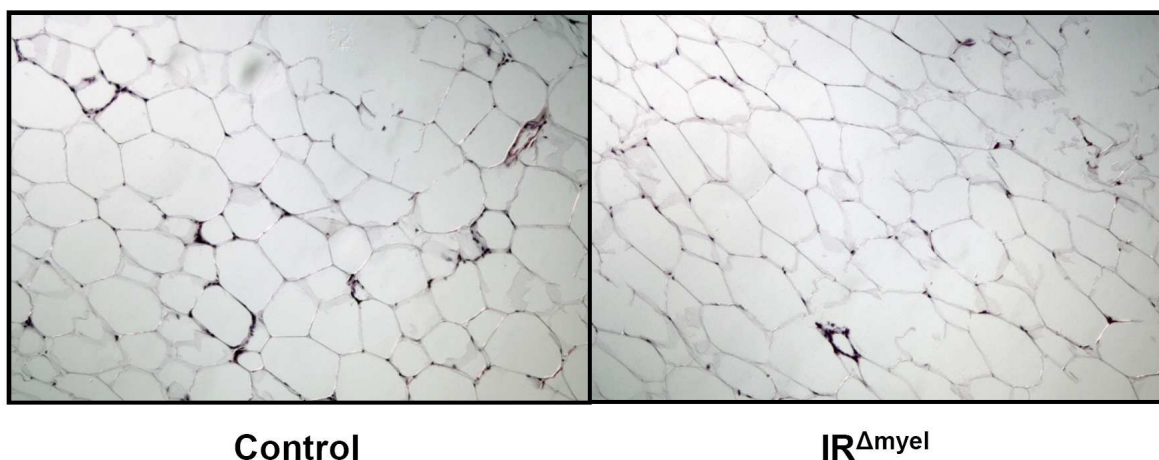


**Fig. 21: Adipose tissue morphology of IR<sup>Δmyel</sup> mice and control mice exposed to HFD.**

H&E staining of paraffin sections from WAT of 16 week old obese control mice and IR<sup>Δmyel</sup> mice. (Magnification: 100-fold)

Additionally, adipocyte size was analyzed in white adipose tissue sections of HFD-fed control mice and IR<sup>Δmyel</sup> mice. As shown in Fig. 22a, the mean cell size reached approximately 10000  $\mu\text{m}^2$  in both genotypes. In addition, adipocyte size occurrence curves displayed Gauss distribution without revealing any significant difference between the genotypes investigated (Fig. 22b).

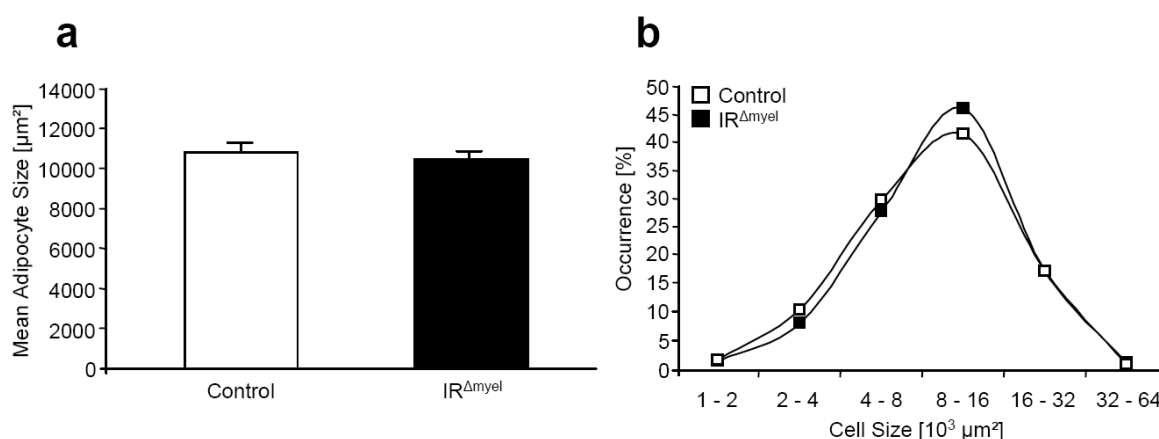


**Fig. 22: Quantification of adipocyte size and size distribution.**

Mean adipocyte size (a) and cell size distribution (b) in WAT was quantified in adipose tissue sections from control mice and IR<sup>Δmyel</sup> mice. (All data are presented as mean  $\pm$  SEM; n = 9 vs 9)

Upon weight gain, macrophages infiltrate the expanding adipose tissue and form crown-like structures (CLS) around dead adipocytes for removal of cell debris and tissue remodeling. Mac-2, a 30-35 kDa galactose-binding protein, is specifically expressed on the surface of macrophages upon activation (203). In order to detect activated macrophages in adipose tissue, immunohistochemical analysis with an antibody directed against Mac-2 was performed. In line with the observed reduction of macrophage marker mRNA expression, microscopical analysis revealed a dramatically reduced number of CLS in adipose tissue sections of obese  $IR^{\Delta myel}$  mice compared to control mice (Fig. 23, upper panel). Likewise, quantification of total CLS area per section revealed a significant reduction in  $IR^{\Delta myel}$  mice (Fig. 23, lower panel).

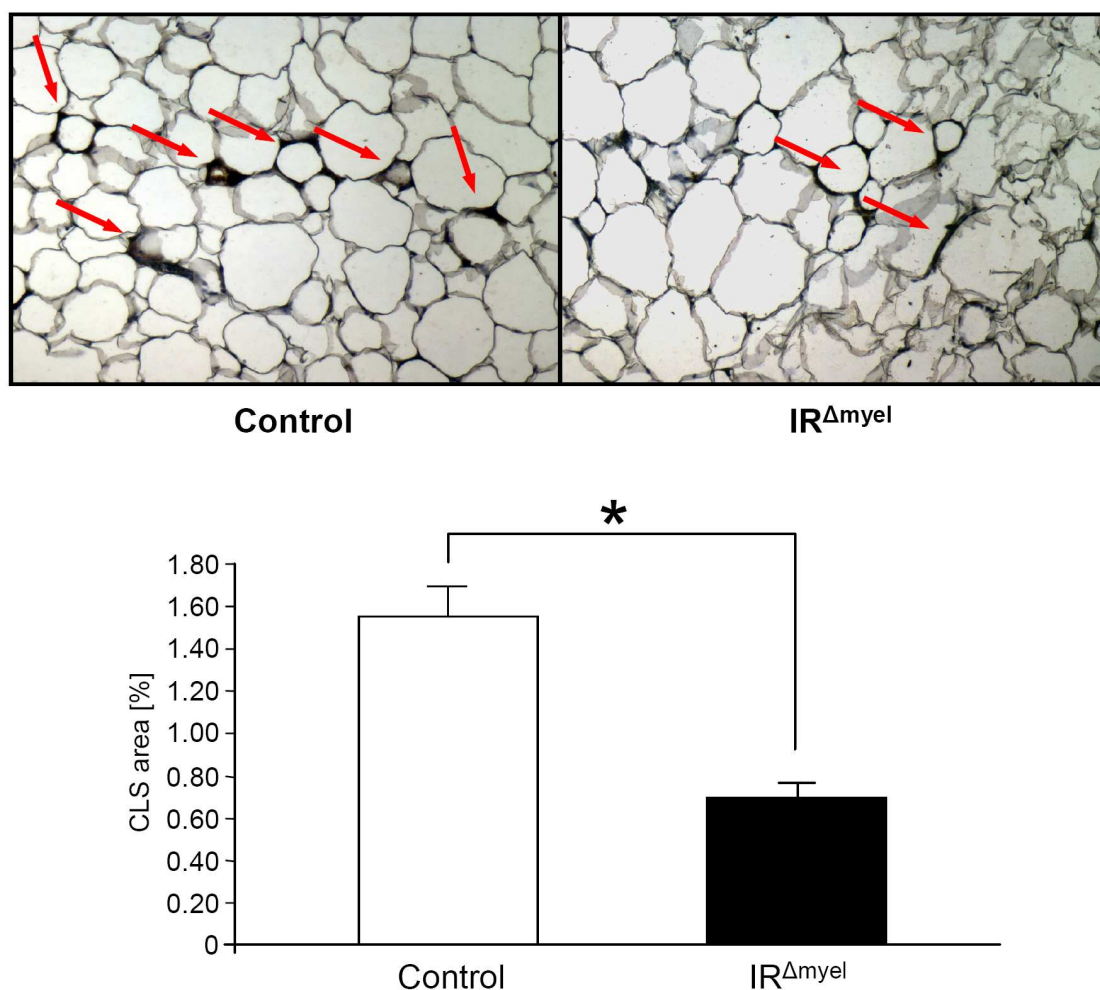


**Fig. 23: Obese adipose tissue of  $IR^{\Delta myel}$  mice shows decreased formation of crown-like structures.**

Paraffin sections from WAT of 16 week old obese control mice and  $IR^{\Delta myel}$  mice were immunohistochemically stained with Mac-2 antibody (upper panel, magnification 100-fold) and the area of Mac-2 positive crown-like structures (CLS) was quantified (lower panel). Red arrows indicate CLS. (All data are presented as mean  $\pm$  SEM; n = 9 vs 9; \*p  $\leq$  0.05)

The adipose tissue consists of two main fractions, adipocytes and stromal vascular cells. To precisely attribute the previously observed reduction of TNF- $\alpha$  mRNA expression to one of these compartments, white adipose tissue of obese control mice and IR <sup>$\Delta$ myel</sup> mice was separated into these two fractions. Quantitative realtime PCR analysis of leptin mRNA, which is exclusively expressed in adipocytes, was taken as a quality control for the separation process. Stromal vascular cells expressed approximately 90% less leptin mRNA compared to adipocytes (Fig. 24). Expression levels of macrophage surface markers F4/80, Mac-2 and CD11c mRNA were 2-fold to 4-fold increased in stromal vascular cells of control mice compared to adipocytes. Concomitant with reduced CLS formation (Fig. 23), expression of Mac-2 as well as F4/80 mRNA was significantly reduced in the stromal vascular fraction of IR <sup>$\Delta$ myel</sup> mice compared to control mice. However, CD11c expression was unchanged between IR <sup>$\Delta$ myel</sup> mice and control mice. Furthermore, TNF- $\alpha$  mRNA expression was 5-fold elevated in stromal vascular cells compared to adipocytes isolated from control mice. Nevertheless, the stromal vascular cells of IR <sup>$\Delta$ myel</sup> mice expressed significantly lower TNF- $\alpha$  mRNA than those of control mice (Fig. 24).

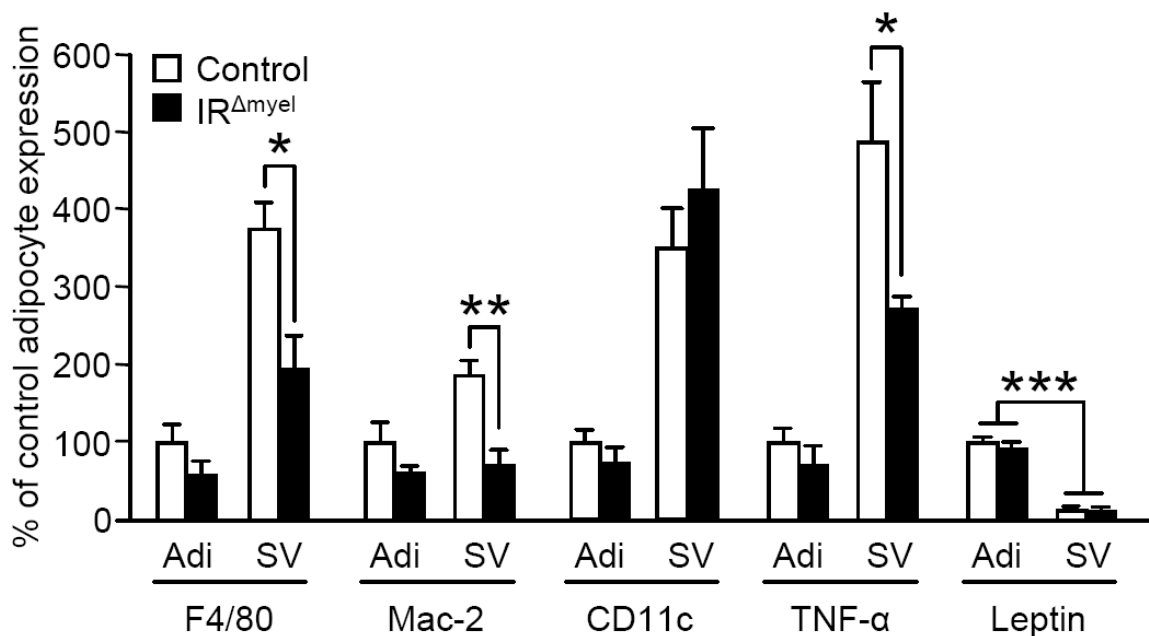


**Fig. 24: Reduced TNF- $\alpha$  expression in adipose tissue-derived stromal vascular cells of IR <sup>$\Delta$ myel</sup> mice.**

WAT of control mice and IR <sup>$\Delta$ myel</sup> mice was separated into adipocytes (Adi) and stromal vascular cells (167). Relative mRNA expression of F4/80, Mac-2, CD11c and TNF- $\alpha$  was determined by quantitative realtime PCR. To estimate fractionation efficiency, Leptin mRNA expression was determined in both fractions. Hprt1 mRNA was used as endogenous control. (All data are presented as mean  $\pm$  SEM; n = 6 vs 5; \*p  $\leq$  0.05; \*\*p  $\leq$  0.01; \*\*\*p  $\leq$  0.001)

Taken together, these data demonstrate that myeloid cell-restricted insulin resistance reduces the inflammatory infiltration of adipose tissue by macrophages, which is generally associated with high fat feeding and obesity. This blunted macrophage accumulation in turn leads to reduced expression of TNF- $\alpha$  mRNA in the stromal vascular compartment of the obese adipose tissue of IR <sup>$\Delta$ myel</sup> mice.

## 3.6 Cell-Autonomous Effects of Insulin Receptor Deficiency on Macrophages

The reason for the observed reduction of adipose tissue macrophage content and inflammatory gene expression in obese IR<sup>Δmyel</sup> mice could arise from (I) enhanced susceptibility to apoptosis, (II) impaired inflammatory response of insulin receptor-deficient macrophages or (III) reduced invasive capacity of these cells.

### 3.6.1 The Effect of Insulin on Macrophage Apoptosis

To investigate the first hypothesis, bone marrow-derived macrophages from control and IR<sup>Δmyel</sup> mice were stimulated with insulin, palmitic acid or both and the number of apoptotic cells was analyzed for DNA fragmentation by TUNEL assay. As depicted in Fig. 25, approximately 10% of control and IR<sup>-/-</sup> macrophages showed DNA fragmentation under basal conditions. Strikingly, exposure to insulin significantly reduced the number of TUNEL positive cells in control but not in IR-deficient macrophages. Furthermore, stimulation with palmitic acid drastically enhanced apoptosis in control and IR-deficient macrophages to approximately 45%. Moreover, costimulation with insulin significantly reduced the number of apoptotic control macrophages by 10%. This anti-apoptotic effect of insulin could not be observed in IR<sup>-/-</sup> macrophages.

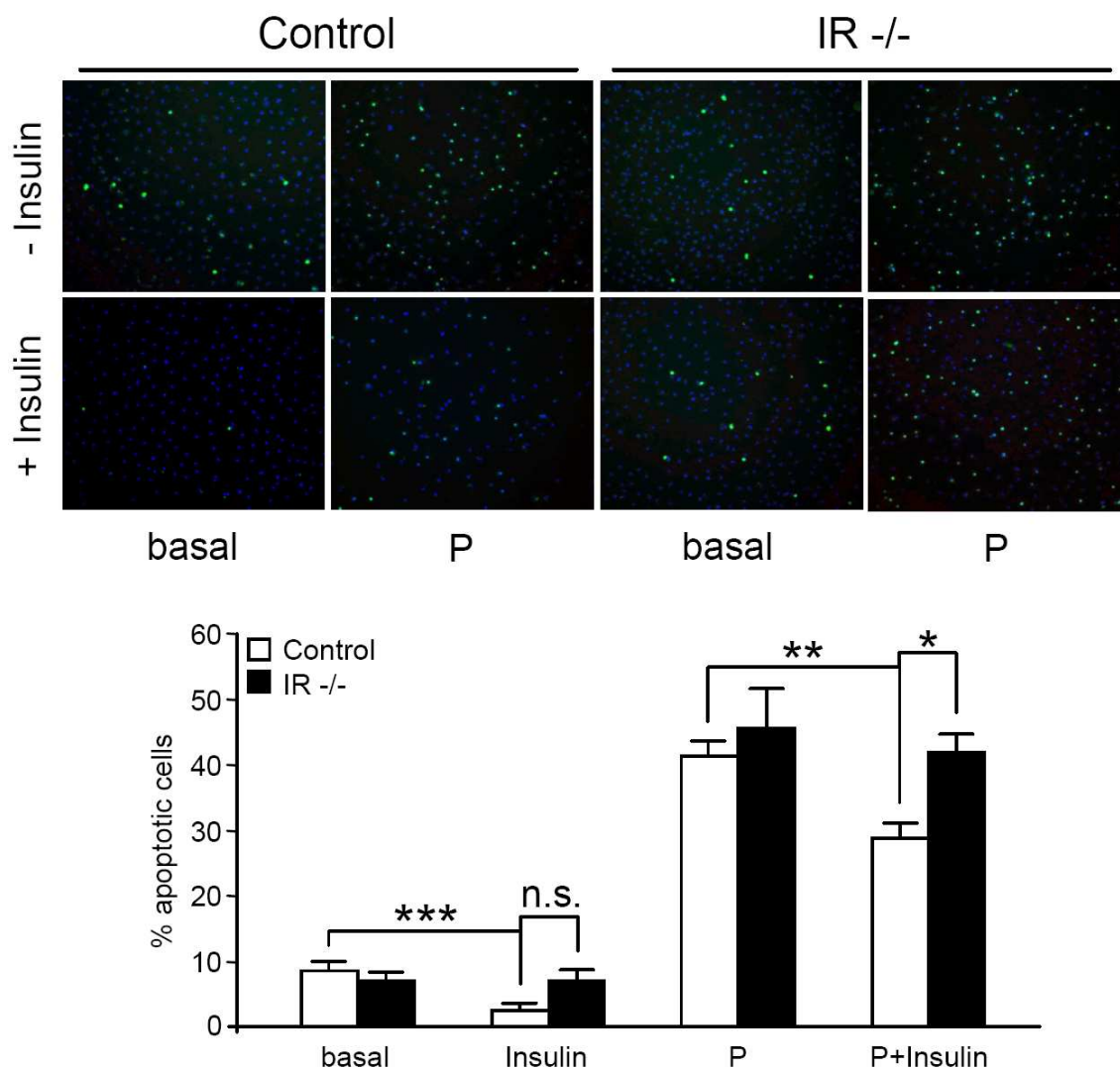


**Fig. 25: Enhanced apoptosis in insulin receptor-deficient macrophages.**

Bone marrow-derived macrophages were stimulated with insulin (50 ng/ml), palmitic acid (P, 500  $\mu$ M) or both for 24 h in serum-free medium and the number of TUNEL-positive (155) cells was determined. DAPI staining of nuclei (blue) was performed for total cell number. (Fluorescence microscopy: upper panel; quantification: lower panel; All data are presented as mean  $\pm$  SEM; n = 4 vs 4; \*p  $\leq$  0.05; \*\*p  $\leq$  0.01; \*\*\*p  $\leq$  0.001)

To further investigate the enhanced palmitic acid-induced apoptosis in insulin receptor-deficient macrophages, quantitative realtime PCR analysis of pro- and anti-apoptotic gene expression was performed. Stimulation with palmitic acid induced a 3-fold increase in mRNA expression of Bcl2-associated X protein (Bax) after 8 h compared to the basal level. However, stimulation with insulin did not alter Bax mRNA levels. Also, no difference could be observed between control and IR-deficient macrophages under any condition analyzed (Fig. 26a).

In contrast, Bcl-2 mRNA expression was strongly reduced after exposure of bone marrow-derived macrophages to palmitic acid compared to the basal level (Fig. 26b). The addition of insulin significantly increased the expression of Bcl-2 in control macrophages. However, this effect was not observed in IR-deficient macrophages. Under the influence of palmitic acid, insulin also induced an increase in Bcl-2 expression of control cells. Nevertheless, this induction was not significant after 8 h of stimulation.

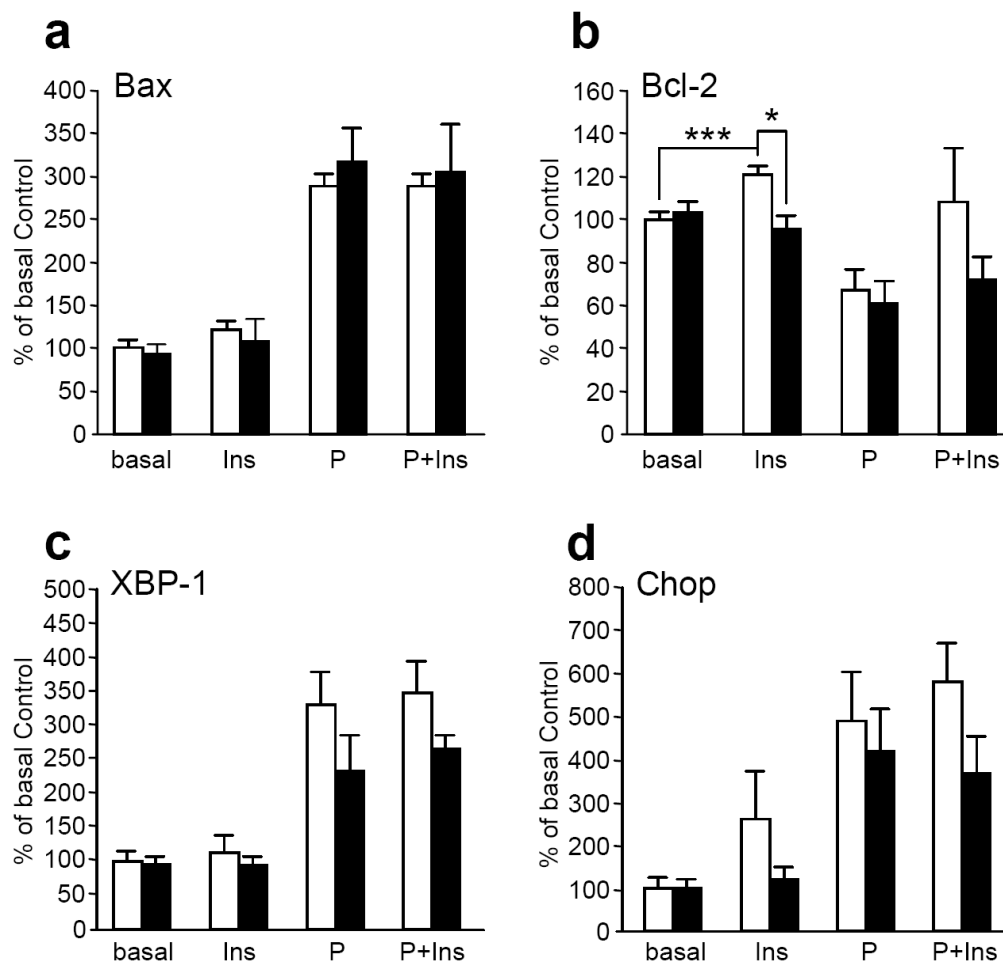


**Fig. 26: Insulin enhances expression of Bcl-2 mRNA in bone marrow-derived macrophages.**

Bone marrow-derived macrophages from control (white columns) or IR<sup>Amyel</sup> mice (black columns) were stimulated with insulin (Ins, 50 ng/ml), palmitic acid (P, 500  $\mu$ M) or both for 8 h in serum-free medium and expression of (a) Bax, (b) Bcl-2, (c) XBP-1 and (d) Chop mRNA was analysed by quantitative realtime PCR. Hprt1 and Gusb mRNA were used as endogenous controls. (All data are presented as mean  $\pm$  SEM; n = 4 vs 4; \*p  $\leq$  0.05; \*\*\*p  $\leq$  0.001)

In addition, the expression of ER stress-induced genes was determined in control and IR-deficient macrophages. Stimulation with palmitic acid significantly induced the expression of XBP-1 and Chop mRNA while no difference could be observed between

genotypes (Fig. 26c, d). Although insulin displayed no significant effect on the expression of the two genes, macrophages of IR<sup>Δmyel</sup> mice exhibited a tendency towards reduced XBP-1 expression after exposure to palmitic acid and reduced Chop expression after combined insulin and palmitic acid stimulation, when compared to control cells.

### 3.6.2 The Effect of Insulin on Pro-inflammatory Gene Expression

To investigate the second hypothesis, namely that insulin regulates pro-inflammatory gene expression, bone marrow-derived macrophages from control and IR<sup>Δmyel</sup> mice were again stimulated with insulin, palmitic acid or both. Induction of pro-inflammatory gene expression was analyzed by quantitative realtime PCR after a stimulation period of 8 h. While mRNA levels of TNF- $\alpha$  and IL-6 were unchanged in non-stimulated cells, exposure to insulin increased the expression of both genes 2-fold in control macrophages. However, insulin failed to enhance TNF- $\alpha$  and IL-6 gene expression in macrophages derived from bone marrow of IR<sup>Δmyel</sup> mice (Fig. 27a). After stimulation with palmitic acid, macrophages of both genotypes displayed a marked increase of TNF- $\alpha$  and IL-6 mRNA expression compared to untreated cells (Fig. 27b). Furthermore, a combination of palmitic acid and insulin slightly increased the expression of TNF- $\alpha$  in control macrophages. In contrast, palmitic acid-induced IL-6 mRNA expression was slightly reduced by insulin in these cells. However, neither the insulin-induced increase of TNF- $\alpha$  nor the decrease of IL-6 mRNA levels under lipid load could be observed in macrophages derived from IR<sup>Δmyel</sup> mice.

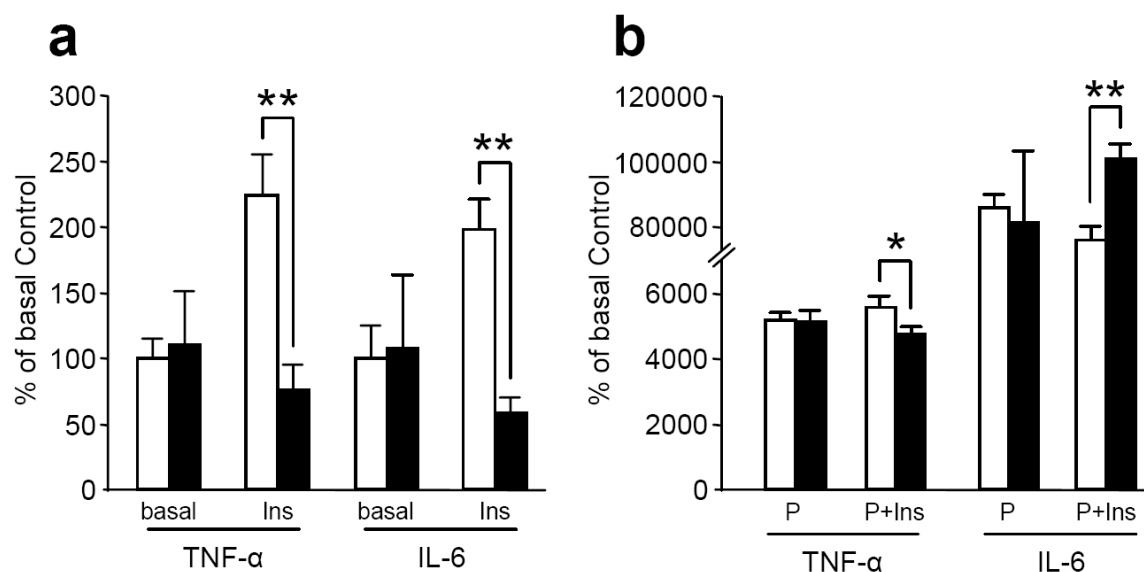


**Fig. 27: Insulin augments pro-inflammatory gene expression in macrophages.**

Bone marrow-derived macrophages from control mice (white columns) or IR<sup>Δmyel</sup> mice (black columns) were stimulated with (a) insulin (Ins, 50 ng/ml), (b) palmitic acid (P, 500 μM) or both for 8 h and expression of TNF-α and IL-6 mRNA was analyzed by quantitative realtime PCR. Hprt1 and Gusb mRNA was used as endogenous control. (All data are presented as mean ± SEM; n = 4 vs 4; \*\*p ≤ 0.01)

To directly assess pro-inflammatory cytokine production in control and insulin receptor-deficient macrophages, TNF-α and IL-6 ELISA was performed with supernatants of these cells. As depicted in Fig. 28a, macrophages of control mice released significantly more TNF-α protein in response to insulin in the absence of other stimuli. Also, in macrophages of IR<sup>Δmyel</sup> mice, stimulation with insulin tended to result in enhanced TNF-α production but this increase was not significant. Upon stimulation with palmitic acid, TNF-α release was further increased compared to insulin. However, no difference was observed between genotypes or after costimulation with palmitic acid and insulin. The release of IL-6 was not affected in macrophages of IR<sup>Δmyel</sup> mice compared to controls under any condition analysed (Fig. 28b).

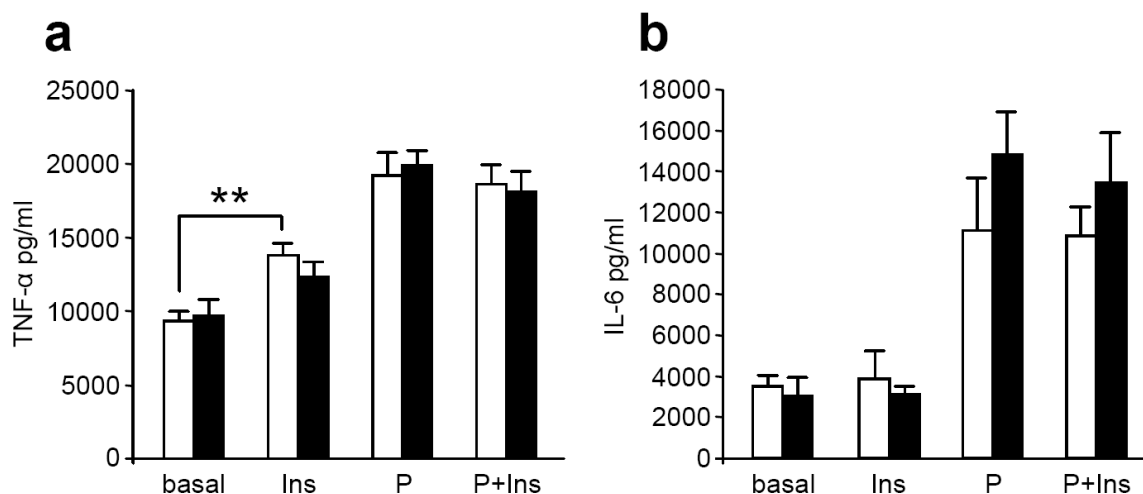


**Fig. 28: Insulin enhances secretion of TNF- $\alpha$  in macrophages.**

Bone marrow-derived macrophages of control and IR<sup>Δmyel</sup> mice were stimulated with insulin (Ins, 50 ng/ml), palmitic acid (P, 500  $\mu$ M) or both for 24 h in serum-free medium and secretion of (a) TNF- $\alpha$  and (b) IL-6 was determined by ELISA. (All data are presented as mean  $\pm$  SEM; n = 4 vs 4; \*\*p  $\leq$  0.01)

### 3.6.3 The Effect of Insulin on Macrophage Migration

An important factor for macrophage migration is their ability to express and secrete matrix metalloproteinases (MMPs) which then help to degrade extracellular matrix (ECM) proteins to allow trans-ECM migration. It has recently been demonstrated that insulin regulates the activity of MMP-9, a member of the type IV collagenase subgroup, in a human monocytic cell line. To investigate the effect of insulin on MMPs in our model, peritoneal macrophages from control and IR<sup>Δmyel</sup> mice were analyzed for expression of MMP-9 mRNA after stimulation with palmitic acid in the presence of serum. As shown in Fig. 29a, MMP-9 mRNA levels were already significantly reduced in untreated macrophages of IR<sup>Δmyel</sup> mice compared to controls. This difference was even more pronounced after stimulation with palmitic acid where MMP-9 mRNA was increased 2.5-fold in control macrophages while insulin receptor-deficient macrophages could enhance MMP-9 expression only 0.5-fold. To directly test the effect of insulin on MMP-9 activity in primary murine macrophages, gelatinase zymography was performed. Stimulation of bone marrow-derived macrophages of control mice with insulin induced MMP-9 activity in the cell culture supernatant (Fig. 29). However, this insulin-mediated increase of MMP-9 gelatinolytic activity could not be observed in supernatant of IR-deficient macrophages.

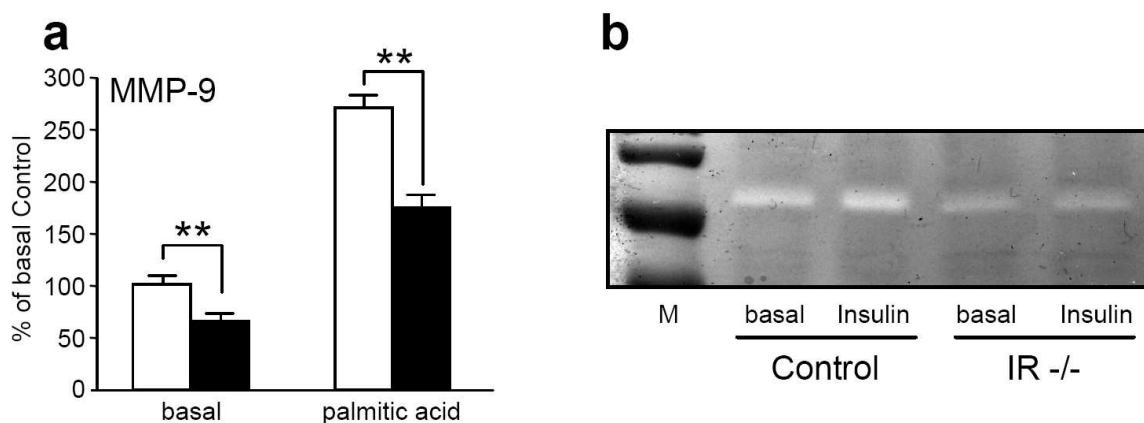


**Fig. 29: Insulin receptor deficiency impairs matrix metalloproteinase 9 expression in macrophages.**

(a) Peritoneal macrophages of control (white columns) and IR<sup>Δmyel</sup> mice (black columns) were treated with palmitic acid or left untreated (basal) for 4 h and expression of MMP-9 mRNA was analysed by quantitative realtime PCR. Hprt1 was used as endogenous control. (b) Cell culture supernatants from 24 h untreated (basal) or insulin-stimulated (50 μg/ml) bone marrow-derived macrophages of control and IR<sup>Δmyel</sup> mice (IR<sup>-/-</sup>) were analyzed by gelatinase zymography. A representative zymogram of three independent experiments is shown (M = protein marker lane; pro-MMP-9 protein size = 105 kDa; All data are presented as mean ± SEM; \*\*p ≤ 0.01)

Boyden chamber analysis, where two compartments are separated by a porous membrane, provides a proper tool for accurate determination of chemotactic behaviour (204). Motile cells are placed into the upper compartment, while the test substance-containing fluid is filled into the lower one. To directly address the migratory potential of insulin receptor-deficient macrophages, Boyden chamber experiments were employed. As depicted in Fig. 30, non-directed (basal) chemotaxis was indistinguishable between control and insulin receptor-deficient macrophages. However, when directed against 25 and 6 ng/ml of the potent chemoattractant MCP-1, control cells showed increased migration towards the lower compartment. Chemotaxis was not induced with 1.5 ng/ml of MCP-1. Strikingly, insulin receptor-deficient macrophages did not increase their migration activity when exposed to MCP-1.

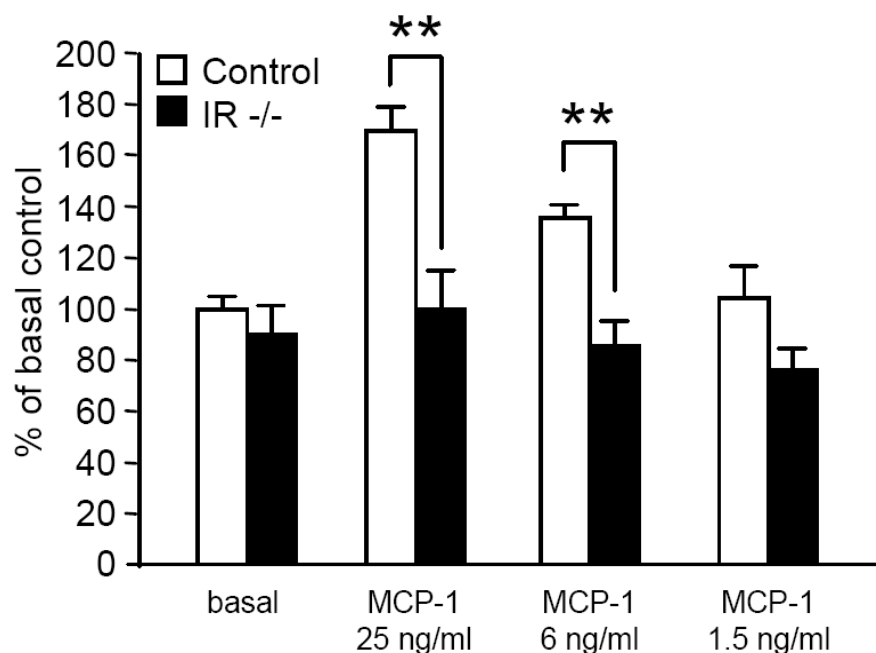


**Fig. 30: Insulin receptor-deficient macrophages show impaired chemotactic abilities.**

Bone marrow-derived macrophages of control and IR<sup>Δmyel</sup> mice were tested for their chemotactic abilities. Chemotaxis against buffer (basal) and different concentrations of MCP-1 was determined. (All data are presented as mean ± SEM; n = 3 vs 3; \*\* p ≤ 0.01)

These data indicate that insulin mediates potent effects on three macrophage key functions. Firstly, it was demonstrated that the hormone promotes macrophage survival under the cytotoxic influence of palmitic acid and enhances expression of Bcl-2. Secondly, insulin was able to increase basal transcription of TNF-α and IL-6 whereas a combination of insulin and palmitic acid augmented the expression of TNF-α while it reduced expression of IL-6. However, secretion of TNF-α and IL-6 by macrophages of IR<sup>Δmyel</sup> mice was not affected although insulin could significantly increase TNF-α release in control macrophages. Finally, insulin was able to enhance expression and secretion of active MMP-9 by control but not IR-deficient macrophages. Additionally, the chemotactic ability of insulin receptor-deficient macrophages towards MCP-1, as assessed by Boyden chamber analysis, was drastically impaired. Taken together, macrophage-autonomous insulin action provides an important signal in controlling metabolic disturbances associated with obesity.

## 4 Discussion

Over the past several years the interplay between inflammatory pathways and insulin action has attracted increasing interest. Interference with certain cytokine-induced signaling pathways and a reduction in obesity-induced inflammation have been demonstrated to provide a potential avenue in the treatment of systemic insulin resistance and impaired glucose metabolism (113, 115). Although the relative contribution and the interaction of cytokine-stimulated JNK and NF $\kappa$ B activation has not been fully elucidated and may exhibit differential, tissue-specific effects, it is evident that inhibiting cytokine-evoked NF $\kappa$ B activation in myeloid cells prevents obesity-associated insulin resistance (114, 115, 205). However, little attention has been given to the effects of insulin itself on macrophage function particularly in the context of the obesity-induced pro-inflammatory state.

In this study, conditional disruption of the insulin receptor was employed to analyze the effect of myeloid cell-autonomous insulin resistance on the development of obesity-induced insulin resistance.

### 4.1 Recombination Efficiency of the LysMCre Transgene

Inactivation of insulin receptor signaling has been achieved through use of the Cre-loxP system. The site-specific DNA recombinase Cre (causes recombination) is a 38 kDa protein of the bacteriophage P1 that recognizes specific 34 bp palindromic sequences, termed *loxP* (locus of crossing (x) over in P1) sites (206). Depending on the orientation of the loxP sites the Cre recombinase mediates the inversion, excision or translocation of the DNA sequence that is flanked by the two loxP sequences (207). DNA sequences flanked by directly repeating loxP sites are excised as a circular molecule, leaving a single loxP sequence at the site of recombination (208). Cre-transgenic mouse strains are generated either by conventional random transgenics, targeted insertion into a gene (knock-in) or by generating bacterial artificial chromosome (BAC)-transgenic mice (209, 210). Regardless of the strategy, the promoter which drives Cre expression determines onset and cell type-specificity of the Cre-mediated recombination. By crossing mice carrying a loxP-flanked mutation of the gene of interest with mice expressing the Cre recombinase restricted to

specific tissues, a conditional mouse mutant is generated that lacks the target gene only in cells in which Cre is expressed.

Expression of the Cre recombinase under control of the lysozyme M promotor (LysMCre) has already successfully been used in numerous studies to conditionally delete loxP-flanked genome regions specifically in myeloid cells (114, 211). Hence, this approach was used in the current study to disrupt the insulin receptor allele in these cells. Ablation efficiency was verified in peritoneal and bone marrow-derived macrophages on genomic DNA, mRNA and protein level. The residual 10% of loxP-flanked alleles detected in bone marrow-derived macrophages of IR<sup>Δmyel</sup> mice can be attributed to contamination with either immune cells of the lymphoid lineage or fibroblasts from the isolation process. Also, the mice generated in this study are heterozygous for the LysMCre allele which could reduce the full Cre-mediated recombination potential (201). Transcription of the insulin receptor mRNA in bone marrow-derived macrophages was also not completely abolished as demonstrated by quantitative realtime PCR. These cells still expressed 15% of insulin receptor mRNA detected in control macrophages. However, western blot analysis of protein lysates from peritoneal macrophages demonstrated a complete absence of immunodetectable insulin receptor protein in cells derived from IR<sup>Δmyel</sup> mice. The discrepancy observed in DNA/mRNA versus protein expression can be attributed to two reasons. Firstly, southern blot analysis and quantitative realtime PCR provide more sensitive detection methods compared to western blot analysis. Secondly, *in vitro* differentiation of macrophages from bone marrow results in a homogenous population of resting macrophages whereas the thioglycolate-elicited peritoneal cell population is heterogenous, consisting mainly of inflammatory, activated macrophages. Since lysozyme is strongly induced in activated macrophages (212), it seems likely that lysozyme M promotor-driven Cre expression is also enhanced in these cells and thus deletion efficiency is increased. Given that obesity results in recruitment of activated macrophages to adipose tissue - although not directly addressed in the present study - it appears very likely that deletion efficiency in these cells is also high. The analysis of insulin receptor protein expression in various tissues of IR<sup>Δmyel</sup> mice revealed no difference compared to control mice although resident macrophages can be found in almost all tissues throughout the body. Isolation and purification of these macrophage populations and subsequent analysis by southern blot or quantitative realtime PCR would provide a superior approach to further investigate the recombination efficiency in tissue resident macrophages.

However, here it has been shown that the LysMCre transgene provides an adequate tool to mediate specific and efficient disruption of the insulin receptor in resting and inflammatory macrophages.

## **4.2 Myeloid Cell-specific Disruption of the Insulin Receptor protects against Obesity-induced Insulin Resistance**

In this study, the commonly employed model of high fat feeding was used to analyze the effect of myeloid cell-restricted insulin resistance on obesity-induced insulin resistance. In control animals, the exposure to a high fat diet (55.2% calories from fat) lead to severe obesity accompanied by a marked increase in circulating leptin, insulin and glucose concentrations compared to lean animals. Moreover, control mice exhibited a pronounced impairment of glucose metabolism and insulin action indicated by increased blood glucose levels and reduced responsiveness to insulin during glucose tolerance test and insulin tolerance test, respectively. Myeloid cell-restricted insulin receptor deficiency did not affect obesity. This was not entirely surprising since myeloid cell-specific disruption of genes that are fundamentally involved in the regulation of macrophage function e.g. IKK $\beta$  and JNK1, either by using the Cre-loxP system or bone marrow transplantation techniques, did not modulate adiposity (114, 158). Until now, changes in body weight after myeloid cell-specific gene deletion were reported only once (168). In this study, transplantation of PPAR $\gamma$ -deficient bone marrow cells into lethally irradiated wildtype mice lead to increased weight gain upon high fat feeding.

However, although adiposity was unchanged, IR <sup>$\Delta$ myel</sup> mice showed a striking protection from obesity-induced hyperglycemia and hyperinsulinemia, two parameters commonly used to define insulin resistance. Furthermore, these mice performed considerably better in glucose and insulin tolerance tests. As demonstrated by euglycemic-hyperinsulinemic clamp analysis, this arises from enhanced insulin-stimulated glucose uptake into skeletal muscle and reduced basal hepatic glucose production. Although glucose uptake into adipose tissue was unaltered during clamp conditions, isolated adipocytes of obese IR <sup>$\Delta$ myel</sup> animals displayed enhanced insulin-stimulated glucose uptake *in vitro*. These cells showed higher sensitivity to insulin, reflected by a shift of the dose response curve without altering the maximal response. Notably, glucose uptake into adipocytes of IR <sup>$\Delta$ myel</sup> mice was markedly increased in response to low rather than high

doses insulin. These experiments explain why glucose uptake was unaltered in adipose tissue of IR<sup>Δmyel</sup> mice during clamp conditions, an experimental setup in which high concentrations of insulin are applied. These data clearly demonstrate that myeloid cell-autonomous insulin resistance protects against the deleterious effect of obesity on glucose metabolism in main insulin target tissues. This is consistent with previous observations that mice with hepatic inactivation of IKKβ retained insulin responsiveness in the liver whereas myeloid cell-restricted disruption of IKKβ resulted in protection against obesity-induced insulin resistance in liver, skeletal muscle and adipose tissue (114). Together with the results of the current study, these findings underline the crucial role of myeloid cells in the control of systemic insulin action under obesity.

### **4.3 Myeloid Cell-specific Disruption of the Insulin Receptor modulates the Obesity-associated Pro-inflammatory Tone**

Aside from improved glucose metabolism and insulin sensitivity, obese IR<sup>Δmyel</sup> mice showed decreased concentration of TNF-α and increased concentration of adiponectin in the circulation when compared to control mice. Circulating TNF-α activates pro-inflammatory kinases like JNK in insulin target tissues leading to S307 phosphorylation of IRS molecules thereby inhibiting insulin action (113). In contrast, adiponectin has been shown to improve glucose metabolism through activation of adenosine monophosphate-activated kinase (AMPK) and inhibition of hepatic gluconeogenesis (213). The observed alteration in concentration of these two proteins may benefit and augment insulin sensitivity in IR<sup>Δmyel</sup> mice upon obesity.

In line with reduced circulating TNF-α, the analysis of JNK in skeletal muscle revealed a dramatic reduction of kinase activity in this tissue. This could potentially explain the enhanced glucose disposal i.e. insulin sensitivity of skeletal muscle, since increased local JNK activity was demonstrated to be positively correlated with muscle insulin resistance (214). However, the question remains why JNK activity in the liver of IR<sup>Δmyel</sup> mice is only slightly decreased although hepatic glucose production is reduced in this tissue. A possible explanation could be that immune cells residing in the liver, maintain local pro-inflammatory signaling (169). Notably, hepatic glucose production is reduced only in the fasted state while remaining unaltered between control and IR<sup>Δmyel</sup> animals after stimulation with insulin. Hence, one could speculate that increased inhibition

of hepatic glucose production i.e. gluconeogenesis in obese  $IR^{\Delta myel}$  mice is a result of the action of adiponectin rather than enhanced hepatic insulin sensitivity. Assessment of AMPK activity, as well as expression of gluconeogenic genes and inflammatory mediators in liver of  $IR^{\Delta myel}$  mice should help to further define the exact cause of decreased basal hepatic glucose production. Moreover, adiponectin has been shown to form higher-order complexes that are differentially distributed in lean, obese and insulin resistant subjects (215). Therefore, determining the abundance of different adiponectin complexes in the circulation of obese  $IR^{\Delta myel}$  mice would be of interest to analyze.

#### **4.4 Myeloid Cell-specific Disruption of the Insulin Receptor blunts the Inflammatory Infiltration of Adipose Tissue by Macrophages**

In the past several years, the inflammatory infiltration of adipose tissue by macrophages and a subsequent increase of pro-inflammatory gene expression has become a central paradigm in obesity-induced insulin resistance (156, 157). Taking the augmented glucose metabolism of  $IR^{\Delta myel}$  mice into consideration, analysis of adipose tissue inflammation and macrophages infiltration represented an interesting approach to further characterize these mice. Diet-induced obese  $IR^{\Delta myel}$  mice showed a dramatic reduction of pro-inflammatory gene expression in adipose tissue indicated by reduced TNF- $\alpha$  mRNA levels. Increased TNF-alpha expression in adipose tissue has been demonstrated to be an important feature of obesity and insulin resistance in humans and rodents (104, 105). Furthermore, neutralization of TNF-alpha in rodents caused a significant increase in peripheral glucose metabolism and insulin action (104). This suggests that the reduction in TNF- $\alpha$  alone, both locally and systemically, reduces the systemic inflammatory tone, thereby exerting a beneficial effect on glucose metabolism and insulin sensitivity in  $IR^{\Delta myel}$  mice.

A considerable amount of TNF- $\alpha$  is expressed by adipocytes. In obesity, however, macrophages are the predominant source of this cytokine (156). Accordingly, we could show that the observed reduction of TNF- $\alpha$  mRNA expression in  $IR^{\Delta myel}$  mice is attributable solely to a reduction in the stromal vascular compartment of the adipose tissue, which is the site of macrophage accumulation, while expression was unchanged in adipocytes. Along with diminished TNF- $\alpha$  expression we observed a striking reduction of

macrophage markers, both on mRNA (F4/80, Mac-2) and protein level (Mac-2). However, expression of CD11c, a surface marker which has recently been shown to be specific for pro-inflammatory M1 macrophages (165), was unchanged in stromal vascular cells of IR<sup>Δmyel</sup> mice. Nonetheless, since CD11c is known to be expressed not only by macrophages but also by dendritic cells (216), the mRNA expression determined in our model could be derived predominantly from these cells, potentially masking any alterations specifically in macrophages.

Chemokines are potent endogenous chemoattractants for macrophages and monocytes. Increased expression of CCL2 (protein: MCP-1) has been associated with obesity and insulin resistance and its production is enhanced during euglycemic hyperinsulinemia in insulin resistant patients (119, 217, 218). It has been postulated that adipose tissue derived MCP-1 contributes to increased macrophage infiltration in obesity (160). In this study, adipose tissue expression of CCL2 was increased by 300% upon high fat feeding. However, with an increase of 2500% in control animals, CCL3 (protein: MIP-1 $\alpha$ ) was induced unequally stronger than CCL2. Furthermore, the increase of CCL3 but not of CCL2 gene expression was significantly abolished in white adipose tissue of obese IR<sup>Δmyel</sup> mice. This indicates that in our model, local changes in CCL3 rather than CCL2 expression are responsible for the reduced infiltration of adipose tissue by macrophages. So far, the increase of MCP-1 but not MIP-1 $\alpha$  serum concentration has been associated with obesity (119). Interestingly, it has been shown that the adipose tissue does not contribute to this systemic increase and adipose tissue-derived MCP-1 only acts in a paracrine fashion (219). Additionally, obese subjects exhibit significantly elevated serum but not adipose tissue-interstitial MCP-1 concentrations, when compared to lean subjects (220). Taken this into account, an intriguing question left to address would be whether local and systemic MCP-1 and MIP-1 $\alpha$  are differentially regulated in IR<sup>Δmyel</sup> mice.

Taken together, the protection from obesity-associated insulin resistance due to impaired insulin action in myeloid cells occurs on two levels. The obesity-induced inflammatory infiltration of macrophages into white adipose tissue is dramatically reduced in IR<sup>Δmyel</sup> mice. This results in reduced local expression and presumably release of TNF- $\alpha$  into the bloodstream, subsequently blunting the obesity-associated rise in circulating inflammatory markers. As a result, the systemic and chronic low-grade inflammation typically found in obese individuals is abrogated (221), thereby preventing the occurrence of obesity-induced insulin resistance.

## 4.5 The Effect of Metabolic Stress on Macrophages

In this study, we sought to expose primary murine macrophages to stimuli which are adequately comparable to the environment encountered in obesity. Special interest was given to hyperlipidemia, here represented by the long chain saturated fatty acid palmitate, as lipids have been demonstrated to exhibit strong modulatory effects on macrophage function (132, 158, 222, 223). The applied amount of palmitic acid (500  $\mu$ M) is comparable to physiological concentrations of fatty acids observed in obese humans and rodents (224, 225). Also, the applied glucose concentration of 200 mg/dl simulates hyperglycemic conditions adequately (226). In the present study, we demonstrate that a cell-autonomous insulin receptor deficiency affects macrophages in terms of survival under metabolic stress conditions, inflammatory gene expression and chemotaxis.

### 4.5.1 Insulin as a Survival Signal for Macrophages

By subjecting primary murine macrophages to the various metabolic stimuli previously mentioned, it became evident that macrophage survival upon fatty acid load is highly dependent on insulin signaling. Insulin efficiently inhibited palmitic acid-induced apoptosis in control macrophages as assessed by DNA fragmentation (TUNEL) assay. Furthermore, basal apoptosis was significantly blocked after exposure to insulin. As expected, the beneficial effect of insulin on macrophage survival was abolished in macrophages from IR <sup>$\Delta$ myel</sup> mice. In line with increasing DNA fragmentation, palmitic acid significantly reduced the expression of anti-apoptotic Bcl-2 and increased that of pro-apoptotic Bax. Treatment with insulin significantly enhanced Bcl-2 expression in control macrophages under basal conditions while after palmitic acid load, only a tendency towards elevated expression of this gene was observed. Taken together, these data suggest that the pro-survival effect of insulin is dependent rather on enhanced anti-apoptotic than reduced pro-apoptotic gene expression.

Additionally, a trend towards higher UPR-related gene expression, represented here by XBP-1 and Chop, was observed in control macrophages. These results are in line with previous observations that insulin, as an inducer of global protein synthesis, increases ER stress, thereby activating several members of the UPR (e.g. GRP78, XBP-1) ultimately

protecting against cell death (185). In the study by Misra et al., the observed anti-apoptotic effect of insulin was mediated by enhanced expression of Bcl-2 and phosphorylation/inhibition of forkhead transcription factor family member FOXO1. Recently, the relevance of these findings has been underlined further by Senokuchi et al. (227), who found that insulin receptor-deficient macrophages exhibited increased susceptibility to cholesterol-induced cell death. The cells could be rescued from apoptosis by either adenoviral introduction of a constitutively active Akt or genetic disruption of FOXO1, thereby restoring the insulin/PI3K-dependent signaling pathways. Notably, in contrast to the design of our study, all experiments were performed in the presence of serum, raising the question whether the effects observed are genuinely insulin-dependent or mediated by the interplay of insulin with other serum-derived factors. Thus, our study demonstrates for the first time that insulin alone can promote macrophage survival in a lipocytotoxic environment, which is potentially dependent on enhanced anti-apoptotic gene expression.

However, the balance between pro- and anti-apoptotic Bcl-2 protein family members localized to the mitochondrial outer membrane plays a central role in the control of apoptosis. Pro-apoptotic proteins such as Bax and Bak, either directly or indirectly, induce the release of proteins from the space between the inner and outer mitochondrial membranes (228, 229). This process of mitochondrial outer membrane permeabilization (MOMP) is likely to be achieved by formation of membrane-spanning pores through which cytochrome *c* and other soluble proteins are released into the cytosol (230, 231). Anti-apoptotic proteins such as Bcl-2 and Bcl-x<sub>L</sub> prevent this release, presumably by blocking pore formation (232). Furthermore, metabolic processing of saturated fatty acids leads to generation of reactive intermediates i.e. reactive oxygen species (ROS). Apoptosis induced by these intermediates is characterized by activation of caspases and DNA-laddering (233). Therefore, analysis of ROS accumulation, caspase activation and cellular localization of Bcl-2 family members would yield further insights into the exact mechanisms underlying insulin's anti-apoptotic effects in macrophages.

#### 4.5.2 Pro-inflammatory Effects of Insulin in Macrophages

In the current study, we demonstrate that insulin has potent effects on inflammatory gene expression in primary murine macrophages. We could show that stimulation with insulin enhances transcription of TNF- $\alpha$  and IL-6 in bone marrow macrophages derived from control mice while this effect was abolished in macrophages from IR <sup>$\Delta$ myel</sup> mice. Furthermore, exposure to palmitic acid drastically exacerbated pro-inflammatory gene expression. Costimulation with palmitic acid and insulin slightly but significantly increased the expression of TNF- $\alpha$  in control macrophages compared to insulin receptor-deficient cells. Conversely, under lipid load, insulin exerted inhibitory effects on IL-6 gene expression in control macrophages. In contrast to its transcriptional effect, insulin could not modulate the secretion of TNF- $\alpha$  and IL-6 under lipid load. However, in the absence of any other stimuli, exposure to insulin induced a significant increase of TNF- $\alpha$  but not IL-6 production in control macrophages. These variable effects of insulin in combination with other pro-inflammatory stimuli on macrophages have been reported previously and seem to be transient. For example, pretreatment with LPS followed by exposure to insulin lead to increased release of TNF- $\alpha$  in a human macrophages cell line (234). On the contrary, when macrophages were primed with insulin followed by subsequent treatment with LPS, activation of NF $\kappa$ B signaling was significantly reduced (235). However, it was previously described that insulin directly induces transcription and release of TNF- $\alpha$  in THP-1 monocytes (182). In terms of mRNA expression, this could be confirmed in murine macrophages and further extended to conditions of hyperlipidemia by the present study. Unexpectedly, this pro-inflammatory effect was only partially conveyed to secretional level. Interestingly, it was recently demonstrated by Iwasaki et al. that insulin exerts short term anti-inflammatory but long term pro-inflammatory effects in hepatocytes (236). In this study, a combined TNF- $\alpha$  and insulin treatment resulted in reduced NF $\kappa$ B-dependent transcription after 6 h but lead to a drastic enhancement after 36-72 h. This long-term effect is in line with previous results obtained in our group, where insulin receptor-deficient macrophages, when compared to control cells, secreted significantly less IL-6 after a 72 h stimulation period with LPS (187). Furthermore, compared to a short-term response, prolonged exposure to insulin and pro-inflammatory stimuli far better matches the conditions encountered in obesity.

A considerable number of inflammatory genes are expressed through activation of NF $\kappa$ B signaling pathways. It has been reported that phosphorylation and proteasomal degradation of inhibitors of NF $\kappa$ B (I $\kappa$ B) is dependent on the activity of Akt/protein kinase

B and that insulin receptor-deficient macrophages exhibit increased I $\kappa$ B $\epsilon$  protein levels (227, 237). Although Akt is classically involved in processes like survival, proliferation, metabolism and glucose uptake especially in the context of insulin signaling, it may also contribute to inflammatory response pathways. Hence, it is plausible that insulin modulates pro-inflammatory signaling events through the PI3K/Akt axis. Additionally, the expression of IL-6 in macrophages is mostly regulated through activation of CCAAT/enhancer binding protein (C/EBP)  $\beta$  also known as nuclear factor IL-6 (NF-IL6) (238). C/EBP $\beta$  is differentially regulated through several cellular kinases including PKC, PKA, Akt and GSK3 $\beta$  (239-241). Also, insulin has been demonstrated to directly activate C/EBP $\beta$  in a PI3K-dependent manner (242). Despite its function as an activator of pro-inflammatory gene expression, C/EBP $\beta$  can also negatively interfere with NF $\kappa$ B-mediated transcription by blocking phosphorylation of p65 (243). Therefore, one could argue that the observed opposing trend of insulin-regulated IL-6 mRNA expression with or without palmitic acid arises from differential activity of C/EBP $\beta$ . Nevertheless, further analysis of inflammatory cascade activation either by insulin alone or in combination with classic pro-inflammatory mediators is required to shed light on these processes.

### **4.5.3 The Effects of Insulin on Macrophage Migration**

The ability to migrate towards loci of inflammation is a central feature of macrophage behaviour. In obesity, chronic inflammation in fat induces the local release of chemokines thereby attracting monocytes from the circulation to enter the tissue which subsequently differentiate into macrophages (157, 166). Proteases like plasminogen (Plg) and matrix metalloproteinases (MMPs) regulate leukocyte recruitment in inflammation by promoting extracellular matrix (ECM) degradation (244, 245). It was recently reported that matrix metalloproteinase 9 (MMP-9) is necessary to provide macrophage trans-ECM migration in inflammation and development of inflammation-associated diseases (246). Interestingly, insulin is able to regulate MMP-9 gelatinolytic activity in a MAPKinase-dependent manner and thereby promotes migration of THP-1 monocytes (247, 248). In the current study we could show that insulin enhances MMP-9 gelatinolytic activity also in primary murine macrophages. Furthermore, it was demonstrated that insulin receptor-deficient macrophages exhibit reduced MMP-9 gene expression in the presence of serum as well as after stimulation with palmitic acid. This implicates a macrophage-autonomous

impairment in ECM-remodeling and migration. Also, after preincubation with insulin, chemotaxis of macrophages from IR<sup>Δmyel</sup> mice towards MCP-1 was significantly blunted compared to controls. These experiments provide an explanation for the reduced macrophage accumulation observed in adipose tissue of diet-induced obese IR<sup>Δmyel</sup> mice. However, *in vivo* evidence for reduced gelatinolytic activity in adipose tissue or reduced circulating matrix metalloproteinase levels in IR<sup>Δmyel</sup> mice is necessary to underline this argument.

Notably, siRNA-mediated knockdown of Cap, which is involved in PI3K-independent insulin-stimulated glucose uptake, leads to impaired motility of RAW264.7 cells *in vitro*. Furthermore, bone marrow-specific deletion of Cap results in reduced obesity-induced macrophage accumulation in adipose tissue of mice (249). In combination with the current study, this underlines the crucial role for insulin in the obesity-induced infiltration of adipose tissue by macrophages. Intriguingly, these results imply a pivotal role for insulin-mediated glucose uptake in macrophages. The dependency of macrophages on hexoses as an energy source in the pro-inflammatory and microhypoxic environment encountered in obesity has been proposed before (174, 250-252). Hypoxia inducible factor (HIF) 1, the central regulator of the hypoxic response, and insulin share common target genes (253). Regulation of these genes is crucial to shift ATP production from the respiratory chain to anaerobic glycolysis thereby maintaining energy supply (254). Thus, the observed phenotype may originate from a fundamental energy problem encountered in insulin receptor-deficient macrophages. Further analysis of hexose metabolism in response to insulin, especially under conditions of hypoxia, hyperlipidemia and hyperglycemia, would provide valuable insight into macrophage function under obesity-associated stress conditions.

## 4.6 Conclusions

Here, we highlight the importance of macrophages as an initiating cell type in the HFD-induced, pro-inflammatory insulin resistance cascade. The findings of the present study reveal an unexpected and pivotal role for insulin signal transduction in the control of innate immune cell behaviour in obesity-induced insulin resistance. Our study demonstrates for the first time *in vivo* that insulin, despite its positive effects on glucose metabolism in target tissues such as liver, skeletal muscle and adipose tissue, can develop a deleterious role in cell types that are not classically involved in metabolic signaling processes. Simulation of the obesity-associated lipidemia by administration of saturated fatty acids to macrophages demonstrates that lipocytotoxicity can eradicate large numbers of these cells *in vitro*. According to our results, high insulin levels might promote the protective signal to maintain macrophage populations in a pro-apoptotic environment *in vivo*. Thereby these cells can perpetuate their devastating behaviour by initiating inflammatory response mechanisms that ultimately induce insulin resistance. In addition, the beneficial effect of hyperinsulinemia on macrophage functions such as pro-inflammatory gene expression and tissue infiltration could further contribute to the harmful role of these cells in obesity-induced insulin resistance. An intriguing question for future experiments is, whether myeloid cells from type 2 diabetic patients are resistant to insulin action. Further exploration of the interaction between metabolic signals and macrophage function offers a promising target for novel interventions in obesity-associated insulin resistance and type 2 diabetes mellitus. Additionally, several other diabetes-associated and macrophage-related diseases such as retinopathy, nephropathy, neuropathy and impaired wound healing represent interesting subjects for further investigation.

## 5 Summary

A major component of obesity-related insulin resistance is the establishment of a chronic inflammatory state with invasion of white adipose tissue by mononuclear cells. This results in release of pro-inflammatory cytokines, which in turn leads to insulin resistance in target tissues such as skeletal muscle and liver. To determine the role of insulin action in macrophages and monocytes in obesity-associated insulin resistance, we have conditionally inactivated the insulin receptor (IR) gene in myeloid cells of mice (IR<sup>Δmyel</sup> mice). While these animals exhibit unaltered glucose metabolism on a normal diet, they are protected from the development of obesity-associated insulin resistance upon high fat feeding. Euglycemic-hyperinsulinemic clamp studies demonstrate that this results from decreased basal hepatic glucose production and from increased insulin-stimulated glucose disposal in skeletal muscle. Furthermore, IR<sup>Δmyel</sup> mice exhibit decreased concentration of circulating tumor necrosis factor (TNF)  $\alpha$  and reduced c-jun N-terminal kinase (JNK) activity in skeletal muscle, reflecting a drastic reduction of the chronic and systemic low-grade inflammatory state associated with obesity. This arises from reduced inflammatory recruitment of macrophages to white adipose tissue. Cell-autonomously, insulin receptor-deficient macrophages are prone to lipid-induced apoptosis and exhibit reduced pro-inflammatory gene transcription. Additionally, these cells show a pronounced impairment of lipid-induced matrix metalloproteinase (MMP) 9 expression and decreased motility in response to macrophage chemoattractant protein (MCP) 1. These data indicate that insulin action in myeloid cells plays an unexpected, critical role in the regulation of macrophage invasion into white adipose tissue and the development of obesity-associated insulin resistance.

## 6 Zusammenfassung

Ein wichtiges Merkmal der Adipositas-assoziierten Insulinresistenz ist die Etablierung einer niedriggradigen aber chronischen Entzündung im Körper. Dieser Entzündungsprozess wird von einer Infiltration des weissen Fettgewebes durch Makrophagen begleitet. Das Resultat dieser Infiltration ist die lokale Ausschüttung proinflammatorischer Zytokine, die dann in die Blutbahn gelangen und eine Insulinresistenz in wichtigen Zielorganen der Insulinwirkung, u.a. Skelettmuskulatur und Leber, verursachen. Um die Rolle der Insulinwirkung auf Makrophagen und Monozyten im Zusammenhang mit der Adipositas-assoziierten Insulinresistenz zu untersuchen, haben wir das Insulinrezeptor (IR) Gen in myeloiden Zellen von Mäusen konditional inaktiviert ( $IR^{\Delta myel}$ ). Während diese Tiere unter Einfluss von Normaldiät einen unveränderten Glukosemetabolismus aufweisen, sind sie vor den verheerenden Konsequenzen einer fettreichen Diät auf die Insulinsensitivität geschützt. Dies ist auf eine verminderte basale, hepatische Glukoseproduktion und eine erhöhte, insulinstimulierte Glukoseaufnahme der Skelettmuskulatur zurückzuführen, was durch euglykämische, hyperinsulinämische Clamp Analyse demonstriert wurde. Darüberhinaus zeigen adipöse  $IR^{\Delta myel}$  Mäuse reduzierte Tumor Nekrose Faktor (TNF)  $\alpha$  Konzentrationen im Blut und verminderte Aktivität der c-jun N-terminalen Kinase (JNK) im Skelettmuskel, was eine drastische Reduktion der Adipositas-assoziierten, chronischen Entzündung reflektiert. Dies resultiert aus einer verminderten inflammatorischen Rekrutierung von Makrophagen in das weisse Fettgewebe. Auf zellautonomer Ebene bewirkt das Fehlen des Insulinrezeptors in Makrophagen eine erhöhte Anfälligkeit für lipidinduzierte Apoptose und eine reduzierte proinflammatorische Gentranskription. Zusätzlich zeigen diese Zellen eine deutliche Beeinträchtigung der lipidinduzierten Expression von Matrix Metalloproteinase (MMP) 9 und eine verminderte Motilität in Reaktion auf Makrophagen Chemoattractant Protein (MCP) 1. Diese Daten belegen, dass Insulin eine entscheidende und kritische Rolle in der Regulation der Infiltration von Makrophagen in das weisse Fettgewebe und der Entwicklung einer Adipositas-assoziierten Insulinresistenz spielen.

## 7 References

1. Mokdad, A.H., Ford, E.S., Bowman, B.A., Dietz, W.H., Vinicor, F., Bales, V.S., and Marks, J.S. 2003. Prevalence of obesity, diabetes, and obesity-related health risk factors, 2001. *Jama* 289:76-79.
2. Silventoinen, K., Sans, S., Tolonen, H., Monterde, D., Kuulasmaa, K., Kesteloot, H., and Tuomilehto, J. 2004. Trends in obesity and energy supply in the WHO MONICA Project. *Int J Obes Relat Metab Disord* 28:710-718.
3. Wang, Y., Monteiro, C., and Popkin, B.M. 2002. Trends of obesity and underweight in older children and adolescents in the United States, Brazil, China, and Russia. *Am J Clin Nutr* 75:971-977.
4. Berghofer, A., Pischon, T., Reinhold, T., Apovian, C.M., Sharma, A.M., and Willich, S.N. 2008. Obesity prevalence from a European perspective: a systematic review. *BMC Public Health* 8:200.
5. WHO. 2005. Obesity and overweight. World Health Organisation.
6. Spiegelman, B.M., and Flier, J.S. 2001. Obesity and the regulation of energy balance. *Cell* 104:531-543.
7. Speakman, J.R. 2004. Obesity: the integrated roles of environment and genetics. *J Nutr* 134:2090S-2105S.
8. Hill, J.O., and Peters, J.C. 1998. Environmental contributions to the obesity epidemic. *Science* 280:1371-1374.
9. James, W.P. 2008. The fundamental drivers of the obesity epidemic. *Obes Rev* 9 Suppl 1:6-13.
10. Mei, Z., Grummer-Strawn, L.M., Pietrobelli, A., Goulding, A., Goran, M.I., and Dietz, W.H. 2002. Validity of body mass index compared with other body-composition screening indexes for the assessment of body fatness in children and adolescents. *Am J Clin Nutr* 75:978-985.
11. Hubert, H.B., Feinleib, M., McNamara, P.M., and Castelli, W.P. 1983. Obesity as an independent risk factor for cardiovascular disease: a 26-year follow-up of participants in the Framingham Heart Study. *Circulation* 67:968-977.
12. Kurth, T., Gaziano, J.M., Berger, K., Kase, C.S., Rexrode, K.M., Cook, N.R., Buring, J.E., and Manson, J.E. 2002. Body mass index and the risk of stroke in men. *Arch Intern Med* 162:2557-2562.

13. Calle, E.E., Rodriguez, C., Walker-Thurmond, K., and Thun, M.J. 2003. Overweight, obesity, and mortality from cancer in a prospectively studied cohort of U.S. adults. *N Engl J Med* 348:1625-1638.
14. Tai, E.S., Lau, T.N., Ho, S.C., Fok, A.C., and Tan, C.E. 2000. Body fat distribution and cardiovascular risk in normal weight women. Associations with insulin resistance, lipids and plasma leptin. *Int J Obes Relat Metab Disord* 24:751-757.
15. Messerli, F.H., Christie, B., DeCarvalho, J.G., Aristimuno, G.G., Suarez, D.H., Dreslinski, G.R., and Frohlich, E.D. 1981. Obesity and essential hypertension. Hemodynamics, intravascular volume, sodium excretion, and plasma renin activity. *Arch Intern Med* 141:81-85.
16. Liuzzi, A., Savia, G., Tagliaferri, M., Lucantoni, R., Berselli, M.E., Petroni, M.L., De Medici, C., and Viberti, G.C. 1999. Serum leptin concentration in moderate and severe obesity: relationship with clinical, anthropometric and metabolic factors. *Int J Obes Relat Metab Disord* 23:1066-1073.
17. Janssen, I., Katzmarzyk, P.T., and Ross, R. 2002. Body mass index, waist circumference, and health risk: evidence in support of current National Institutes of Health guidelines. *Arch Intern Med* 162:2074-2079.
18. Stolk, R.P., Meijer, R., Mali, W.P., Grobbee, D.E., and van der Graaf, Y. 2003. Ultrasound measurements of intraabdominal fat estimate the metabolic syndrome better than do measurements of waist circumference. *Am J Clin Nutr* 77:857-860.
19. Garaulet, M., Perez-Llomas, F., Zamora, S., and Tebar, F.J. 2002. Interrelationship between serum lipid profile, serum hormones and other components of the metabolic syndrome. *J Physiol Biochem* 58:151-160.
20. Rosenbaum, M., and Leibel, R.L. 1999. The role of leptin in human physiology. *N Engl J Med* 341:913-915.
21. Frederich, R.C., Lollmann, B., Hamann, A., Napolitano-Rosen, A., Kahn, B.B., Lowell, B.B., and Flier, J.S. 1995. Expression of ob mRNA and its encoded protein in rodents. Impact of nutrition and obesity. *J Clin Invest* 96:1658-1663.
22. Zhang, Y., Guo, K.Y., Diaz, P.A., Heo, M., and Leibel, R.L. 2002. Determinants of leptin gene expression in fat depots of lean mice. *Am J Physiol Regul Integr Comp Physiol* 282:R226-234.
23. Arita, Y., Kihara, S., Ouchi, N., Takahashi, M., Maeda, K., Miyagawa, J., Hotta, K., Shimomura, I., Nakamura, T., Miyaoka, K., et al. 1999. Paradoxical decrease of an adipose-specific protein, adiponectin, in obesity. *Biochem Biophys Res Commun* 257:79-83.

24. Combs, T.P., Berg, A.H., Obici, S., Scherer, P.E., and Rossetti, L. 2001. Endogenous glucose production is inhibited by the adipose-derived protein Acrp30. *J Clin Invest* 108:1875-1881.
25. Tomas, E., Tsao, T.S., Saha, A.K., Murrey, H.E., Zhang Cc, C., Itani, S.I., Lodish, H.F., and Ruderman, N.B. 2002. Enhanced muscle fat oxidation and glucose transport by ACRP30 globular domain: acetyl-CoA carboxylase inhibition and AMP-activated protein kinase activation. *Proc Natl Acad Sci U S A* 99:16309-16313.
26. MedlinePlus. 2008. The Metabolic Syndrome. National Institute of Diabetes and Digestive and Kidney Diseases.
27. Eckel, R.H., Grundy, S.M., and Zimmet, P.Z. 2005. The metabolic syndrome. *Lancet* 365:1415-1428.
28. Grundy, S.M. 2006. Metabolic syndrome: connecting and reconciling cardiovascular and diabetes worlds. *J Am Coll Cardiol* 47:1093-1100.
29. Ferrannini, E. 2006. Is insulin resistance the cause of the metabolic syndrome? *Ann Med* 38:42-51.
30. Centers for Disease Control and Prevention. 2007. National diabetes fact sheet: general information and national estimates on diabetes in the United States, 2007.: Atlanta, GA: U.S. Department of Health and Human Services, Centers for Disease Control and Prevention, 2007.
31. WHO. 2005. Diabetes. World Health Organisation.
32. King, H., Aubert, R.E., and Herman, W.H. 1998. Global burden of diabetes, 1995-2025: prevalence, numerical estimates, and projections. *Diabetes Care* 21:1414-1431.
33. Tisch, R., and McDevitt, H. 1996. Insulin-dependent diabetes mellitus. *Cell* 85:291-297.
34. 2007. Standards of medical care in diabetes--2007. *Diabetes Care* 30 Suppl 1:S4-S41.
35. Lillioja, S., Mott, D.M., Spraul, M., Ferraro, R., Foley, J.E., Ravussin, E., Knowler, W.C., Bennett, P.H., and Bogardus, C. 1993. Insulin resistance and insulin secretory dysfunction as precursors of non-insulin-dependent diabetes mellitus. Prospective studies of Pima Indians. *N Engl J Med* 329:1988-1992.
36. Muoio, D.M., and Newgard, C.B. 2008. Mechanisms of disease: molecular and metabolic mechanisms of insulin resistance and beta-cell failure in type 2 diabetes. *Nat Rev Mol Cell Biol* 9:193-205.

37. Prentki, M., and Nolan, C.J. 2006. Islet beta cell failure in type 2 diabetes. *J Clin Invest* 116:1802-1812.
38. Steil, G.M., Trivedi, N., Jonas, J.C., Hasenkamp, W.M., Sharma, A., Bonner-Weir, S., and Weir, G.C. 2001. Adaptation of beta-cell mass to substrate oversupply: enhanced function with normal gene expression. *Am J Physiol Endocrinol Metab* 280:E788-796.
39. Srinivasan, S., Bernal-Mizrachi, E., Ohsugi, M., and Permutt, M.A. 2002. Glucose promotes pancreatic islet beta-cell survival through a PI 3-kinase/Akt-signaling pathway. *Am J Physiol Endocrinol Metab* 283:E784-793.
40. van Citters, G.W., Kabir, M., Kim, S.P., Mittelman, S.D., Dea, M.K., Brubaker, P.L., and Bergman, R.N. 2002. Elevated glucagon-like peptide-1-(7-36)-amide, but not glucose, associated with hyperinsulinemic compensation for fat feeding. *J Clin Endocrinol Metab* 87:5191-5198.
41. Shimabukuro, M., Higa, M., Zhou, Y.T., Wang, M.Y., Newgard, C.B., and Unger, R.H. 1998. Lipoapoptosis in beta-cells of obese prediabetic fa/fa rats. Role of serine palmitoyltransferase overexpression. *J Biol Chem* 273:32487-32490.
42. Prentki, M., Joly, E., El-Assaad, W., and Roduit, R. 2002. Malonyl-CoA signaling, lipid partitioning, and glucolipotoxicity: role in beta-cell adaptation and failure in the etiology of diabetes. *Diabetes* 51 Suppl 3:S405-413.
43. Linn, T., Strate, C., and Schneider, K. 1999. Diet promotes beta-cell loss by apoptosis in prediabetic nonobese diabetic mice. *Endocrinology* 140:3767-3773.
44. Saltiel, A.R., and Kahn, C.R. 2001. Insulin signalling and the regulation of glucose and lipid metabolism. *Nature* 414:799-806.
45. Reaven, G.M. 1995. Pathophysiology of insulin resistance in human disease. *Physiol Rev* 75:473-486.
46. Lewis, G.F., Carpentier, A., Adeli, K., and Giacca, A. 2002. Disordered fat storage and mobilization in the pathogenesis of insulin resistance and type 2 diabetes. *Endocr Rev* 23:201-229.
47. Hundal, R.S., Krssak, M., Dufour, S., Laurent, D., Lebon, V., Chandramouli, V., Inzucchi, S.E., Schumann, W.C., Petersen, K.F., Landau, B.R., et al. 2000. Mechanism by which metformin reduces glucose production in type 2 diabetes. *Diabetes* 49:2063-2069.
48. Phillips, L.S., Grunberger, G., Miller, E., Patwardhan, R., Rappaport, E.B., and Salzman, A. 2001. Once- and twice-daily dosing with rosiglitazone improves glycemic control in patients with type 2 diabetes. *Diabetes Care* 24:308-315.

49. King, A.B. 2000. A comparison in a clinical setting of the efficacy and side effects of three thiazolidinediones. *Diabetes Care* 23:557.
50. Zimmerman, B.R. 1997. Sulfonylureas. *Endocrinol Metab Clin North Am* 26:511-522.
51. Yuan, M., Konstantopoulos, N., Lee, J., Hansen, L., Li, Z.W., Karin, M., and Shoelson, S.E. 2001. Reversal of obesity- and diet-induced insulin resistance with salicylates or targeted disruption of Ikkbeta. *Science* 293:1673-1677.
52. Hundal, R.S., Petersen, K.F., Mayerson, A.B., Randhawa, P.S., Inzucchi, S., Shoelson, S.E., and Shulman, G.I. 2002. Mechanism by which high-dose aspirin improves glucose metabolism in type 2 diabetes. *J Clin Invest* 109:1321-1326.
53. Knowler, W.C., Barrett-Connor, E., Fowler, S.E., Hamman, R.F., Lachin, J.M., Walker, E.A., and Nathan, D.M. 2002. Reduction in the incidence of type 2 diabetes with lifestyle intervention or metformin. *N Engl J Med* 346:393-403.
54. Booth, F.W., Chakravarthy, M.V., Gordon, S.E., and Spangenburg, E.E. 2002. Waging war on physical inactivity: using modern molecular ammunition against an ancient enemy. *J Appl Physiol* 93:3-30.
55. Gariano, R.F., and Gardner, T.W. 2005. Retinal angiogenesis in development and disease. *Nature* 438:960-966.
56. Reiber, G.E., Vileikyte, L., Boyko, E.J., del Aguila, M., Smith, D.G., Lavery, L.A., and Boulton, A.J. 1999. Causal pathways for incident lower-extremity ulcers in patients with diabetes from two settings. *Diabetes Care* 22:157-162.
57. Remuzzi, G., Schieppati, A., and Ruggenenti, P. 2002. Clinical practice. Nephropathy in patients with type 2 diabetes. *N Engl J Med* 346:1145-1151.
58. Adler, A.I., Stevens, R.J., Manley, S.E., Bilous, R.W., Cull, C.A., and Holman, R.R. 2003. Development and progression of nephropathy in type 2 diabetes: the United Kingdom Prospective Diabetes Study (UKPDS 64). *Kidney Int* 63:225-232.
59. 2007. Genome-wide association study of 14,000 cases of seven common diseases and 3,000 shared controls. *Nature* 447:661-678.
60. Killilea, T. 2002. Long-term consequences of type 2 diabetes mellitus: economic impact on society and managed care. *Am J Manag Care* 8:S441-449.
61. Bluher, M., Michael, M.D., Peroni, O.D., Ueki, K., Carter, N., Kahn, B.B., and Kahn, C.R. 2002. Adipose tissue selective insulin receptor knockout protects against obesity and obesity-related glucose intolerance. *Dev Cell* 3:25-38.

62. Brady, M.J., and Saltiel, A.R. 1999. Closing in on the cause of insulin resistance and type 2 diabetes. *J Clin Invest* 104:675-676.
63. Cushman, S.W., and Wardzala, L.J. 1980. Potential mechanism of insulin action on glucose transport in the isolated rat adipose cell. Apparent translocation of intracellular transport systems to the plasma membrane. *J Biol Chem* 255:4758-4762.
64. Cushman, S.W., Wardzala, L.J., Simpson, I.A., Karnieli, E., Hissin, P.J., Wheeler, T.J., Hinkle, P.C., and Salans, L.B. 1984. Insulin-induced translocation of intracellular glucose transporters in the isolated rat adipose cell. *Fed Proc* 43:2251-2255.
65. Terrettaz, J., Assimacopoulos-Jeannet, F., and Jeanrenaud, B. 1986. Inhibition of hepatic glucose production by insulin in vivo in rats: contribution of glycolysis. *Am J Physiol* 250:E346-351.
66. Claus, T.H., and Pilkis, S.J. 1976. Regulation by insulin of gluconeogenesis in isolated rat hepatocytes. *Biochim Biophys Acta* 421:246-262.
67. Michael, M.D., Kulkarni, R.N., Postic, C., Previs, S.F., Shulman, G.I., Magnuson, M.A., and Kahn, C.R. 2000. Loss of insulin signaling in hepatocytes leads to severe insulin resistance and progressive hepatic dysfunction. *Mol Cell* 6:87-97.
68. Roth, J. 1973. Peptide hormone binding to receptors: a review of direct studies in vitro. *Metabolism* 22:1059-1073.
69. Patti, M.E., and Kahn, C.R. 1998. The insulin receptor--a critical link in glucose homeostasis and insulin action. *J Basic Clin Physiol Pharmacol* 9:89-109.
70. Eck, M.J., Dhe-Paganon, S., Trub, T., Nolte, R.T., and Shoelson, S.E. 1996. Structure of the IRS-1 PTB domain bound to the juxtamembrane region of the insulin receptor. *Cell* 85:695-705.
71. Miralpeix, M., Sun, X.J., Backer, J.M., Myers, M.G., Jr., Araki, E., and White, M.F. 1992. Insulin stimulates tyrosine phosphorylation of multiple high molecular weight substrates in Fao hepatoma cells. *Biochemistry* 31:9031-9039.
72. White, M.F., Livingston, J.N., Backer, J.M., Lauris, V., Dull, T.J., Ullrich, A., and Kahn, C.R. 1988. Mutation of the insulin receptor at tyrosine 960 inhibits signal transmission but does not affect its tyrosine kinase activity. *Cell* 54:641-649.
73. Kahn, C.R., Baird, K.L., Jarrett, D.B., and Flier, J.S. 1978. Direct demonstration that receptor crosslinking or aggregation is important in insulin action. *Proc Natl Acad Sci U S A* 75:4209-4213.

74. Burks, D.J., Wang, J., Towery, H., Ishibashi, O., Lowe, D., Riedel, H., and White, M.F. 1998. IRS pleckstrin homology domains bind to acidic motifs in proteins. *J Biol Chem* 273:31061-31067.
75. Jacobs, A.R., LeRoith, D., and Taylor, S.I. 2001. Insulin receptor substrate-1 pleckstrin homology and phosphotyrosine-binding domains are both involved in plasma membrane targeting. *J Biol Chem* 276:40795-40802.
76. Sun, X.J., Rothenberg, P., Kahn, C.R., Backer, J.M., Araki, E., Wilden, P.A., Cahill, D.A., Goldstein, B.J., and White, M.F. 1991. Structure of the insulin receptor substrate IRS-1 defines a unique signal transduction protein. *Nature* 352:73-77.
77. Sun, X.J., Wang, L.M., Zhang, Y., Yenush, L., Myers, M.G., Jr., Glasheen, E., Lane, W.S., Pierce, J.H., and White, M.F. 1995. Role of IRS-2 in insulin and cytokine signalling. *Nature* 377:173-177.
78. White, M.F. 1998. The IRS-signalling system: a network of docking proteins that mediate insulin action. *Mol Cell Biochem* 182:3-11.
79. Holgado-Madruga, M., Emllet, D.R., Moscatello, D.K., Godwin, A.K., and Wong, A.J. 1996. A Grb2-associated docking protein in EGF- and insulin-receptor signalling. *Nature* 379:560-564.
80. Yamanashi, Y., and Baltimore, D. 1997. Identification of the Abl- and rasGAP-associated 62 kDa protein as a docking protein, Dok. *Cell* 88:205-211.
81. Pessin, J.E., and Saltiel, A.R. 2000. Signaling pathways in insulin action: molecular targets of insulin resistance. *J Clin Invest* 106:165-169.
82. De Fea, K., and Roth, R.A. 1997. Protein kinase C modulation of insulin receptor substrate-1 tyrosine phosphorylation requires serine 612. *Biochemistry* 36:12939-12947.
83. Myers, M.G., Jr., Sun, X.J., Cheatham, B., Jachna, B.R., Glasheen, E.M., Backer, J.M., and White, M.F. 1993. IRS-1 is a common element in insulin and insulin-like growth factor-I signaling to the phosphatidylinositol 3'-kinase. *Endocrinology* 132:1421-1430.
84. Skolnik, E.Y., Batzer, A., Li, N., Lee, C.H., Lowenstein, E., Mohammadi, M., Margolis, B., and Schlessinger, J. 1993. The function of GRB2 in linking the insulin receptor to Ras signaling pathways. *Science* 260:1953-1955.
85. Myers, M.G., Jr., Backer, J.M., Sun, X.J., Shoelson, S., Hu, P., Schlessinger, J., Yoakim, M., Schaffhausen, B., and White, M.F. 1992. IRS-1 activates phosphatidylinositol 3'-kinase by associating with src homology 2 domains of p85. *Proc Natl Acad Sci U S A* 89:10350-10354.

86. Boulton, T.G., Nye, S.H., Robbins, D.J., Ip, N.Y., Radziejewska, E., Morgenbesser, S.D., DePinho, R.A., Panayotatos, N., Cobb, M.H., and Yancopoulos, G.D. 1991. ERKs: a family of protein-serine/threonine kinases that are activated and tyrosine phosphorylated in response to insulin and NGF. *Cell* 65:663-675.
87. Lazar, D.F., Wiese, R.J., Brady, M.J., Mastick, C.C., Waters, S.B., Yamauchi, K., Pessin, J.E., Cuatrecasas, P., and Saltiel, A.R. 1995. Mitogen-activated protein kinase kinase inhibition does not block the stimulation of glucose utilization by insulin. *J Biol Chem* 270:20801-20807.
88. Aikawa, R., Nawano, M., Gu, Y., Katagiri, H., Asano, T., Zhu, W., Nagai, R., and Komuro, I. 2000. Insulin prevents cardiomyocytes from oxidative stress-induced apoptosis through activation of PI3 kinase/Akt. *Circulation* 102:2873-2879.
89. Shepherd, P.R., Nave, B.T., and Siddle, K. 1995. Insulin stimulation of glycogen synthesis and glycogen synthase activity is blocked by wortmannin and rapamycin in 3T3-L1 adipocytes: evidence for the involvement of phosphoinositide 3-kinase and p70 ribosomal protein-S6 kinase. *Biochem J* 305 ( Pt 1):25-28.
90. Cross, D.A., Alessi, D.R., Cohen, P., Andjelkovich, M., and Hemmings, B.A. 1995. Inhibition of glycogen synthase kinase-3 by insulin mediated by protein kinase B. *Nature* 378:785-789.
91. Nave, B.T., Ouwens, M., Withers, D.J., Alessi, D.R., and Shepherd, P.R. 1999. Mammalian target of rapamycin is a direct target for protein kinase B: identification of a convergence point for opposing effects of insulin and amino-acid deficiency on protein translation. *Biochem J* 344 Pt 2:427-431.
92. Baumann, C.A., Ribon, V., Kanzaki, M., Thurmond, D.C., Mora, S., Shigematsu, S., Bickel, P.E., Pessin, J.E., and Saltiel, A.R. 2000. CAP defines a second signalling pathway required for insulin-stimulated glucose transport. *Nature* 407:202-207.
93. Bastard, J.P., Maachi, M., Van Nhieu, J.T., Jardel, C., Bruckert, E., Grimaldi, A., Robert, J.J., Capeau, J., and Hainque, B. 2002. Adipose tissue IL-6 content correlates with resistance to insulin activation of glucose uptake both in vivo and in vitro. *J Clin Endocrinol Metab* 87:2084-2089.
94. Trischitta, V., Brunetti, A., Chiavetta, A., Benzi, L., Papa, V., and Vigneri, R. 1989. Defects in insulin-receptor internalization and processing in monocytes of obese subjects and obese NIDDM patients. *Diabetes* 38:1579-1584.
95. Patki, V., Buxton, J., Chawla, A., Lifshitz, L., Fogarty, K., Carrington, W., Tuft, R., and Corvera, S. 2001. Insulin action on GLUT4 traffic visualized in single 3T3-L1 adipocytes by using ultra-fast microscopy. *Mol Biol Cell* 12:129-141.

96. Liu, J., Kimura, A., Baumann, C.A., and Saltiel, A.R. 2002. APS facilitates c-Cbl tyrosine phosphorylation and GLUT4 translocation in response to insulin in 3T3-L1 adipocytes. *Mol Cell Biol* 22:3599-3609.
97. JeBailey, L., Rudich, A., Huang, X., Di Ciano-Oliveira, C., Kapus, A., and Klip, A. 2004. Skeletal muscle cells and adipocytes differ in their reliance on TC10 and Rac for insulin-induced actin remodeling. *Mol Endocrinol* 18:359-372.
98. Chiang, S.H., Baumann, C.A., Kanzaki, M., Thurmond, D.C., Watson, R.T., Neudauer, C.L., Macara, I.G., Pessin, J.E., and Saltiel, A.R. 2001. Insulin-stimulated GLUT4 translocation requires the CAP-dependent activation of TC10. *Nature* 410:944-948.
99. Chandra, R.K. 1996. Nutrition, immunity and infection: from basic knowledge of dietary manipulation of immune responses to practical application of ameliorating suffering and improving survival. *Proc Natl Acad Sci U S A* 93:14304-14307.
100. Blackburn, G.L. 2001. Pasteur's Quadrant and malnutrition. *Nature* 409:397-401.
101. Khovidhunkit, W., Kim, M.S., Memon, R.A., Shigenaga, J.K., Moser, A.H., Feingold, K.R., and Grunfeld, C. 2004. Effects of infection and inflammation on lipid and lipoprotein metabolism: mechanisms and consequences to the host. *J Lipid Res* 45:1169-1196.
102. Wellen, K.E., and Hotamisligil, G.S. 2005. Inflammation, stress, and diabetes. *J Clin Invest* 115:1111-1119.
103. Shoelson, S.E., Lee, J., and Goldfine, A.B. 2006. Inflammation and insulin resistance. *J Clin Invest* 116:1793-1801.
104. Hotamisligil, G.S., Shargill, N.S., and Spiegelman, B.M. 1993. Adipose expression of tumor necrosis factor-alpha: direct role in obesity-linked insulin resistance. *Science* 259:87-91.
105. Hotamisligil, G.S., Arner, P., Caro, J.F., Atkinson, R.L., and Spiegelman, B.M. 1995. Increased adipose tissue expression of tumor necrosis factor-alpha in human obesity and insulin resistance. *J Clin Invest* 95:2409-2415.
106. Kanety, H., Feinstein, R., Papa, M.Z., Hemi, R., and Karasik, A. 1995. Tumor necrosis factor alpha-induced phosphorylation of insulin receptor substrate-1 (IRS-1). Possible mechanism for suppression of insulin-stimulated tyrosine phosphorylation of IRS-1. *J Biol Chem* 270:23780-23784.
107. Brenner, D.A., O'Hara, M., Angel, P., Chojkier, M., and Karin, M. 1989. Prolonged activation of jun and collagenase genes by tumour necrosis factor-alpha. *Nature* 337:661-663.

108. Mercurio, F., Zhu, H., Murray, B.W., Shevchenko, A., Bennett, B.L., Li, J., Young, D.B., Barbosa, M., Mann, M., Manning, A., et al. 1997. IKK-1 and IKK-2: cytokine-activated I $\kappa$ B kinases essential for NF- $\kappa$ B activation. *Science* 278:860-866.
109. Hotamisligil, G.S., Peraldi, P., Budavari, A., Ellis, R., White, M.F., and Spiegelman, B.M. 1996. IRS-1-mediated inhibition of insulin receptor tyrosine kinase activity in TNF- $\alpha$ - and obesity-induced insulin resistance. *Science* 271:665-668.
110. Aguirre, V., Uchida, T., Yenush, L., Davis, R., and White, M.F. 2000. The c-Jun NH(2)-terminal kinase promotes insulin resistance during association with insulin receptor substrate-1 and phosphorylation of Ser(307). *J Biol Chem* 275:9047-9054.
111. Aguirre, V., Werner, E.D., Giraud, J., Lee, Y.H., Shoelson, S.E., and White, M.F. 2002. Phosphorylation of Ser307 in insulin receptor substrate-1 blocks interactions with the insulin receptor and inhibits insulin action. *J Biol Chem* 277:1531-1537.
112. Paz, K., Hemi, R., LeRoith, D., Karasik, A., Elhanany, E., Kanety, H., and Zick, Y. 1997. A molecular basis for insulin resistance. Elevated serine/threonine phosphorylation of IRS-1 and IRS-2 inhibits their binding to the juxtamembrane region of the insulin receptor and impairs their ability to undergo insulin-induced tyrosine phosphorylation. *J Biol Chem* 272:29911-29918.
113. Hirosumi, J., Tuncman, G., Chang, L., Gorgun, C.Z., Uysal, K.T., Maeda, K., Karin, M., and Hotamisligil, G.S. 2002. A central role for JNK in obesity and insulin resistance. *Nature* 420:333-336.
114. Arkan, M.C., Hevener, A.L., Greten, F.R., Maeda, S., Li, Z.W., Long, J.M., Wynshaw-Boris, A., Poli, G., Olefsky, J., and Karin, M. 2005. IKK-beta links inflammation to obesity-induced insulin resistance. *Nat Med* 11:191-198.
115. Cai, D., Yuan, M., Frantz, D.F., Melendez, P.A., Hansen, L., Lee, J., and Shoelson, S.E. 2005. Local and systemic insulin resistance resulting from hepatic activation of IKK-beta and NF- $\kappa$ B. *Nat Med* 11:183-190.
116. Rotter, V., Nagaev, I., and Smith, U. 2003. Interleukin-6 (IL-6) induces insulin resistance in 3T3-L1 adipocytes and is, like IL-8 and tumor necrosis factor- $\alpha$ , overexpressed in human fat cells from insulin-resistant subjects. *J Biol Chem* 278:45777-45784.
117. Juge-Aubry, C.E., Somm, E., Giusti, V., Pernin, A., Chicheportiche, R., Verdumo, C., Rohner-Jeanraud, F., Burger, D., Dayer, J.M., and Meier, C.A. 2003. Adipose tissue is a major source of interleukin-1 receptor antagonist: upregulation in obesity and inflammation. *Diabetes* 52:1104-1110.
118. Straczkowski, M., Dzienis-Straczkowska, S., Stepień, A., Kowalska, I., Szelachowska, M., and Kinalska, I. 2002. Plasma interleukin-8 concentrations are

- increased in obese subjects and related to fat mass and tumor necrosis factor-alpha system. *J Clin Endocrinol Metab* 87:4602-4606.
119. Sartipy, P., and Loskutoff, D.J. 2003. Monocyte chemoattractant protein 1 in obesity and insulin resistance. *Proc Natl Acad Sci U S A* 100:7265-7270.
  120. Derosa, G., Ferrari, I., D'Angelo, A., Tinelli, C., Salvadeo, S.A., Ciccarelli, L., Piccinni, M.N., Gravina, A., Ramondetti, F., Maffioli, P., et al. 2008. Matrix metalloproteinase-2 and -9 levels in obese patients. *Endothelium* 15:219-224.
  121. Deepa, R., Velmurugan, K., Arvind, K., Sivaram, P., Sientay, C., Uday, S., and Mohan, V. 2006. Serum levels of interleukin 6, C-reactive protein, vascular cell adhesion molecule 1, and monocyte chemotactic protein 1 in relation to insulin resistance and glucose intolerance--the Chennai Urban Rural Epidemiology Study (CURES). *Metabolism* 55:1232-1238.
  122. Solinas, G., Naugler, W., Galimi, F., Lee, M.S., and Karin, M. 2006. Saturated fatty acids inhibit induction of insulin gene transcription by JNK-mediated phosphorylation of insulin-receptor substrates. *Proc Natl Acad Sci U S A* 103:16454-16459.
  123. Gao, Z., Zhang, X., Zuberi, A., Hwang, D., Quon, M.J., Lefevre, M., and Ye, J. 2004. Inhibition of insulin sensitivity by free fatty acids requires activation of multiple serine kinases in 3T3-L1 adipocytes. *Mol Endocrinol* 18:2024-2034.
  124. Nguyen, M.T., Satoh, H., Favelyukis, S., Babendure, J.L., Imamura, T., Sbodio, J.I., Zalevsky, J., Dahiyat, B.I., Chi, N.W., and Olefsky, J.M. 2005. JNK and tumor necrosis factor-alpha mediate free fatty acid-induced insulin resistance in 3T3-L1 adipocytes. *J Biol Chem* 280:35361-35371.
  125. Yu, C., Chen, Y., Cline, G.W., Zhang, D., Zong, H., Wang, Y., Bergeron, R., Kim, J.K., Cushman, S.W., Cooney, G.J., et al. 2002. Mechanism by which fatty acids inhibit insulin activation of insulin receptor substrate-1 (IRS-1)-associated phosphatidylinositol 3-kinase activity in muscle. *J Biol Chem* 277:50230-50236.
  126. Griffin, M.E., Marcucci, M.J., Cline, G.W., Bell, K., Barucci, N., Lee, D., Goodyear, L.J., Kraegen, E.W., White, M.F., and Shulman, G.I. 1999. Free fatty acid-induced insulin resistance is associated with activation of protein kinase C theta and alterations in the insulin signaling cascade. *Diabetes* 48:1270-1274.
  127. Kim, J.K., Fillmore, J.J., Sunshine, M.J., Albrecht, B., Higashimori, T., Kim, D.W., Liu, Z.X., Soos, T.J., Cline, G.W., O'Brien, W.R., et al. 2004. PKC-theta knockout mice are protected from fat-induced insulin resistance. *J Clin Invest* 114:823-827.
  128. Medzhitov, R. 2001. Toll-like receptors and innate immunity. *Nat Rev Immunol* 1:135-145.

129. Zuany-Amorim, C., Hastewell, J., and Walker, C. 2002. Toll-like receptors as potential therapeutic targets for multiple diseases. *Nat Rev Drug Discov* 1:797-807.
130. Hwang, D. 2001. Modulation of the expression of cyclooxygenase-2 by fatty acids mediated through toll-like receptor 4-derived signaling pathways. *Faseb J* 15:2556-2564.
131. Lee, J.Y., Sohn, K.H., Rhee, S.H., and Hwang, D. 2001. Saturated fatty acids, but not unsaturated fatty acids, induce the expression of cyclooxygenase-2 mediated through Toll-like receptor 4. *J Biol Chem* 276:16683-16689.
132. Shi, H., Kokoeva, M.V., Inouye, K., Tzameli, I., Yin, H., and Flier, J.S. 2006. TLR4 links innate immunity and fatty acid-induced insulin resistance. *J Clin Invest* 116:3015-3025.
133. Morino, K., Petersen, K.F., and Shulman, G.I. 2006. Molecular mechanisms of insulin resistance in humans and their potential links with mitochondrial dysfunction. *Diabetes* 55 Suppl 2:S9-S15.
134. Schenk, S., and Horowitz, J.F. 2007. Acute exercise increases triglyceride synthesis in skeletal muscle and prevents fatty acid-induced insulin resistance. *J Clin Invest* 117:1690-1698.
135. Liu, L., Zhang, Y., Chen, N., Shi, X., Tsang, B., and Yu, Y.H. 2007. Upregulation of myocellular DGAT1 augments triglyceride synthesis in skeletal muscle and protects against fat-induced insulin resistance. *J Clin Invest* 117:1679-1689.
136. Summers, S.A. 2006. Ceramides in insulin resistance and lipotoxicity. *Prog Lipid Res* 45:42-72.
137. Ron, D., and Walter, P. 2007. Signal integration in the endoplasmic reticulum unfolded protein response. *Nat Rev Mol Cell Biol* 8:519-529.
138. Ozcan, U., Cao, Q., Yilmaz, E., Lee, A.H., Iwakoshi, N.N., Ozdelen, E., Tuncman, G., Gorgun, C., Glimcher, L.H., and Hotamisligil, G.S. 2004. Endoplasmic reticulum stress links obesity, insulin action, and type 2 diabetes. *Science* 306:457-461.
139. Hetz, C., Bernasconi, P., Fisher, J., Lee, A.H., Bassik, M.C., Antonsson, B., Brandt, G.S., Iwakoshi, N.N., Schinzel, A., Glimcher, L.H., et al. 2006. Proapoptotic BAX and BAK modulate the unfolded protein response by a direct interaction with IRE1alpha. *Science* 312:572-576.
140. Wei, M.C., Zong, W.X., Cheng, E.H., Lindsten, T., Panoutsakopoulou, V., Ross, A.J., Roth, K.A., MacGregor, G.R., Thompson, C.B., and Korsmeyer, S.J. 2001. Proapoptotic BAX and BAK: a requisite gateway to mitochondrial dysfunction and death. *Science* 292:727-730.

141. Nakagawa, T., Zhu, H., Morishima, N., Li, E., Xu, J., Yankner, B.A., and Yuan, J. 2000. Caspase-12 mediates endoplasmic-reticulum-specific apoptosis and cytotoxicity by amyloid-beta. *Nature* 403:98-103.
142. Urano, F., Wang, X., Bertolotti, A., Zhang, Y., Chung, P., Harding, H.P., and Ron, D. 2000. Coupling of stress in the ER to activation of JNK protein kinases by transmembrane protein kinase IRE1. *Science* 287:664-666.
143. Yoneda, T., Imaizumi, K., Oono, K., Yui, D., Gomi, F., Katayama, T., and Tohyama, M. 2001. Activation of caspase-12, an endoplasmic reticulum (ER) resident caspase, through tumor necrosis factor receptor-associated factor 2-dependent mechanism in response to the ER stress. *J Biol Chem* 276:13935-13940.
144. Iwakoshi, N.N., Lee, A.H., Vallabhajosyula, P., Otipoby, K.L., Rajewsky, K., and Glimcher, L.H. 2003. Plasma cell differentiation and the unfolded protein response intersect at the transcription factor XBP-1. *Nat Immunol* 4:321-329.
145. Ozcan, U., Yilmaz, E., Ozcan, L., Furuhashi, M., Vaillancourt, E., Smith, R.O., Gorgun, C.Z., and Hotamisligil, G.S. 2006. Chemical chaperones reduce ER stress and restore glucose homeostasis in a mouse model of type 2 diabetes. *Science* 313:1137-1140.
146. van Furth, R., and Cohn, Z.A. 1968. The origin and kinetics of mononuclear phagocytes. *J Exp Med* 128:415-435.
147. Ebert, R.H., and Florey, H.W. 1939. The extravascular development of the monocyte observed in vivo. *Brit. J. Exp. Pathol.* 20:342-356.
148. Van Furth, R., Diesselhoff-den Dulk, M.C., and Mattie, H. 1973. Quantitative study on the production and kinetics of mononuclear phagocytes during an acute inflammatory reaction. *J Exp Med* 138:1314-1330.
149. Franke-Ullmann, G., Pfortner, C., Walter, P., Steinmuller, C., Lohmann-Matthes, M.L., Kobzik, L., and Freihorst, J. 1995. Alteration of pulmonary macrophage function by respiratory syncytial virus infection in vitro. *J Immunol* 154:268-280.
150. Medzhitov, R., and Janeway, C., Jr. 2000. Innate immunity. *N Engl J Med* 343:338-344.
151. Naito, M. 2008. Macrophage differentiation and function in health and disease. *Pathol Int* 58:143-155.
152. Tesch, G.H. 2007. Role of macrophages in complications of type 2 diabetes. *Clin Exp Pharmacol Physiol* 34:1016-1019.
153. Trayhurn, P., and Beattie, J.H. 2001. Physiological role of adipose tissue: white adipose tissue as an endocrine and secretory organ. *Proc Nutr Soc* 60:329-339.

154. Ye, J., Gao, Z., Yin, J., and He, Q. 2007. Hypoxia is a potential risk factor for chronic inflammation and adiponectin reduction in adipose tissue of ob/ob and dietary obese mice. *Am J Physiol Endocrinol Metab* 293:E1118-1128.
155. Cinti, S., Mitchell, G., Barbatelli, G., Murano, I., Ceresi, E., Faloia, E., Wang, S., Fortier, M., Greenberg, A.S., and Obin, M.S. 2005. Adipocyte death defines macrophage localization and function in adipose tissue of obese mice and humans. *J Lipid Res* 46:2347-2355.
156. Xu, H., Barnes, G.T., Yang, Q., Tan, G., Yang, D., Chou, C.J., Sole, J., Nichols, A., Ross, J.S., Tartaglia, L.A., et al. 2003. Chronic inflammation in fat plays a crucial role in the development of obesity-related insulin resistance. *J Clin Invest* 112:1821-1830.
157. Weisberg, S.P., McCann, D., Desai, M., Rosenbaum, M., Leibel, R.L., and Ferrante, A.W., Jr. 2003. Obesity is associated with macrophage accumulation in adipose tissue. *J Clin Invest* 112:1796-1808.
158. Solinas, G., Vilcu, C., Neels, J.G., Bandyopadhyay, G.K., Luo, J.L., Naugler, W., Grivennikov, S., Wynshaw-Boris, A., Scadeng, M., Olefsky, J.M., et al. 2007. JNK1 in hematopoietically derived cells contributes to diet-induced inflammation and insulin resistance without affecting obesity. *Cell Metab* 6:386-397.
159. Weisberg, S.P., Hunter, D., Huber, R., Lemieux, J., Slaymaker, S., Vaddi, K., Charo, I., Leibel, R.L., and Ferrante, A.W., Jr. 2006. CCR2 modulates inflammatory and metabolic effects of high-fat feeding. *J Clin Invest* 116:115-124.
160. Kanda, H., Tateya, S., Tamori, Y., Kotani, K., Hiasa, K., Kitazawa, R., Kitazawa, S., Miyachi, H., Maeda, S., Egashira, K., et al. 2006. MCP-1 contributes to macrophage infiltration into adipose tissue, insulin resistance, and hepatic steatosis in obesity. *J Clin Invest* 116:1494-1505.
161. Gordon, S., and Taylor, P.R. 2005. Monocyte and macrophage heterogeneity. *Nat Rev Immunol* 5:953-964.
162. Mosser, D.M. 2003. The many faces of macrophage activation. *J Leukoc Biol* 73:209-212.
163. Mantovani, A., Sica, A., Sozzani, S., Allavena, P., Vecchi, A., and Locati, M. 2004. The chemokine system in diverse forms of macrophage activation and polarization. *Trends Immunol* 25:677-686.
164. Lumeng, C.N., Deyoung, S.M., Bodzin, J.L., and Saltiel, A.R. 2007. Increased inflammatory properties of adipose tissue macrophages recruited during diet-induced obesity. *Diabetes* 56:16-23.
165. Lumeng, C.N., Bodzin, J.L., and Saltiel, A.R. 2007. Obesity induces a phenotypic switch in adipose tissue macrophage polarization. *J Clin Invest* 117:175-184.

166. Lumeng, C.N., Delproposto, J.B., Westcott, D.J., and Saltiel, A.R. 2008. Phenotypic switching of adipose tissue macrophages with obesity is generated by spatiotemporal differences in macrophage subtypes. *Diabetes*.
167. Wahli, W., Devchand, P.R., A, I.J., and Desvergne, B. 1999. Fatty acids, eicosanoids, and hypolipidemic agents regulate gene expression through direct binding to peroxisome proliferator-activated receptors. *Adv Exp Med Biol* 447:199-209.
168. Odegaard, J.I., Ricardo-Gonzalez, R.R., Goforth, M.H., Morel, C.R., Subramanian, V., Mukundan, L., Eagle, A.R., Vats, D., Brombacher, F., Ferrante, A.W., et al. 2007. Macrophage-specific PPARgamma controls alternative activation and improves insulin resistance. *Nature* 447:1116-1120.
169. Hevener, A.L., Olefsky, J.M., Reichart, D., Nguyen, M.T., Bandyopadhyay, G., Leung, H.Y., Watt, M.J., Benner, C., Febbraio, M.A., Nguyen, A.K., et al. 2007. Macrophage PPAR gamma is required for normal skeletal muscle and hepatic insulin sensitivity and full antidiabetic effects of thiazolidinediones. *J Clin Invest* 117:1658-1669.
170. Patsouris, D., Li, P.P., Thapar, D., Chapman, J., Olefsky, J.M., and Neels, J.G. 2008. Ablation of CD11c-positive cells normalizes insulin sensitivity in obese insulin resistant animals. *Cell Metab* 8:301-309.
171. Cani, P.D., Amar, J., Iglesias, M.A., Poggi, M., Knauf, C., Bastelica, D., Neyrinck, A.M., Fava, F., Tuohy, K.M., Chabo, C., et al. 2007. Metabolic endotoxemia initiates obesity and insulin resistance. *Diabetes* 56:1761-1772.
172. Nguyen, M.T., Favelyukis, S., Nguyen, A.K., Reichart, D., Scott, P.A., Jenn, A., Liu-Bryan, R., Glass, C.K., Neels, J.G., and Olefsky, J.M. 2007. A subpopulation of macrophages infiltrates hypertrophic adipose tissue and is activated by free fatty acids via Toll-like receptors 2 and 4 and JNK-dependent pathways. *J Biol Chem* 282:35279-35292.
173. Lee, J.Y., Ye, J., Gao, Z., Youn, H.S., Lee, W.H., Zhao, L., Sizemore, N., and Hwang, D.H. 2003. Reciprocal modulation of Toll-like receptor-4 signaling pathways involving MyD88 and phosphatidylinositol 3-kinase/AKT by saturated and polyunsaturated fatty acids. *J Biol Chem* 278:37041-37051.
174. Cramer, T., Yamanishi, Y., Clausen, B.E., Forster, I., Pawlinski, R., Mackman, N., Haase, V.H., Jaenisch, R., Corr, M., Nizet, V., et al. 2003. HIF-1alpha is essential for myeloid cell-mediated inflammation. *Cell* 112:645-657.
175. Beck-Nielsen, H., Pedersen, O., Kragballe, K., and Sorensen, N.S. 1977. The monocyte as a model for the study of insulin receptors in man. *Diabetologia* 13:563-569.

176. Whitson, R.H., and Kaplan, S.A. 1983. In vitro regulation of human monocyte insulin receptors by insulin and 1-methyl-3-isobutylxanthine. *Am J Physiol* 245:E494-501.
177. Carpentier, J.L., Dayer, J.M., Lang, U., Silverman, R., Orci, L., and Gorden, P. 1984. Down-regulation and recycling of insulin receptors. Effect of monensin on IM-9 lymphocytes and U-937 monocyte-like cells. *J Biol Chem* 259:14190-14195.
178. Rhodes, J. 1975. Modulation of macrophage Fc receptor expression in vitro by insulin and cyclic nucleotides. *Nature* 257:597-599.
179. Zhilina, I.L., Elkina, S.I., and Boichenko, M.N. 1984. [Effect of insulin and isoproterenol on macrophage phagocytic activity]. *Zh Mikrobiol Epidemiol Immunobiol*:98-101.
180. Leiter, E.H. 1987. Murine macrophages and pancreatic beta cells. Chemotactic properties of insulin and beta-cytostatic action of interleukin 1. *J Exp Med* 166:1174-1179.
181. Costa Rosa, L.F., Safi, D.A., Cury, Y., and Curi, R. 1996. The effect of insulin on macrophage metabolism and function. *Cell Biochem Funct* 14:33-42.
182. Iida, K.T., Shimano, H., Kawakami, Y., Sone, H., Toyoshima, H., Suzuki, S., Asano, T., Okuda, Y., and Yamada, N. 2001. Insulin up-regulates tumor necrosis factor-alpha production in macrophages through an extracellular-regulated kinase-dependent pathway. *J Biol Chem* 276:32531-32537.
183. Iida, K.T., Suzuki, H., Sone, H., Shimano, H., Toyoshima, H., Yatoh, S., Asano, T., Okuda, Y., and Yamada, N. 2002. Insulin inhibits apoptosis of macrophage cell line, THP-1 cells, via phosphatidylinositol-3-kinase-dependent pathway. *Arterioscler Thromb Vasc Biol* 22:380-386.
184. Leffler, M., Hrach, T., Stuerzl, M., Horch, R.E., Herndon, D.N., and Jeschke, M.G. 2007. Insulin attenuates apoptosis and exerts anti-inflammatory effects in endotoxemic human macrophages. *J Surg Res* 143:398-406.
185. Misra, U.K., and Pizzo, S.V. 2005. Up-regulation of GRP78 and antiapoptotic signaling in murine peritoneal macrophages exposed to insulin. *J Leukoc Biol* 78:187-194.
186. Han, S., Liang, C.P., DeVries-Seimon, T., Ranalletta, M., Welch, C.L., Collins-Fletcher, K., Accili, D., Tabas, I., and Tall, A.R. 2006. Macrophage insulin receptor deficiency increases ER stress-induced apoptosis and necrotic core formation in advanced atherosclerotic lesions. *Cell Metab* 3:257-266.
187. Baumgartl, J., Baudler, S., Scherner, M., Babaev, V., Makowski, L., Suttles, J., McDuffie, M., Fazio, S., Kahn, C.R., Hotamisligil, G.S., et al. 2006. Myeloid

- lineage cell-restricted insulin resistance protects apolipoproteinE-deficient mice against atherosclerosis. *Cell Metab* 3:247-256.
188. Sambrook, J., and Russell, D.W. 2001. *Molecular Cloning: A Laboratory Manual*: CSHL Press. 2344 pp.
189. Chomczynski, P., and Qasba, P.K. 1984. Alkaline transfer of DNA to plastic membrane. *Biochem Biophys Res Commun* 122:340-344.
190. Mullis, K.B., and Faloona, F.A. 1987. Specific synthesis of DNA in vitro via a polymerase-catalyzed chain reaction. *Methods Enzymol* 155:335-350.
191. Saiki, R.K., Gelfand, D.H., Stoffel, S., Scharf, S.J., Higuchi, R., Horn, G.T., Mullis, K.B., and Erlich, H.A. 1988. Primer-directed enzymatic amplification of DNA with a thermostable DNA polymerase. *Science* 239:487-491.
192. Abel, E.D., Peroni, O., Kim, J.K., Kim, Y.B., Boss, O., Hadro, E., Minnemann, T., Shulman, G.I., and Kahn, B.B. 2001. Adipose-selective targeting of the GLUT4 gene impairs insulin action in muscle and liver. *Nature* 409:729-733.
193. Laemmli, U.K. 1970. Cleavage of structural proteins during the assembly of the head of bacteriophage T4. *Nature* 227:680-685.
194. Hogan, B., Costantini, F., and Lacey, E. 1986. *Manipulating the mouse embryo: A Laboratory Manual*. Cold Spring Harbor, New York: Cold Spring Harbor Laboratory Press.
195. Silver, L.M. 1995. *Mouse Genetics: Concepts and Applications*: Oxford University Press. 376 Seiten pp.
196. Bruning, J.C., Michael, M.D., Winnay, J.N., Hayashi, T., Horsch, D., Accili, D., Goodyear, L.J., and Kahn, C.R. 1998. A muscle-specific insulin receptor knockout exhibits features of the metabolic syndrome of NIDDM without altering glucose tolerance. *Mol Cell* 2:559-569.
197. Seibler, J., Zevnik, B., Kuter-Luks, B., Andreas, S., Kern, H., Hennek, T., Rode, A., Heimann, C., Faust, N., Kauselmann, G., et al. 2003. Rapid generation of inducible mouse mutants. *Nucleic Acids Res* 31:e12.
198. Etherton, T.D., Thompson, E.H., and Allen, C.E. 1977. Improved techniques for studies of adipocyte cellularity and metabolism. *J Lipid Res* 18:552-557.
199. Ferre, P., Leturque, A., Burnol, A.F., Penicaud, L., and Girard, J. 1985. A method to quantify glucose utilization in vivo in skeletal muscle and white adipose tissue of the anaesthetized rat. *Biochem J* 228:103-110.

200. Cross, M., Mangelsdorf, I., Wedel, A., and Renkawitz, R. 1988. Mouse lysozyme M gene: isolation, characterization, and expression studies. *Proc Natl Acad Sci U S A* 85:6232-6236.
201. Clausen, B.E., Burkhardt, C., Reith, W., Renkawitz, R., and Forster, I. 1999. Conditional gene targeting in macrophages and granulocytes using LysMcre mice. *Transgenic Res* 8:265-277.
202. Semple, R.K., Soos, M.A., Luan, J., Mitchell, C.S., Wilson, J.C., Gurnell, M., Cochran, E.K., Gorden, P., Chatterjee, V.K., Wareham, N.J., et al. 2006. Elevated plasma adiponectin in humans with genetically defective insulin receptors. *J Clin Endocrinol Metab* 91:3219-3223.
203. Sato, S., and Hughes, R.C. 1994. Regulation of secretion and surface expression of Mac-2, a galactoside-binding protein of macrophages. *J Biol Chem* 269:4424-4430.
204. Boyden, S. 1962. The chemotactic effect of mixtures of antibody and antigen on polymorphonuclear leucocytes. *J Exp Med* 115:453-466.
205. Rohl, M., Pasparakis, M., Baudler, S., Baumgartl, J., Gautam, D., Huth, M., De Lorenzi, R., Krone, W., Rajewsky, K., and Bruning, J.C. 2004. Conditional disruption of IkappaB kinase 2 fails to prevent obesity-induced insulin resistance. *J Clin Invest* 113:474-481.
206. Sternberg, N., Hamilton, D., and Hoess, R. 1981. Bacteriophage P1 site-specific recombination. II. Recombination between loxP and the bacterial chromosome. *J Mol Biol* 150:487-507.
207. Sauer, B., and Henderson, N. 1988. Site-specific DNA recombination in mammalian cells by the Cre recombinase of bacteriophage P1. *Proc Natl Acad Sci U S A* 85:5166-5170.
208. Abremski, K., Hoess, R., and Sternberg, N. 1983. Studies on the properties of P1 site-specific recombination: evidence for topologically unlinked products following recombination. *Cell* 32:1301-1311.
209. Rickert, R.C., Rajewsky, K., and Roes, J. 1995. Impairment of T-cell-dependent B-cell responses and B-1 cell development in CD19-deficient mice. *Nature* 376:352-355.
210. Testa, G., Zhang, Y., Vintersten, K., Benes, V., Pijnappel, W.W., Chambers, I., Smith, A.J., Smith, A.G., and Stewart, A.F. 2003. Engineering the mouse genome with bacterial artificial chromosomes to create multipurpose alleles. *Nat Biotechnol* 21:443-447.
211. Cho, I.H., Hong, J., Suh, E.C., Kim, J.H., Lee, H., Lee, J.E., Lee, S., Kim, C.H., Kim, D.W., Jo, E.K., et al. 2008. Role of microglial IKK{beta} in kainic acid-induced hippocampal neuronal cell death. *Brain*.

212. Keshav, S., Chung, P., Milon, G., and Gordon, S. 1991. Lysozyme is an inducible marker of macrophage activation in murine tissues as demonstrated by in situ hybridization. *J Exp Med* 174:1049-1058.
213. Yamauchi, T., Kamon, J., Minokoshi, Y., Ito, Y., Waki, H., Uchida, S., Yamashita, S., Noda, M., Kita, S., Ueki, K., et al. 2002. Adiponectin stimulates glucose utilization and fatty-acid oxidation by activating AMP-activated protein kinase. *Nat Med* 8:1288-1295.
214. Hilder, T.L., Tou, J.C., Grindeland, R.E., Wade, C.E., and Graves, L.M. 2003. Phosphorylation of insulin receptor substrate-1 serine 307 correlates with JNK activity in atrophic skeletal muscle. *FEBS Lett* 553:63-67.
215. Schraw, T., Wang, Z.V., Halberg, N., Hawkins, M., and Scherer, P.E. 2008. Plasma adiponectin complexes have distinct biochemical characteristics. *Endocrinology* 149:2270-2282.
216. Maroof, A., English, N.R., Bedford, P.A., Gabrilovich, D.I., and Knight, S.C. 2005. Developing dendritic cells become 'lacy' cells packed with fat and glycogen. *Immunology* 115:473-483.
217. Huber, J., Kiefer, F.W., Zeyda, M., Ludvik, B., Silberhumer, G.R., Prager, G., Zlabinger, G.J., and Stulnig, T.M. 2008. CC chemokine and CC chemokine receptor profiles in visceral and subcutaneous adipose tissue are altered in human obesity. *J Clin Endocrinol Metab* 93:3215-3221.
218. Westerbacka, J., Corner, A., Kolak, M., Makkonen, J., Turpeinen, U., Hamsten, A., Fisher, R.M., and Yki-Jarvinen, H. 2008. Insulin regulation of MCP-1 in human adipose tissue of obese and lean women. *Am J Physiol Endocrinol Metab* 294:E841-845.
219. Dahlman, I., Kaaman, M., Olsson, T., Tan, G.D., Bickerton, A.S., Wahlen, K., Andersson, J., Nordstrom, E.A., Blomqvist, L., Sjogren, A., et al. 2005. A unique role of monocyte chemoattractant protein 1 among chemokines in adipose tissue of obese subjects. *J Clin Endocrinol Metab* 90:5834-5840.
220. Murdolo, G., Hammarstedt, A., Sandqvist, M., Schmelz, M., Herder, C., Smith, U., and Jansson, P.A. 2007. Monocyte chemoattractant protein-1 in subcutaneous abdominal adipose tissue: characterization of interstitial concentration and regulation of gene expression by insulin. *J Clin Endocrinol Metab* 92:2688-2695.
221. Maachi, M., Pieroni, L., Bruckert, E., Jardel, C., Fellahi, S., Hainque, B., Capeau, J., and Bastard, J.P. 2004. Systemic low-grade inflammation is related to both circulating and adipose tissue TNFalpha, leptin and IL-6 levels in obese women. *Int J Obes Relat Metab Disord* 28:993-997.
222. de Lima, T.M., de Sa Lima, L., Scavone, C., and Curi, R. 2006. Fatty acid control of nitric oxide production by macrophages. *FEBS Lett* 580:3287-3295.

- 
223. Martins de Lima, T., Cury-Boaventura, M.F., Giannocco, G., Nunes, M.T., and Curi, R. 2006. Comparative toxicity of fatty acids on a macrophage cell line (J774). *Clin Sci (Lond)* 111:307-317.
224. Santomauro, A.T., Boden, G., Silva, M.E., Rocha, D.M., Santos, R.F., Ursich, M.J., Strassmann, P.G., and Wajchenberg, B.L. 1999. Overnight lowering of free fatty acids with Acipimox improves insulin resistance and glucose tolerance in obese diabetic and nondiabetic subjects. *Diabetes* 48:1836-1841.
225. Chou, C.J., Cha, M.C., Jung, D.W., Boozer, C.N., Hashim, S.A., and Pi-Sunyer, F.X. 2001. High-fat diet feeding elevates skeletal muscle uncoupling protein 3 levels but not its activity in rats. *Obes Res* 9:313-319.
226. Giugliano, D., Marfella, R., Coppola, L., Verrazzo, G., Acampora, R., Giunta, R., Nappo, F., Lucarelli, C., and D'Onofrio, F. 1997. Vascular effects of acute hyperglycemia in humans are reversed by L-arginine. Evidence for reduced availability of nitric oxide during hyperglycemia. *Circulation* 95:1783-1790.
227. Senokuchi, T., Liang, C.P., Seimon, T.A., Han, S., Matsumoto, M., Banks, A.S., Paik, J.H., DePinho, R.A., Accili, D., Tabas, I., et al. 2008. Forkhead transcription factors (FoxOs) promote apoptosis of insulin-resistant macrophages during cholesterol-induced endoplasmic reticulum stress. *Diabetes* 57:2967-2976.
228. Epand, R.F., Martinou, J.C., Montessuit, S., and Epand, R.M. 2002. Membrane perturbations induced by the apoptotic Bax protein. *Biochem J* 367:849-855.
229. Nechushtan, A., Smith, C.L., Lamensdorf, I., Yoon, S.H., and Youle, R.J. 2001. Bax and Bak coalesce into novel mitochondria-associated clusters during apoptosis. *J Cell Biol* 153:1265-1276.
230. Kluck, R.M., Esposti, M.D., Perkins, G., Renken, C., Kuwana, T., Bossy-Wetzel, E., Goldberg, M., Allen, T., Barber, M.J., Green, D.R., et al. 1999. The pro-apoptotic proteins, Bid and Bax, cause a limited permeabilization of the mitochondrial outer membrane that is enhanced by cytosol. *J Cell Biol* 147:809-822.
231. Chipuk, J.E., Bouchier-Hayes, L., and Green, D.R. 2006. Mitochondrial outer membrane permeabilization during apoptosis: the innocent bystander scenario. *Cell Death Differ* 13:1396-1402.
232. Newmeyer, D.D., Farschon, D.M., and Reed, J.C. 1994. Cell-free apoptosis in *Xenopus* egg extracts: inhibition by Bcl-2 and requirement for an organelle fraction enriched in mitochondria. *Cell* 79:353-364.
233. Listenberger, L.L., Ory, D.S., and Schaffer, J.E. 2001. Palmitate-induced apoptosis can occur through a ceramide-independent pathway. *J Biol Chem* 276:14890-14895.

234. Brundage, S.I., Kirilcuk, N.N., Lam, J.C., Spain, D.A., and Zautke, N.A. 2008. Insulin increases the release of proinflammatory mediators. *J Trauma* 65:367-372.
235. Cuschieri, J., Bulger, E., Grinsell, R., Garcia, I., and Maier, R.V. 2008. Insulin regulates macrophage activation through activin A. *Shock* 29:285-290.
236. Iwasaki, Y., Nishiyama, M., Taguchi, T., Asai, M., Yoshida, M., Kambayashi, M., Terada, Y., and Hashimoto, K. 2008. Insulin exhibits short-term anti-inflammatory but long-term proinflammatory effects in vitro. *Mol Cell Endocrinol*.
237. Ozes, O.N., Mayo, L.D., Gustin, J.A., Pfeffer, S.R., Pfeffer, L.M., and Donner, D.B. 1999. NF-kappaB activation by tumour necrosis factor requires the Akt serine-threonine kinase. *Nature* 401:82-85.
238. Uematsu, S., Kaisho, T., Tanaka, T., Matsumoto, M., Yamakami, M., Omori, H., Yamamoto, M., Yoshimori, T., and Akira, S. 2007. The C/EBP beta isoform 34-kDa LAP is responsible for NF-IL-6-mediated gene induction in activated macrophages, but is not essential for intracellular bacteria killing. *J Immunol* 179:5378-5386.
239. Chano, F., and Descoteaux, A. 2002. Modulation of lipopolysaccharide-induced NF-IL6 activation by protein kinase C-alpha in a mouse macrophage cell line. *Eur J Immunol* 32:2897-2904.
240. Piwien-Pilipuk, G., Van Mater, D., Ross, S.E., MacDougald, O.A., and Schwartz, J. 2001. Growth hormone regulates phosphorylation and function of CCAAT/enhancer-binding protein beta by modulating Akt and glycogen synthase kinase-3. *J Biol Chem* 276:19664-19671.
241. Trautwein, C., van der Geer, P., Karin, M., Hunter, T., and Chojkier, M. 1994. Protein kinase A and C site-specific phosphorylations of LAP (NF-IL6) modulate its binding affinity to DNA recognition elements. *J Clin Invest* 93:2554-2561.
242. Sekine, O., Nishio, Y., Egawa, K., Nakamura, T., Maegawa, H., and Kashiwagi, A. 2002. Insulin activates CCAAT/enhancer binding proteins and proinflammatory gene expression through the phosphatidylinositol 3-kinase pathway in vascular smooth muscle cells. *J Biol Chem* 277:36631-36639.
243. Zwergal, A., Quirling, M., Saugel, B., Huth, K.C., Sydlik, C., Poli, V., Neumeier, D., Ziegler-Heitbrock, H.W., and Brand, K. 2006. C/EBP beta blocks p65 phosphorylation and thereby NF-kappa B-mediated transcription in TNF-tolerant cells. *J Immunol* 177:665-672.
244. Moser, T.L., Enghild, J.J., Pizzo, S.V., and Stack, M.S. 1993. The extracellular matrix proteins laminin and fibronectin contain binding domains for human plasminogen and tissue plasminogen activator. *J Biol Chem* 268:18917-18923.

- 
245. Lijnen, H.R. 2001. Plasmin and matrix metalloproteinases in vascular remodeling. *Thromb Haemost* 86:324-333.
246. Gong, Y., Hart, E., Shchurin, A., and Hoover-Plow, J. 2008. Inflammatory macrophage migration requires MMP-9 activation by plasminogen in mice. *J Clin Invest* 118:3012-3024.
247. Fiscoeder, A., Meyborg, H., Stibenz, D., Fleck, E., Graf, K., and Stawowy, P. 2007. Insulin augments matrix metalloproteinase-9 expression in monocytes. *Cardiovasc Res* 73:841-848.
248. Kappert, K., Meyborg, H., Clemenz, M., Graf, K., Fleck, E., Kintscher, U., and Stawowy, P. 2008. Insulin facilitates monocyte migration: a possible link to tissue inflammation in insulin-resistance. *Biochem Biophys Res Commun* 365:503-508.
249. Lesniewski, L.A., Hosch, S.E., Neels, J.G., de Luca, C., Pashmforoush, M., Lumeng, C.N., Chiang, S.H., Scadeng, M., Saltiel, A.R., and Olefsky, J.M. 2007. Bone marrow-specific Cap gene deletion protects against high-fat diet-induced insulin resistance. *Nat Med* 13:455-462.
250. Kawaguchi, T., Veech, R.L., and Uyeda, K. 2001. Regulation of energy metabolism in macrophages during hypoxia. Roles of fructose 2,6-bisphosphate and ribose 1,5-bisphosphate. *J Biol Chem* 276:28554-28561.
251. Leppanen, O., Bjornheden, T., Evaldsson, M., Boren, J., Wiklund, O., and Levin, M. 2006. ATP depletion in macrophages in the core of advanced rabbit atherosclerotic plaques in vivo. *Atherosclerosis* 188:323-330.
252. Rosa, L.F., Cury, Y., and Curi, R. 1992. Effects of insulin, glucocorticoids and thyroid hormones on the activities of key enzymes of glycolysis, glutaminolysis, the pentose-phosphate pathway and the Krebs cycle in rat macrophages. *J Endocrinol* 135:213-219.
253. Yim, S., Choi, S.M., Choi, Y., Lee, N., Chung, J., and Park, H. 2003. Insulin and hypoxia share common target genes but not the hypoxia-inducible factor-1alpha. *J Biol Chem* 278:38260-38268.
254. Seagroves, T.N., Ryan, H.E., Lu, H., Wouters, B.G., Knapp, M., Thibault, P., Laderoute, K., and Johnson, R.S. 2001. Transcription factor HIF-1 is a necessary mediator of the pasteur effect in mammalian cells. *Mol Cell Biol* 21:3436-3444.

## 8 Acknowledgements

Mein spezieller Dank geht an Prof. Dr. Jens Brüning für seine Unterstützung, für die Möglichkeit an diesem interessanten Thema zu arbeiten und für den intellektuellen Freiraum, den er mir immer gewährt hat.

Ich möchte Prof. Dr. Thomas Langer, Prof. Dr. Peter Kloppenburg und Dr. Ursula Lichtenberg dafür danken, dass sie sich dazu bereit erklärt haben mein Prüfungskomitee zu bilden.

Mein besonderer Dank gilt Bengt Belgardt, Thomas Wunderlich, André Kleinriders, Bhagirath Chaurasia und Carsten Merkwirth für Freundschaft, Rat und Inspiration. Ich danke Brigitte Hampel für ihre tollen Färbungen sowie Ruth Kuschewski und Leona Plum für Ihre kompetente Hilfe bei den Clamp-Operationen. Zudem möchte ich Julia Baumgartl für ihre technische Unterstützung und die schöne Zeit in "unserem kleinen Labor" danken. Liebe Linda, auch Dir danke ich ganz besonders für die exzellente Korrekturarbeit und eine Freundschaft, die uns hoffentlich noch lange erhalten bleibt. Darüberhinaus möchte ich allen meinen Kollegen für die wunderbare und unterhaltsame Zeit danken, die ich während meiner Arbeit in der AG Brüning hatte.

Unendlich dankbar bin ich meinen Eltern Beatrice und Bernd, die mich immer unterstützt, inspiriert und begeistert haben, die mir jegliche Freiheit ließen und doch immer da waren, wenn ich sie gebraucht habe. Ausserdem möchte ich Julia für die liebevolle Unterstützung und Zuneigung danken die sie mir zuteil werden lässt. Mein Dank gilt auch meiner Schwester Anna-Katalin, ohne die ich bestimmt ein anderer Mensch wäre.

## 9 Erklärung

Ich versichere, daß ich die von mir vorgelegte Dissertation selbständig angefertigt, die benutzten Quellen und Hilfsmittel vollständig angegeben und die Stellen der Arbeit - einschließlich Tabellen, Karten und Abbildungen -, die anderen Werken im Wortlaut oder dem Sinn nach entnommen sind, in jedem Einzelfall als Entlehnung kenntlich gemacht habe; daß diese Dissertation noch keiner anderen Fakultät oder Universität zur Prüfung vorgelegen hat; daß sie - abgesehen von unten angegebenen Teilpublikationen - noch nicht veröffentlicht worden ist sowie, daß ich eine solche Veröffentlichung vor Abschluß des Promotionsverfahrens nicht vornehmen werde. Die Bestimmungen dieser Promotionsordnung sind mir bekannt. Die von mir vorgelegte Dissertation ist von Prof. Dr. Jens C. Brüning betreut worden.

Köln, Dezember 2008

Jan Mauer

## 10 Curriculum Vitae

### Persönliche Daten

Name	Jan Mauer
Geburt	12.09.1978 in Köln
Adresse	Zülpicher Str. 47, 50674 Köln
Email	j.mauer@uni-koeln.de
Nationalität	deutsch

### Bildungsweg

Seit 11/2004	Promotion in der Abteilung Mausgenetik und Metabolismus des Instituts für Genetik der Universität zu Köln
1999 - 2004	Studium der Biologie an der Mathematisch-Naturwissenschaftlichen Fakultät der Universität zu Köln  Diplomarbeit in der Abteilung Mausgenetik und Metabolismus des Instituts für Genetik der Universität zu Köln zum Thema: „Bedeutung der insulinrezeptorvermittelten Signaltransduktion in Makrophagen“  Diplomprüfungen im Hauptfach Genetik und in den Nebenfächern Biochemie und Entwicklungsbiologie
1998-1999	Zivildienst bei den Zentren für Senioren und Behinderte der Stadt Köln
1989 - 1998	Johann-Gottfried-Herder Gymnasium Köln-Buchheim Abschluss: Abitur
1985-1989	Gemeinschaftsgrundschule Köln Dellbrück

### Publikationen

2005	Seibler J, Küter-Luks B, Kern H, Streu S, Plum L, Mauer J, Kühn R, Brüning JC, Schwenk F. 2005 Single copy shRNA configuration for ubiquitous gene knockdown in mice. <i>Nucleic Acids Res.</i> 33 e67.
------	---